Preliminary indian ocean bigeye tuna stock assessment 1950-2021 (stock synthesis)

DAN FU[1], GORKA MERINO[2], HENNING WINKER[3]

02 OCTOBER 2022

[1] IOTC Secretariat, Dan.Fu@fao.org;
[2] AZTI Secretariat, gorka.merino@azti.es;
[3] henning.winker@gmail.com;

Contents

SUMMARY

This report presents a preliminary stock assessment for Indian Ocean bigeye tuna (*Thunnus albacares*) using *Stock Synthesis 3* (SS3). The assessment uses a spatially structured, age-based model that integrates catch rate indices, length-compositions, and tagging data. The assessment model covers the period 1975–2021 and represents an update and revision of the 2019 assessment model, taking into account newly available information since the previous assessment. The assessment assumes that the Indian Ocean bigeye tuna constitute a single stock, modelled as spatially disaggregated four regions, with 12 fisheries. Standardised CPUE series from the main longline fleets 1975 – 2021 were included in the models as the relative abundance index of exploitable biomass in each region. Standardised indices of bigeye tuna caught by European purse seiners from sets on associated tuna schools (2010 – 2021) in the western tropical region were also included. Tag release and recovery data from the Indian Ocean regional tuna tagging program were included in the model to inform abundance, movement, and mortality rates

A range of sensitivity models is presented to explore the impact of key data sets and to assess the effects of alternative model assumptions, including the utility of CPUE and length compositions, data weighting, and spatial and temporal model structures. The proposed final assessment model options correspond to a combination of model configurations, including alternative assumptions about key biological parameters. The final models involved running a combination of options on selectivity configurations for the main longline fisheries in region 2 and 3 (2 scenario), steepness (3 values), growth (2 scenario), natural morality (2 levels). These models encompass a wide range of stock trajectories. Estimates of stock status were combined across from the 24 models and incorporated uncertainty estimates from both within and across the model ensemble.

The overall stock status estimate is more pessimistic than the previous assessment. Considering the quantified uncertainty, spawning stock biomass in 2021 was estimated to be 25% of the unfished levels and 90% of the level that can support MSY (SSB_{2021}/SSB_{MSY} = 0.90), current fishing mortality was estimated to be higher than F_{MSY} (F_{2021}/F_{MSY} = 1.43). The probability of the stock being currently in the red Kobe quadrant is estimated to be 79%. Therefore, the stock is considered be overfished and is subject to overfishing in 2021. However, the recent catches have been lower than the estimated MSY and the spawning biomass has been increasing in the last three years. Considering the quantified uncertainty, the stock is considered be overfished and is subject to overfishing in 2021. The estimated stock status is summarized as below:

- Catch in 2021: 87 728
- Average catch 2017–2021: 95 021
- MSY (1000 mt) (plausible range): 96 (83 –108)
- F_{MSY}: 0.26 (0.18–0.34)
- SB_0(1000 mt) (80% CI): 1831 (1445–2218)
- SB_{2021} (1000 mt) (80% CI): 450 (322–577)
- SB_{MSY} (80% CI) 513 (332–694)
- SB_{2021} / SB_0 (80% CI): 0.25 (0.23–0.27)
- SB_{2021} / SB_{MSY} (80% CI): 0.90 (0.75–1.05)
- F_{2021} / F_{MSY} (80% CI): 1.43 (1.10–1.77)

1. INTRODUCTION

This paper presents a preliminary stock assessment of bigeye tuna (*Thunnus albacares*) in the Indian Ocean (IO) including fishery data up to the end of 2021. The assessment implements an age- and spatially structured population model using the Stock Synthesis software (Methot 2013, Methot & Wetzel 2013).

Previous assessments of the Indian Ocean bigeye tuna stock have been conducted using Stock Synthesis (Shono et al 2009, Kolody et al 2010, Langley et al 2013a, b, 2016, Fu 2019) and ASPM (Nishida & Rademeyer 2011). The assessment of Langley et al (2013a, b) conducted a thorough examination of the key model assumptions, and the results of that assessment provided the basis for the management advice for bigeye tuna formulated by WPTT15. However, the spatial dynamics of these models were not considered to adequately represent the dynamics of the IO bigeye tuna stock, specifically the regional distribution of biomass and the movement dynamics. The model results were sensitive to the spatial structure of the model (1 or 3 regions), the tag mixing period (4 quarters vs 8 quarters) and the relative weighting of the length frequency data. The final assessment models did not incorporate the available IO bigeye tag release/recovery data.

In 2016, the stock assessment of the IO bigeye tuna stock included a review of the spatial stratification and parameterization of the assessment model to enable the integration of the tagging data into the assessment model (Langley 2016, IOTC 2016). The 2016 assessment model utilized the new composite longline CPUE indices derived from main distant water longline fleets, replacing the Japanese longline CPUE indices used in the previous assessment. A range of model sensitivities were conducted, specifically related to natural mortality, selectivity and SRR steepness. The assessment captured the uncertainty on stock recruitment relationship and the influence of tagging information. Spawning stock biomass in 2015 was estimated be above SSB_{MSY}, and fishing mortality was below F_{MSY}.

The 2019 assessment adopted of a new regional weighting scheme for the longline CPUE indices and a revised procedure to correct for tag loss and reporting. The assessment model estimated a substantial increase in fishing mortality in 2018, driven by the significant increase of the catches from the EU purse seine FAD fishery in 2018. The WPTT considered that this was primarily due to the changes in the estimation of the species composition for catches reported by the EU purse seine fleet in 2018 (IOTC 2019a). The magnitude of increase of this catch component was deemed not credible and for that reason the WPTT21 adopted an approach to revising the bigeye tuna catch, which applied the species composition recorded for the log-associated component of EU,Spain purse seine catches in 2017 to the total catches (log-associated) reported in 2018 by the same fleet (scientific catch estimates, see IOTC 2019a). The revised catches were used in the final assessment models. The final assessment adopted an ensemble of 12 models covering major components of structural uncertainty to characterise the stock status and to predict future fishing risks (IOTC 2019a). The assessment estimated that the spawning stock biomass in 2018 was above SB_{MSY}, but the fishing mortality was above F_{MSY}. As such, the stock status was determined to be not overfished but experiencing overfishing.

In 2022, the IOTC adopted a Management Procedure (MP) to recommend the total allowable catch (TAC) for bigeye tuna (Resolution 22/03). The adopted MP schedule requires the MP to be run by the IOTC Scientific Committee in 2022 to derive a recommended TAC through pre-agreed data input and a harvest control rule (Williams et al. 2021a). Given that bigeye tuna MP has been adopted, the stock assessment is no longer used to provide TAC advice. The stock assessment now provides information on bigeye tuna stock status, which can also be used to evaluate the performance of the MP (Williams et al. 2021b).

This report documents the next iteration of the stock assessment of the IO bigeye tuna stock for consideration at 24th WPTT meeting. This stock assessment is based on the 2019 modelling framework and has incorporated revised and updated data up to the end of 2021 and newly available biological information. The assessment implements an age-structured and spatially explicit population model and

is fitted to catch rate indices, length-compositions, and tagging data. The assessment is implemented using Stock Synthesis (version V3.30).

1.1 Biology and stock structure

Bigeye are distributed throughout the tropical and sub-tropical waters of the Indian Ocean. Qualitatively, the tagging data suggest that BET migrate reasonably quickly, and indicate at least some basin-scale movements. Unfortunately, the limited distribution of tag releases, and small number of returns (and absence of tag reporting rate estimates) outside of the European/Seychelles purse seine fleets, mainly operating in the western equatorial Indian Ocean, makes it difficult to quantify large-scale movements. While there may be some relatively discreet sub-populations, or slow mixing rates among sub-regions, there is no evidence that this is the case in the core area where most of the catch is taken, and presumably where the bulk of the population is located.

The differences in fish growth between oceans support the hypothesis of separate bigeye stocks in the Indian and Pacific Oceans (Farley et al. 2004). Genetic studies indicate that bigeye tuna form a single stock in the Indian Ocean, which is not connected to stocks in the Pacific or Atlantic Oceans (Appleyard et al. 2002; Chiang et al. 2008; Díaz-Arce et al. 2020). The current assessment assumes the Indian Ocean bigeye tuan consists of a single stock. However, the assessment model partitions the population by regions to account for differences in exploitation level and fishery operations (Figure 1).

1.2 Fishery overview

The distant-water longline fishery commenced operation in the Indian Ocean during the early 1950s (Figure 2). Bigeye tuna represented a significant component of the total catch from the longline fishery and catches increased steadily over the subsequent decades, reaching a peak in the late 1990s–early 2000s. The purse-seine fisheries and fresh-chilled longline fisheries developed from the mid-1980s, and total bigeye tuna catches peaked at about 150,000 t in the late 1990s (Figure 2). During the mid-2000s, the total annual bigeye catch declined considerably, primarily due to a decline in the longline catch in the western equatorial region in response to the threat of piracy off the Somali coast. The total annual catch declined to around 85,000 t in 2010 but recovered somewhat over the following years, reaching around 125,000 t in 2012. The total annual catch has declined since then and was 96,000 in 2018 (there were exceptionally high catches from the purse seine fisheries during 2018 which were potentially biased by changes in data processing methodologies confirmed by EU,Spain for its purse seine fleet for that year, see IOTC 2019a,b). The annual catch decreased in 2019, but increased in 2020, and was around 95 022 t in 2021.

During the middle 1970s, target species for Japanese longliners was rapidly shifted from yellowfin to bigeye, which was accompanied by the introduction of deep freezer that enhanced the value of bigeye as the Sashimi material (Okamoto 2005). However, since 1990s, the bigeye ratio decreased, and the catch of yellowfin exceeded that of bigeye. The changes were thought to be caused by shift of fishing ground (distribution of effort concentration) to yellowfin dominant region in western Indian ocean.

All the small bigeye taken by purse seiners are caught in equatorial warm surface waters. In contrast, a wide majority of adult bigeye catches taken by longliners in each ocean are caught in association with warm surface waters, close to the equatorial zones (Fonteneau et al. 2004). Most of the bigeye tuna catch from the Indian Ocean is caught within the latitudinal range 35° S to 10° N (Figure 3). This area of the Indian Ocean was used as the spatial domain of the assessment model. The small amount of bigeye catch from higher latitudes was reassigned to fisheries of the appropriate method within the model domain.

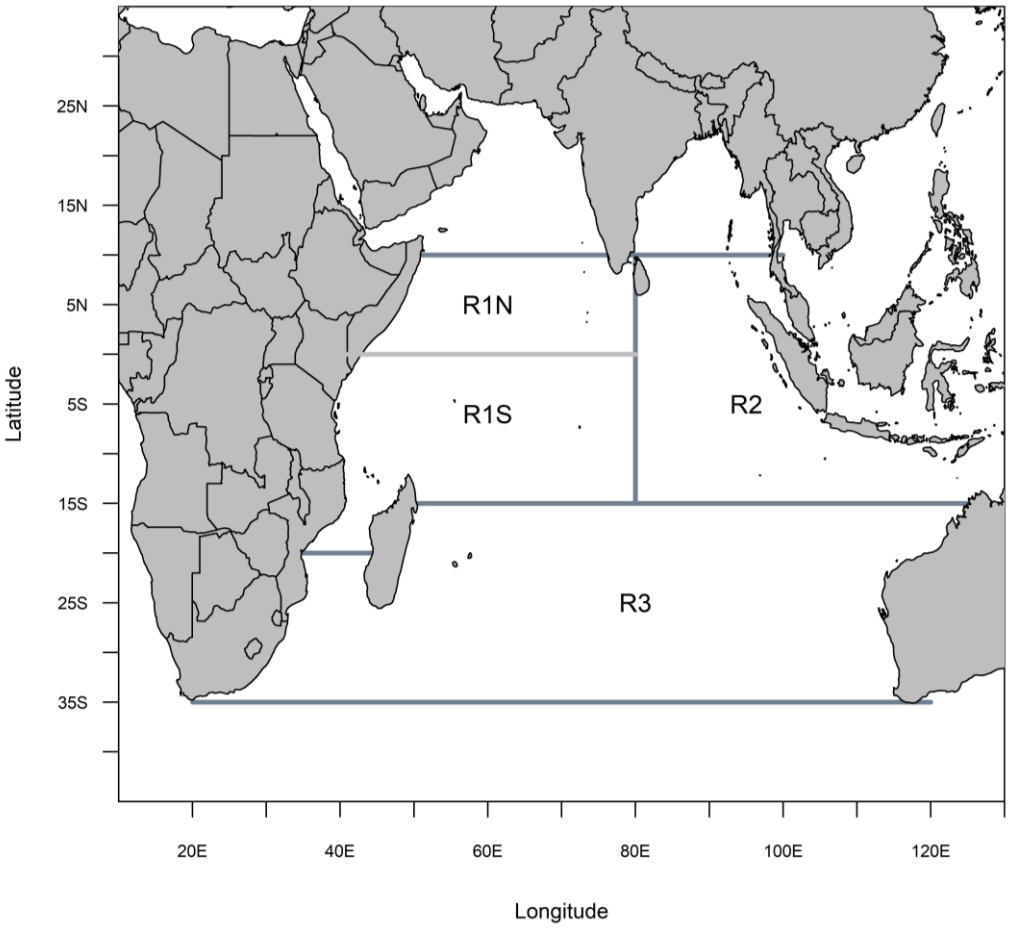

Figure 1: Spatial stratification of the Indian Ocean for the four-region assessment model.

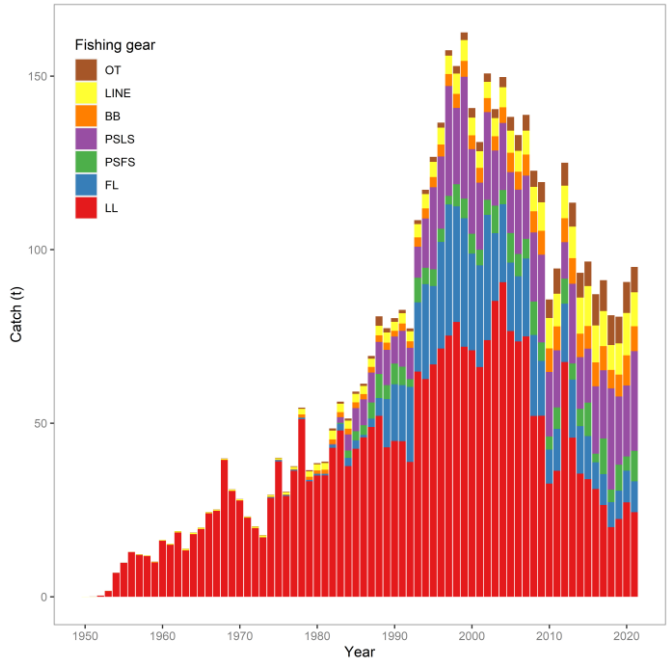

Figure 2: Total annual catch (1000s t) of bigeye tuna by fishing gear from 1950 to 2021. Gear codes are described in Table 1.

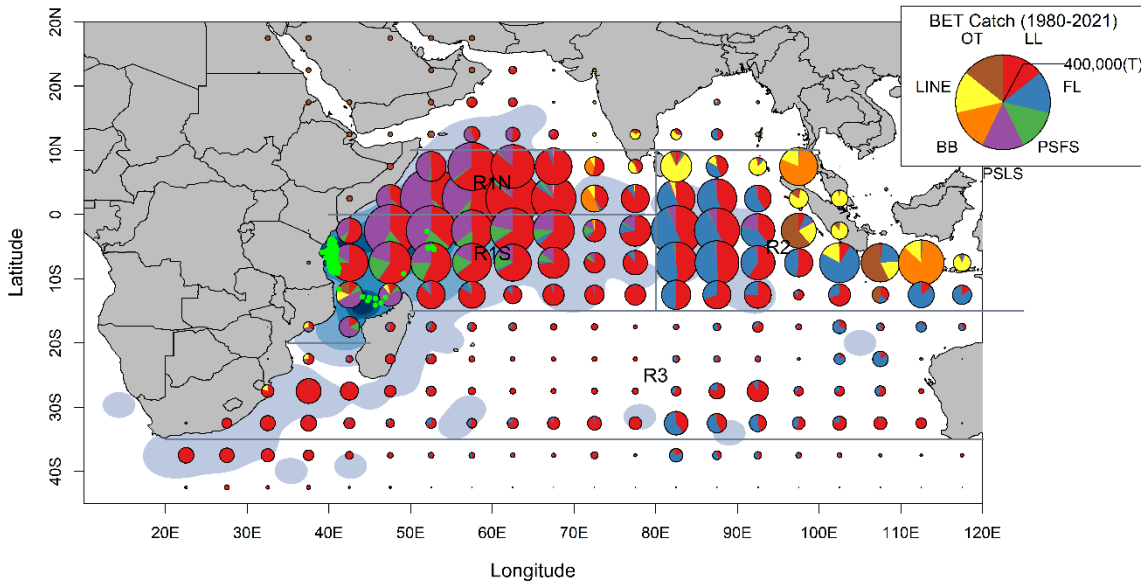

Figure 3: Spatial distribution of Indian Ocean bigeye catches by main gear types aggregated for1980-2021, overlaid with the dispersion of tag releases and recoveries from the Indian Ocean Tuna Tagging Program (IOTTP) 2005 – 2015.

2. OBSERVATIONS AND MODEL INPUTS

The data used in the bigeye tuna assessment consist of catch and length composition data for the fisheries defined in the analysis, longline CPUE indices and tag release-recapture data. The details of the configuration of the fishery specific data sets are described below.

2.1 Spatial stratification

Stock assessment models often adopted region structures to account for differences in biological characteristics of the species, regional exploitation pattern, or the level of mixing amongst subpopulations (Vincent, et al. 2018). In the 2013 bigeye assessment (Langley *et al* 2013a), the spatial domain of the bigeye assessment model was stratified into three regions: western equatorial region (region 1), eastern equatorial region (region 2) and southern region (region 3). Most of the longline catch is taken within the two equatorial regions (15° S to 10° N), while the purse seine catch is predominantly taken within the western equatorial region. A seasonal longline fishery operates in the southern region. The longitudinal partitioning of the equatorial area subdivides the distribution of tagged fish recoveries from releases that occurred in the western area of region 1. There are also some differences in the temporal trends in the longline CPUE indices from the three regions. This regional restructure was further refined in the 2016 assessment where the western equatorial region (region 1) was subdivided to account for differences in the distribution of tags within this region (Section 2.5 of Langley 2015). The region was partitioned at the equator: the area south of the equator and the area north of the equator, denoted as Region 1S and Region 1N, respectively (Figure 1). The four-region structure was adopted in the 2019 assessment, is also used in the current assessment.

2.2 Temporal stratification

The model commenced in 1975 and assumed an exploited, equilibrium initial state. Within this model period, the annual data were compiled into quarters (Jan–Mar, Apr–Jun, Jul–Sep, Oct–Dec) (representing a total of 176-time steps), and model is iterated a quarterly time step which as treated as a model year the SS3. The time steps were used to define model "years" (of 3-month duration) enabling recruitment to be estimated for each quarter to approximate the continuous recruitment of bigeye.

2.3 Definition of fisheries

The assessment adopted the equivalent fisheries definitions used in the previous SS3 stock assessment. These "fisheries" represent relatively homogeneous fishing units, with similar selectivity and catchability characteristics that do not vary greatly over time. Fifteen fisheries were defined based on the fishing gear type and the regional stratification (Table 1). The longline fishery was split into two main components based on vessel types. The Purse seine fishery was also partitioned by the fishing mode (set type).

Freezing longline fisheries, or those using drifting longlines for which one of the following conditions apply: (i) the vessel hull is made up of steel; (ii) vessel length overall of 30 m or greater; (iii) most of the catches of target species are preserved frozen or deep-frozen. A composite longline fishery was defined in each region (LL 1N, 1S, 2,3) aggregating the longline catch from all freezing longline fleets.

Fresh-tuna longline fisheries, or all those using drifting longlines and made of vessels (i) having fibreglass, FRP, or wooden hull; (ii) having length overall less than 30 m; (iii) preserving the catches of target species fresh or in refrigerated seawater. A composite longline fishery was defined aggregating the longline catch from all fresh-tuna longline fleets (principally Indonesia and Taiwan) in region 2 (FL 2), which is where most of the fresh-tuna longlines have traditionally operated.

The purse-seine catch and effort data were apportioned into two separate method fisheries: catches from sets on associated schools of tuna (log and drifting FAD sets; PSLS) and from sets on unassociated schools (free schools; PS FS). Purse-seine fisheries operate within regions 1N, 1S, and 2 and separate purse-seine fisheries were defined in regions 1N, 1S, and 2.

A single baitboat fishery was defined within region 1N. The fishery included the pole-and-line (essentially the Maldives fishery) and small seine fisheries (catching small fish). A small proportion of the total baitboat catch and effort occurs on the periphery of region 1N, within regions 1S and 2. The additional catch was assigned to the region 1N fishery.

A Line fishery was defined within region 2, representing a mixture of gears using handlines, and small longlines (including the gillnet and longline combination fishery of Sri Lanka). Moderate handline catches are also taken in regions 1, the catch and effort from these components of the fishery were reassigned to the fishery within region 2.

For regions 1N and 2, a miscellaneous ("Other") fishery was defined comprising catches from artisanal fisheries other than those specified above (e.g. gillnet, trolling and a range of small gears.)

Table 1: Definition of fisheries for the four-region assessment model for bigeye tuna

Code	Method	Region	Flag	Notes
FL2	Longline, fresh tuna fleets	2	All	
LL1N	Longline, distant water	1N	All	
LL1S	Longline, distant water	1S	All	
LL2	Longline, distant water	2	All	
LL3	Longline, distant water	3	All	
PSFS1N	Purse seine, free school	1N	All	
PSFS1S	Purse seine, free school	1S	All	
PSFS2	Purse seine, free school	2	All	
PSLS1N	Purse seine, associated sets	1N	All	
PSLS1S	Purse seine, associated sets	1S	All	
PSLS2	Purse seine, associated sets	2	All	
BB1N	Baitboat and small-scale encircling gears (PSS, RN)	1N	All	Primarily catch from the Maldives baitboat fishery.
LINE2	Mixed gears (hand-line, gillnet/longline combination)	2	All	Gears grouped on the basis that primarily catch large bigeye.
OT1N	Other (trolling, gillnet, unclassified)	1N	All	
OT2	Other (trolling, gillnet, unclassified)	2	All	

2.4 Catch history

Catch data were compiled based on the fisheries definitions. An update of quarterly catches by fishery was provided by the IOTC Secretariat, including catches from 2019–2021 (2022-WPTT24-DATA14-BET). The time series of catches were very similar to the catch series included in the 2019 assessment except for some minor differences for a few fisheries (Figure 4). There was a small error in the previous assessment where the catches for LL 1N was off by one quarter throughout the time series (Figure 4). Total annual catches for 2019, 2020 and 2021 included in the updated catch history are 80 674, 90 659, 95 022 t respectively (Table 2). The total catch in 2021 is the highest amongst the last five years.

Longline, distant-water (LL 1N, LL1S, LL2, LL3). The longline fishery operates throughout the Indian Ocean although catches are concentrated in the equatorial region (Figure 3). Catches are primarily from the Japanese, Korean and Taiwanese distant-water longline fleets. Most (62%) of the distant-water longline catch has been taken from the western equatorial region and annual catches from the LL1 fishery (LL1S and LL 1N) steadily increased from the early 1950s to reach a peak of 64,000 t in 2003−2004. Catches of about 55,000 t were maintained during 2005−07, declined rapidly to about 15,000 t in 2010−2011, recovered to about 50,000 t in 2012 and then declined to about 14000 t in 2018 (Figure **4**). The catch in 2020 has increased to about 20000 t.

Annual catches from the LL2 fishery fluctuated between about 10,000−15,000 t during 1975−2011. In the subsequent years, catches declined sharply to about 3,000−4,000 t during 2017−2021 (Figure 4).

Annual longline catches from the southern area were comparatively low, averaging about 3,000 t, from 1960 to 1990 (Figure 4). Catches then increased to a peak of 22,000 t in 1995, declined steadily to about 5,000 t in 2007 and remained at that level over subsequent years. However, catches during 2018 – 2021 declined to about 3000 t.

Longline, fresh tuna fleet (FL2). The fishery developed in the late 1980s and annual catches rapidly increased to reach a peak of about 30−35,000 t in the late 1990s–early 2000s, due to increased activity of small longliners fishing tuna to be marketed fresh. Catches declined sharply in 2003 and then again in 2010, as some vessels have moved south to target albacore. Annual catches were about 12,000−15,000 t during 2011−2015 but decline to about 7,000−9,000 t during 2017–2021(Figure **4**).

Purse seine (PSFS1N, PSFS1S, PSFS2, PSLS1N, PSLS1S, PSLS2). Almost all of the industrial purse-seine catch is taken within the western equatorial region (Figure 3) and catches are dominated by the fishery on associated schools (PSLS1N and PSLS1S) (Figure **4**). Annual catches from the PSLS1 (N and S) fisheries reached a peak of about 30,000 t in the late 1990s and have fluctuated at 15−25,000 t over the last decade, with the exception of a lower catch in 2012. Since the late 1990s, annual catches from the purse-seine free-school fishery (PSFS1N and PSFS1S) have fluctuated between 5,000−10,000 mt. While the activities of purse seiners have also been affected by piracy in the Indian Ocean, the decline in catches have not been as marked as for longline fleets (IOTC 2018a, b). Relatively minor catches were taken intermittently by the purse-seine fisheries in the eastern equatorial region.

There was a marked increase of reported catches on the purse seine associated schools in 2018. The WPTT21 considered this magnitude of increase of catches is not credible and is likely to have reflected several changes related to the methodologies to produce catch statistics by EU,Spain in 2018. The WPTT21 identified a methodology to revise the bigeye tuna catches reported by EU,Spain in 2018 (limited to their log-associated school component), which applied the species composition recorded for the log-associated component of EU,Spain purse seine catches in 2017 to the total catches (log-associated) reported in 2018 by the same fleet (IOTC 2019a). The method was subsequently developed further during the WPDCS15 (IOTC 2019b), which applied a spatial-temporal re-estimation procedure, based on several proxying scenarios. The WPTT24(DP) in 2022 agreed to use the proxying scenario number four (as recommended by the WPDCS15) to re-estimate Spanish purse seine catch for the 2022 stock assessment model (IOTC 2022). This approach causes marked reductions in catches of bigeye

tuna reported by the EU purse seine fleet component in 2018 (around 12,000 t). The purse seine associated sets' catch has significantly increased in 2021, with catches from region 1N more than doubling those of the previous year (Table 2).

Baitboat (BB1N). Bigeye catches from the Maldives baitboat fishery are estimated to have increased steadily from a minimal level in the late 1970s to about 6–7,000 t in recent years (Figure **4**). The catch decreased to around 5,000 t in 2018 and increased significantly to around 8,600 t in 2020, but declined to around 7000 t in 2021 (Table 2).

Line (LINE2). The LINE2 fishery includes small scale fisheries using handlines, small longlines and the gillnet/longline combination fishery of Sri Lanka. Annual catches are estimated to have increased steadily from a minimal level in the 1970s to about 10,000 t in recent years (Figure **4**). The catch decreased to around 7000 t in 2018, and increased significantly to around 12,000 in 2020, but declined to around 9800 t in 2021 (Table 2).

Other (OT1N and OT2). The "Other" fisheries include gillnet, trolling and other minor artisanal gears. The fisheries are aggregated by region for the two equatorial areas. Within the western region the OT1 fishery is primarily comprised of the Iranian driftnet fishery operating in the high seas. Total catches were negligible prior to 2005 but subsequently increased to about 2,500 t per annum (Figure **4**). The increase in catches was mainly attributed to major changes to some fleets, including increases in boat size, developments in fishing techniques and fishing grounds (IOTC 2018). For the Other 2 (OT2) fishery, recent catches were primarily taken by the Indonesian troll and gillnet fleets.

Table 2: Recent bigeye tuna catches (mt) by fishery included in the stock assessment model. The annual catches are presented for 2013- 2018.

Fishery	Time period				
	2017	2018	2019	2020	2021
FL2	8 910	7 201	8 172	9 152	8 893
LL1N	3 050	2 488	2 680	5 578	2 653
LL1S	14 002	11 139	13 091	14 328	14 308
LL2	4 354	2 813	3 843	4 155	4 239
LL3	5 008	3 602	2 760	3 107	3 138
PSFS1N	4 376	2 292	2 211	2 117	6 733
PSFS1S	5 807	1 342	5 272	1 969	2 077
PSFS2	65	–	–	–	–
PSLS1N	9 381	13 855	10 601	10 425	21 011
PSLS1S	9 628	9 941	8 166	9 979	6 586
PSLS2	639	5 360	897	60	1 099
BB1	6 961	5 295	6 293	8 678	7 180
LINE2	10 121	7 177	9 009	12 210	9 784
OT1	4 502	5 001	3 519	2 983	1 604
OT2	4 395	3 574	4 160	5 918	5 717
Total	91 199	81 080	80 674	90 659	95 022

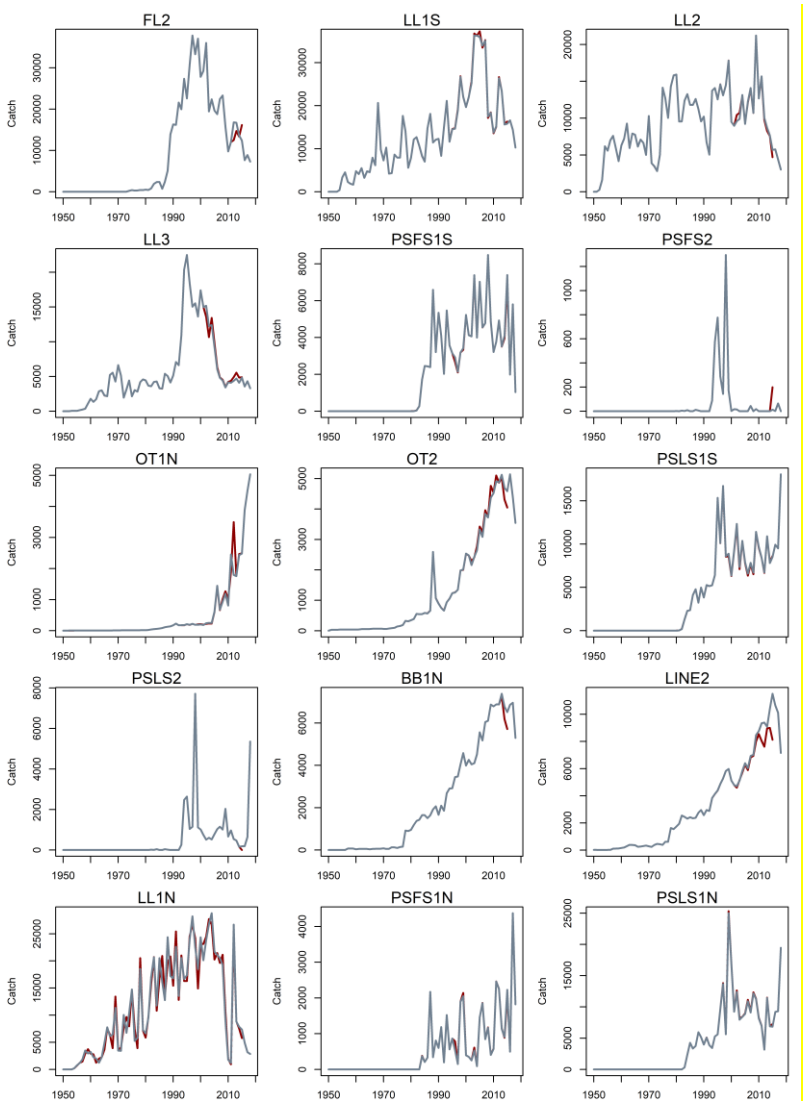

Figure 4: Fishery catches (metric tonnes) aggregated by year. Note the y-axis differs among plots. Red lines are catches used in the 2019 assessment.

2.5 CPUE indices

2.5.1 Longline CPUE

Standardised CPUE indices were derived using generalized linear models (GLM) from longline catch and effort data (agrreated by month and 1° grid resolution) provided by Japan, Korea, Taiwan,China (Kitakado et al. 2022). Cluster analyses of species composition data for each fleet were used to separate datasets into fisheries understood to target different species. Selected clusters were then combined and standardized using generalized linear models. bigeye catch (numbers of fish) was the dependent variable of the positive catch model (lognormal error structure), while the presence/absence of bigeye tuna in the catch was the dependent variable in the binomial model. In addition to the year-quarter, models included covariates for 5° square location, number of hooks, and vessels. The CPUE for regions 1N, 1S, and 2 are based on the lognormal model whereas for region R3 are based on a a delta lognormal (including the binomial model component). The CPUE indices represented the time series of abundance (1979–2021) for each of the four model regions (1N, 1S, 2, and 3).

The earlier assessment used the indices developed from the longer time series (1953–2015) but excluded the years prior to 1979 for a number of reasons: the decline in the indices during the late 1960s–early 1970s is inconsistent with the relatively low level of catch. The 2–3 fold increase in the indices during

1976–1978 was considered to be related to factors other than abundance (Kolody et al 2010, Langley et al 2013b, Langley 2016, Hoyle et al. 2017a).

The standardised quarterly CPUE indices are shown in Figure 5. The CPUE indices from the four regions exhibit broadly comparable trends, declining by about 65–75% from the early 1980s to 2010s. In the western equatorial region, the decline from 1979 to the early 2000s is slightly less in the southern subregion, but steeper in the northern subregion. The indices in both R1N and R1S peaked in 2011 when the main fleets returned to the main fishing ground but declined rapidly to the lowest level in 2018. Both indices, however increased moderately during 2019 – 2021. The very large recent spike in bigeye catch rates in the western tropical Indian Ocean 2011–12 has some similarities to the 1976–78 peak. It is believed to have occurred when vessels returned to the area that had been unfished for several years due to piracy. It may have reflected a major increase in catchability because of changes in population density, fishing effort, and/or fish behaviour (Hoyle et al. 2017a). In the eastern tropical region (R2) there is also a general decline in CPUE after 1980, with an increase in CPUE after 2010 that is much smaller than in the west. The CPUE in R2 exhibited a large fluctuation during 2019 –2021 and is currently also close to the lowest level observed. Since the 1990s, the indices for the temperate area (R3) have generally declined, which is different from the previous index, which was largely stable throughout the same period.

In each region, the annul trend in the index are generally very consistent among all quarters. The CPUE indices from region 3 exhibit considerable seasonal variation, with lower CPUE in the first and fourth quarters (austral summer), and relatively high CPUE in the second and third quarters (austral winter). This seasonality is also somewhat reflected in the longline length samples, with large fish caught in the third quarter and smaller fish in the first and second quarter. Stock Synthesis does not have the flexibility to estimate seasonal catchability or movement dynamics when the model is configured based on a quarterly time step. Consequently, to account for the seasonal variation in the CPUE indices, the Region 3 CPUE indices were incorporated in the model as four separate sets of abundance indices (i.e. one series for each quarter).

For the regional longline fisheries, a common catchability coefficient was estimated in the assessment model, thereby, linking the respective CPUE indices among regions. This significantly increases the power of the model to estimate the relative (and absolute) level of biomass among regions. However, as CPUE indices are essentially density estimates it is necessary to scale the CPUE indices to account for the relative abundance of the stock among regions. The approach used was to determine regional scaling factors that incorporated both the size of the region and the relative catch rate to estimate the relative level of exploitable longline biomass among regions (Hoyle & Langley 2018). The relative scaling factors are R1N 0.63, R1S 0.80, R2 1.00, R3 0.6 (see method ‘8’ of Hoyle & Langley 2018) For each of the principal longline fisheries, the standardised CPUE index was normalised to the mean of the period for which the region scaling factors were derived (i.e. the GLM index from 1979–1994). The normalised GLM index was then scaled by the respective regional scaling factor to account for the regional differences in the relative level of exploitable longline biomass among regions.

2.5.2 Purse seine CPUE

The European and associated flags purse seine fishing activities in the Indian Ocean during 1981–2021 have been monitored through the collection of logbooks and observer sampling. Standardised indices of the biomass of bigeye tuna caught by European purse seiners from sets on associated tuna schools (2010 – 2021) were developed by Akia al (2022). The standardisation was based on the application of the VAST methodology which considered a comprehensive list of candidate covariates, including the effect of the technological improvement related to the use of echosounder buoys. This index is assumed to represent the juvenile part of the population vulnerable to the purse seine fishery in Region 1S.

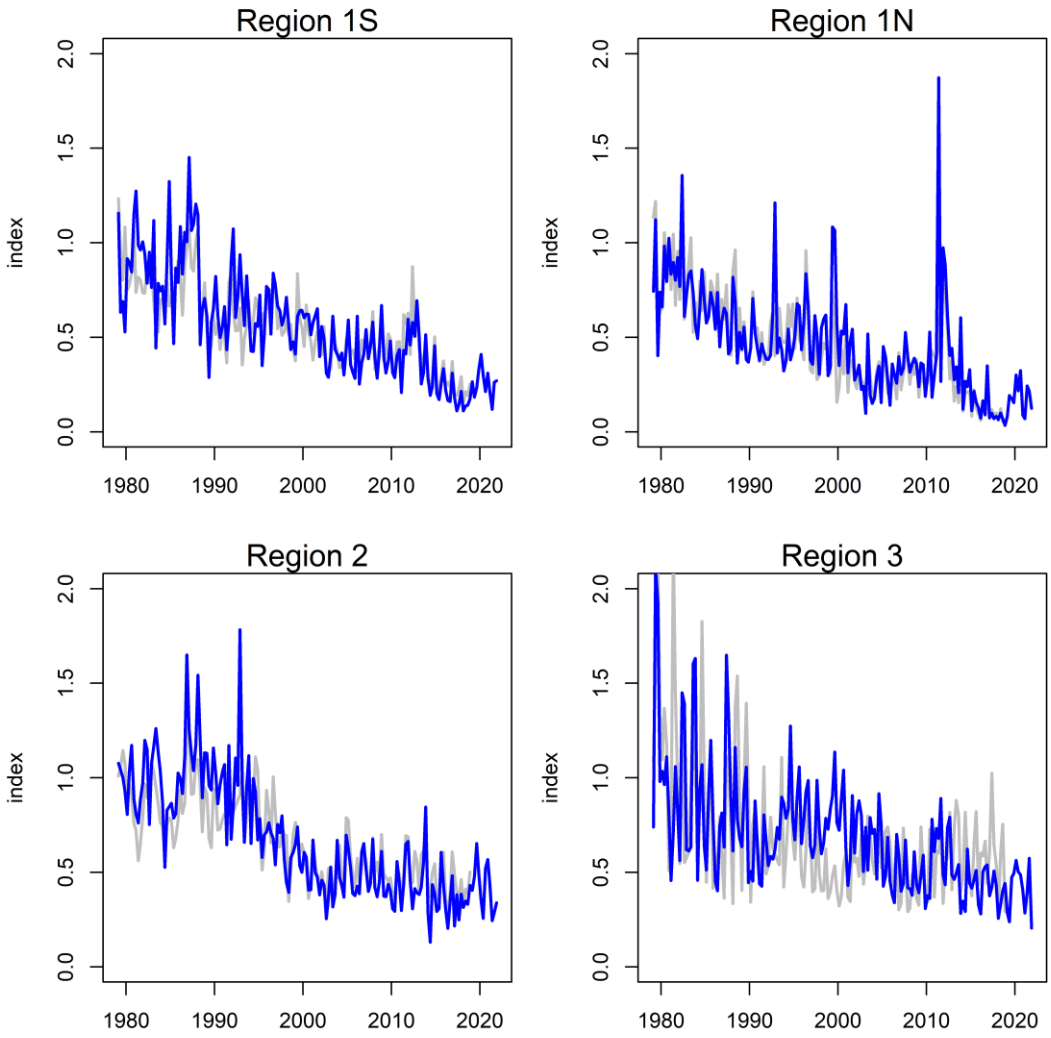

Figure 5: A comparison of the longline CPUE indices included in the 2019 stock assessment (grey line) and the 2021 stock assessment (blue line). The 2019 indices are rescaled to have the same mean of the 2021 indices for each region.

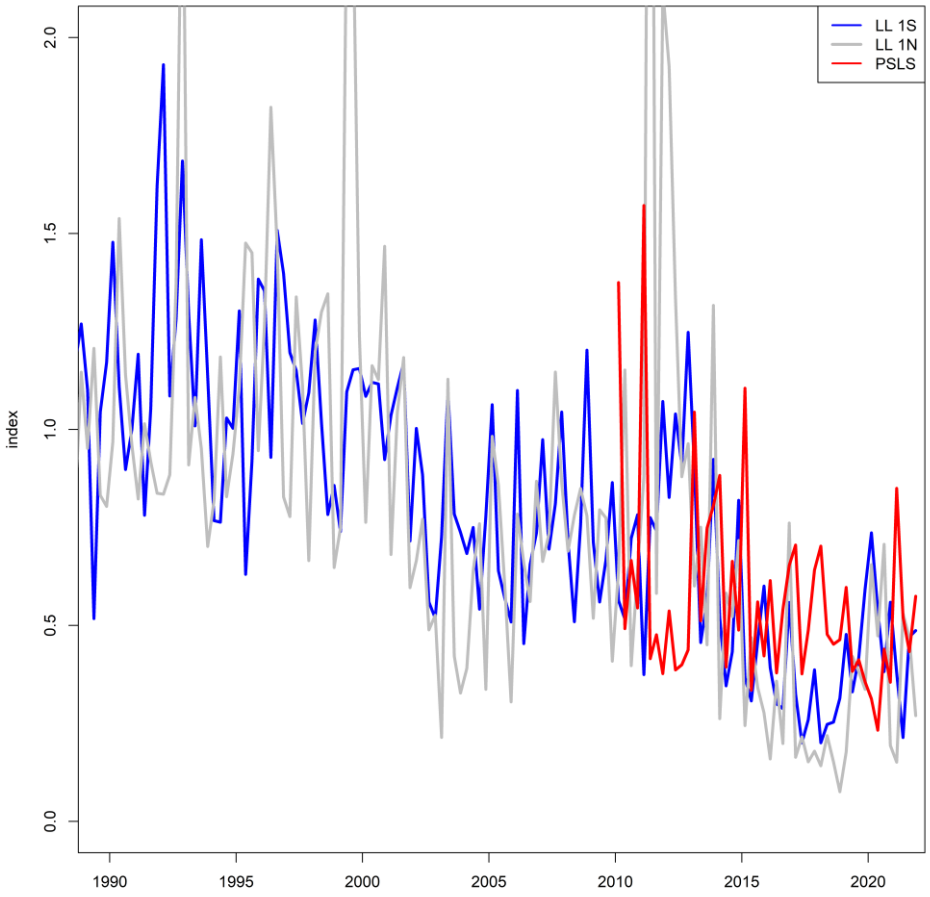

Figure 6: Other CPUE indices for yellowfin tuna: Index from the purse seine associated sets on juvenile 2010–2021. Longline CPUE indices in region 1 are included for comparison.

2.6 Length frequency data

Available length-frequency data for each of the defined fisheries were compiled into 95 2-cm size classes (10–12 cm to 198–200 cm) and were aggregated to provide a composite length composition for each year/quarter. Each length frequency observation for purse seine fisheries represents the number of fish sampled raised to the sampling units (sets in the fish compartment) while for fisheries other than purse seine each observation consisted of the actual number of bigeye tuna measured. Each aggregated length sample was assigned an initial sample size. The sample size was determined based on the number of fish included in the aggregated sample, up to a maximum of 1000. The sample size was then divided by 100 resulting in a maximum initial sample size of 10. Purse seine length samples were also assigned an initial sample size of 10. A graphical representation of the availability of length samples is provided in Figure 7.

Longline, distant-water (LL1N, 1S, 2, 3). Size frequency data are available for the LL1–3 fisheries from 1965 to 2021. Prior to 1995, the length compositions were dominated by sampling from the Japanese longline fleet, while in the subsequent period the size data were increasingly dominated by data collected from the Taiwanese distant-water longline fleet. In recent years, length frequency data were also collected from locally based longline fleets (e.g., Seychelles).

Length and weight data were collected from sampling aboard Japanese commercial, research and training vessels. Weight frequency data collected from the fleet have been converted to length frequency data via a processed weight-whole weight conversion factor and a weight-length key. While in recent years most of the samples available have come from scientific observers on commercial vessels, in the

past samples came from training and research vessels, and commercial vessels. Matsumoto (2016) suggested that length distribution was similar between sampling sources (commercial and non-commercial vessels) or platform (fishermen, scientists, observers) in the Indian Ocean. Length frequency data from the Taiwanese longline fleet are also available from 1980−2021. Length samples from this component come from commercial vessels and include lengths recorded by fishermen and, to a lesser extent, lengths measured by scientific observers on some of those vessels.

Previous assessments of IO bigeye tuna have highlighted the temporal variability in the length composition data from the main longline fisheries. Langley (2016) examined the longline length data to investigate potential sources of variation in fish length. For the LL 1 area, there were marked differences in the sizes of fish sampled from the various longline fleets during the late 1980s and early 2000s. There were also divergent temporal trends in the lengths of fish sampled amongst the fleets (see Figure A1 of Langley 2016). A similar trend is also apparent in the length composition data from the eastern equatorial region. Langley (2016) restricted the length data were restricted to the main area of catch from the bigeye tuna longline fishery (core area) for each model region to minimise potential variation in length composition attributable to the collection of length samples from the periphery of the fishery.

The lengths of fish sampled from the Taiwanese fleet increased markedly during the early 2000s and the length compositions of the samples from catches of most fleets were comprised of larger fish during 2005–2015 (see Figure A1 Appendix 1 of Langley 2016). The increase in Taiwanese fish sizes during the period coincided with a large shift in the ratio of the Taiwanese bigeye and yellowfin longline catches in the region during the same period; the ratio of bigeye in the longline catch increased during the late 2000s and remained at a higher level in the subsequent years (Hoyle et al 2015, see Figure 20). A review of the recent Taiwanese length composition data by Geehan & Hoyle (2013) recommended *excluding from stock assessments the size data for BET, YFT and ALB from the Taiwanese DWLL fleet after the early-2000s, until the cause of changes in the size frequency data have been determined by the WPTT*". A more recent review shows that the sampling behaviour of Taiwanese and Seychelles fleets (mostly reflagged Taiwanese vessels) have changed over time, with patterns in the logbook length data inconsistent with other fleet (Hoyle et al. 2021), and as such the WPTT23 (DP) recommended omitting all Taiwanese and Seychelles logbook length data from the current assessment (IOTC 2021). However, the length data collected by the scientific observers in the period 2005–2021 were included in the assessment.

For the final data sets, the length compositions of the LL1N, 1S, 2, and 3 fisheries are dominated by fish in the 90−150 cm length range (Figure 8). The average lengths of fish in the sampled catch fluctuated over the study period, with regions 2 and 3 having smaller average sizes than regions 1N and 1S, particularly in the early years (Figure 9**Error! Reference source not found.**).

Longline, fresh tuna fleet (FL2). Length and weight data were collected during the unloading of catches at several ports, primarily from fresh-tuna longline vessels flagged in Indonesia and Taiwan/China (IOTC-OFCF sampling). Length data from 1998−2008 were included in the previous assessment. But most samples were subsequently found to be biased (F. Fiorellato per. comm., IOTC Secretariat). For the current assessment, only ten years of data are included (2012–2021).

The composite length composition of the catch is similar to the distant water longline fleet (Figure 8) and remained relatively stable over the sampling period except in 2012 when there are larger fish in the samples (Figure 9**Error! Reference source not found.**).

Purse seine (PSFS1, PSFS2, PSLS1, PSLS2). Length-frequency samples from purse seiners have been collected from a variety of port sampling programmes since the mid-1980s. The samples are comprised of large numbers of individual fish measurements and represent comprehensive sampling of the main period of the fishery (

Figure 7). Limited size data are available from the purse-seine fisheries within region 2.

The associated purse-seine fishery (PSLS) primarily catches smaller bigeye tuna, while the size composition of the catch from the free-school fishery is bimodal, being comprised of the smaller size

range of bigeye and a broad mode of larger fish (Figure 8). There was a general decline in the average length of fish caught by the PSLS1 fishery from 1990 to 2018 (Figure 9**Error! Reference source not found.**). The average size of fish sampled from the free-school fishery was variable among quarters, although fish tended to have increased through the 1990s and the early 2000s (Figure 9**Error! Reference source not found.**). It is unknown whether the trends in the length composition of the purse seine catch are representative of the population or reflect changes in the operation of the fishery.

Baitboat (BB1N). Limited length samples are available from the fishery (Figure 7

Figure 7) and the sampled catch was dominated by fish in the smaller length classes (50−70 cm) (Figure 8 and Figure 9**Error! Reference source not found.**). It has been suggested that these samples are not adequate to be used for the assessment.

Line (LINE2). Negligible length frequency data are available from the fishery although the available data indicate that the catch was predominantly composed of larger fish (Figure 8). Fish sampled from this fishery are generally larger than the fish sampled from the other main longline fisheries. In 2020–21 and 2021, the Indonesia Line fishery sampled a considerable number of small fish (around 50 cm). It is not known how well these small fish are representative of this fishery therefore these samples are not included in the current assessment.

Other (OT1N and OT2). While catches from the OT1 fishery are dominated by the Iranian driftnet fleet, there are no length samples available from this component of the fishery. Instead, the available OT1 length samples were collected from the 'other' fisheries that operated prior to 2005 (Figure 7). The aggregate length samples encompass a broad length range (Figure 8).

For the Other 2 (OT2) fishery, limited length samples were collected from the Indonesian small purse seine and troll fisheries. The aggregate length frequency data available include two size modes from the small-scale purse seine samples (Figure 8). This is probably due to different sizes of fish taken by different modes of fishing (e.g., fishing at night with light, around anchored FADs, etc.).

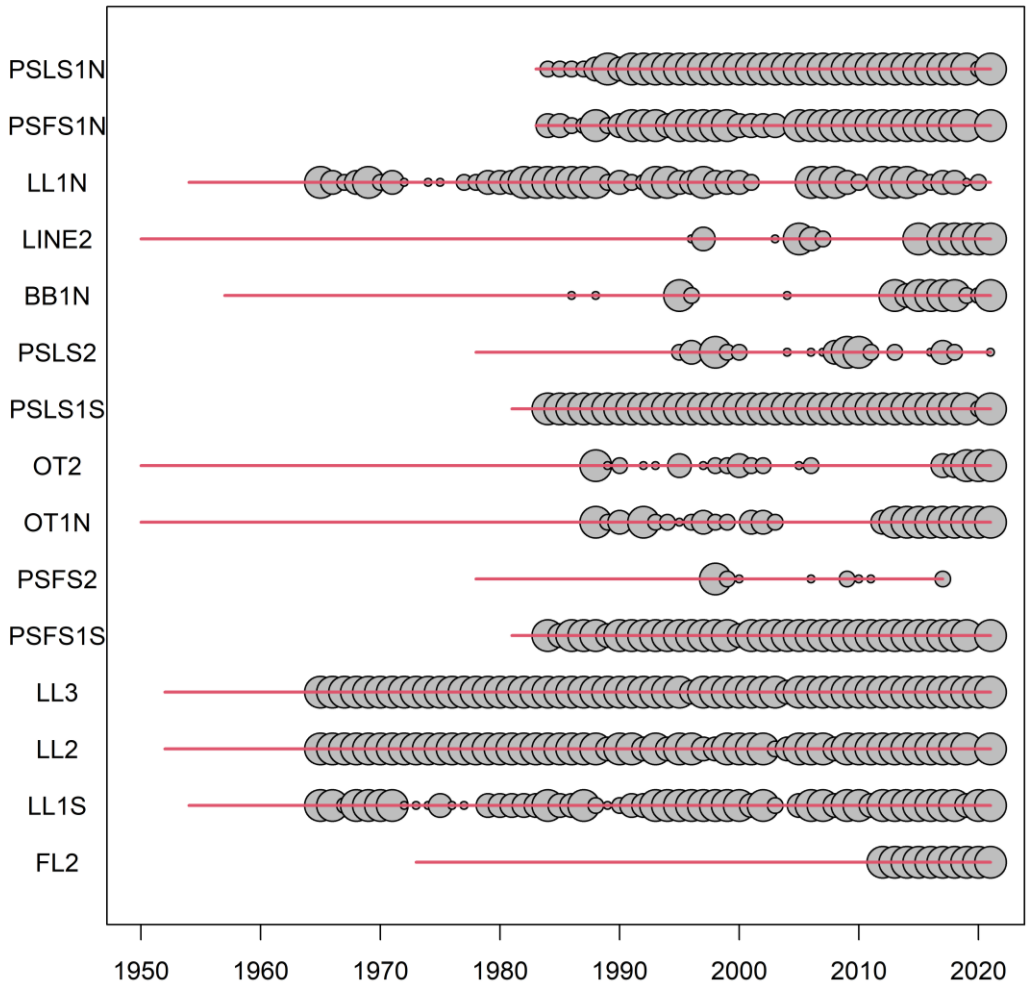

Figure 7: The availability of length sampling data from each fishery by year. The grey circles denote the presence of samples in a specific year (the size indicate number of quarters being sampled). The red horizontal lines indicate the time period over which each fishery operated.

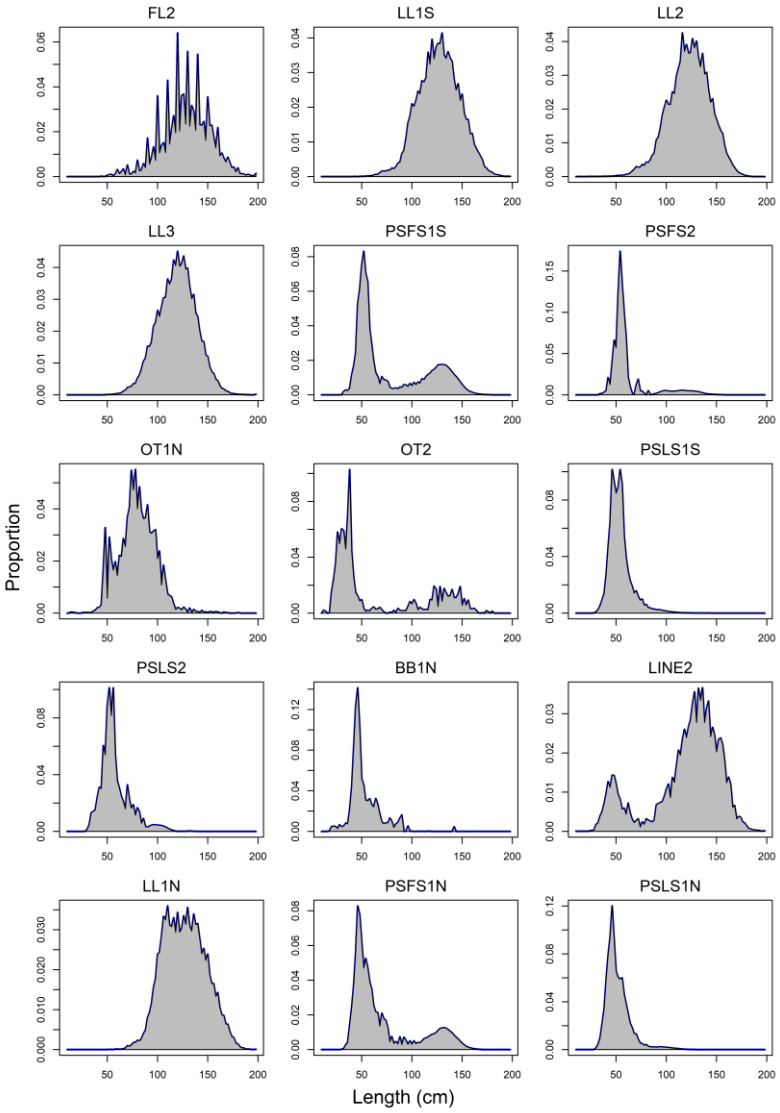

Figure 8: Length compositions of bigeye tuna samples aggregated by fishery.

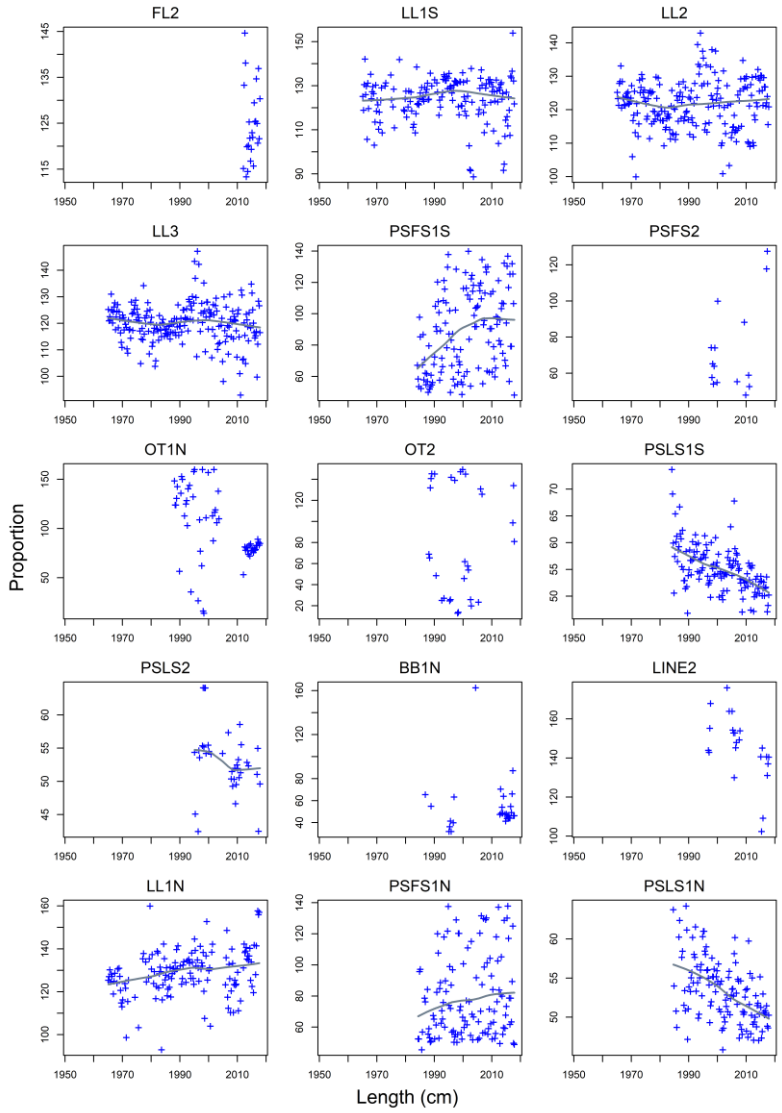

Figure 9: Mean length (fork length, cm) of bigeye sampled from the principal fisheries by year quarter. The grey line represents the fit of a loess smoother to the dataset.

2.7 Tagging data

A considerable amount of tagging data was available for inclusion in the assessment model. The data used consisted of bigeye tuna tag releases and returns from the Regional Tuna Tagging Project-Indian Ocean (RTTP-IO) phase of the Indian Ocean Tuna Tagging Programme (IOTTP). Tags were released during 2005–2007 and recoveries were monitored by the IOTTP during 2005–2009 and by the IOTC in the subsequent years.

A total of 34,478 bigeye tuna were released by the RTTP-IO program (removed tagged fish with unknown length). All the bigeye tag releases of the RTTP-IO occurred in a localized area off the Tanzania coast within the western equatorial region (region 1S) (Figure 10). Most of the releases occurred during the second and third quarters of 2006 and the third quarter of 2007 (Figure 11).

In total, 5674 tag recoveries (removed tags with unknown recovery dates) could be assigned to the fisheries included in the model. A relatively high proportion of tag recoveries occurred in the vicinity of the main release location (Figure 10). There was also a relatively large number of tags recovered from bigeye tuna catches from the Mozambique Channel. Overall, most of the tags were recovered in the home region, some recoveries occurred in adjacent regions, particularly region 1N. A very small

number of tags were recovered in regions 2 and 3 (less than 1%) (Table 3).

Most of the tag recoveries occurred between mid-2006 and 2008 (Figure 12). The number of tag recoveries started to attenuate in 2009 although small numbers of tags were recovered up to the end of 2015. Most of the recaptures near main release locations were from purse seine associated sets during 2007 and were comprised of tagged fish at liberty for 6–12 months. Recoveries from the purse seine fishery for fish at liberty for at least 12 months were more evenly distributed over the main area fished by the purse seine fleet.

A significant proportion of the tag returns from purse seiners were not accompanied by information concerning the set type. These tag recoveries were assigned to either the free-school or FAD fishery based on the assumed age of the fish at the time of recapture; i.e. based on the age assigned to the release group and the period at liberty. Fish "older" than 12 quarters were assumed to be recaptured by the free-school fishery; "younger" fish were assumed to be recovered by the FAD set fishery.

Langley (2016) identified considerable differences in the recovery rate (number of tags per tonne of catch) from the PSLS fishery amongst latitudinal zones for tags at liberty for at least 12 months (Tag recovery rates from south of 2°S were consistently higher than from north of 2°S during the main recovery period). The difference in tag recovery rates between the two main areas of the fishery indicates that the dispersal of tagged bigeye during the 12 month "mixing period" was insufficient to redistribute tagged fish throughout the bigeye population resident within the western equatorial region (Region 1). Consequently, the distribution of PSLS fishery effort (and catch) would have strongly influenced the number of tags recovered from the fishery. Following Langley (2016), the western equatorial region has been partitioned into two regions (Region 1N and Region 1S) in the assessment model account for the potential incomplete mixing of tagged fish.

For incorporation into the assessment model, tag releases were stratified by release region, time period of release (quarter) and age class. The returns from each tag release group were classified by recapture fishery and recapture time period (quarter). The tag data were further adjusted for tag losses and reporting rates to minimize the bias on estimates of fishing mortality and abundance in the assessment model. The procedure is described in below.

Age assignment of tag release. For the current assessment, the age at release was converted based on the mean growth function. In the previous assessment, the use of an age-length key approach that admits the uncertainty in the size distribution at age had been explored.

Tagging mortality. The number of tags in each release group was reduced by 30% to account for initial tag mortality. The initial tag mortality estimates of 20.5% was increased by a further 10% to account for an assumed level of tag mortality associated with the best (base) tagger (Hoyle *et al* 2015)**.**

Reporting rate. The results of the tag seeding experiments conducted during 2005–2008, have revealed considerable temporal variability in tag reporting rates from the IO purse-seine fishery (Hillary *et al.* 2008a). Reporting rates were lower in 2005 (57%) compared to 2006 and 2007 (89% and 94%). Quarterly estimates were also available and were similar in magnitude (Hillary *et al.* 2008b). This large increase over time was the result of the development of publicity campaign and tag recovery scheme raising the awareness of the stakeholders, *i.e.* stevedores and crew. SS3 assumes a constant fishery-specific reporting rate. To account for the temporal change in reporting rate, the number of tag returns from the purse-seine fishery in each stratum (tag group, year/quarter, and length class) were corrected using the respective estimate of the annual reporting rate (Langley 2016).

The approach to correct the number of tag returns for the reporting rate follows Kolody (2011), Fu (2017), and Fu et al. (2018): tags recovered at-sea are assumed to have a 100% reporting rate; tags recovered from landings in Seychelles were corrected for the quarterly estimates of reporting rates from Hillary *et al* (2008b). The tag recoveries were further increased by the proportions of EU PS catches landed outside the Seychelles, to account for purse-seine catches that were not examined for tags. For example, the adjusted number of observed recaptures for a PSLS fishery as input to the model, R'_L was calculated using the following equation:

$$R'_L = R_L^{sea} + \frac{R_L^{sez}}{P^{sez} r^{sez}}$$

where

R_L^{sea} = the number of observed recaptures recovered at sea for the PSLS fishery.
R_L^{sez} = the number of observed recaptures recovered in Seychelles for the PSLS fishery.
r^{sez} = the reporting rates for PS tags removed from the Seychelles
P^{sez} = the scaling factor to account for the EU PS recaptures not landed in the Seychelles.

The adjusted number of observed recaptures for a PSFS fishery was calculated similarly. A reporting rate of 94% was assumed for the correction of the 2009−2015 tag recoveries. The numbers of tag recoveries were also adjusted for long-term tag loss (tag shedding) based on an analysis by Gaertner and Hallier (2015). Tag shedding rates for bigeye tuna were estimated to be approximately 1.7% per annum.

A total of 34 427 releases were classified into 68 tag release groups. Most of the tag releases were in the 5−12 quarter age classes (Figure 11) A total of 5,666 actual tag recoveries were included in the tagging data set. The cumulative effect of processing the tag recovery data increased the number of recoveries to 6,788 tags.

Table 3: Tag recoveries by year of recovery (box), region of release (number released in bracket), and region of recovery. Region of recovery is defined by the definitions of the fisheries included in the model.

Recovery year	Release region		Recovery region		
		1S	1N	2	3
2005	1S (1 375)	6	5		
2006	1S (19 042)	478	256	4	1
2007	1S (14 061)	2 407	613		3
2008		1 191	160		9
2009		178	18	3	13
2010		107	8	2	15
2011		36	17	2	15
2012		72	14		5
2013		13			1
2014		11			
2015		10			1

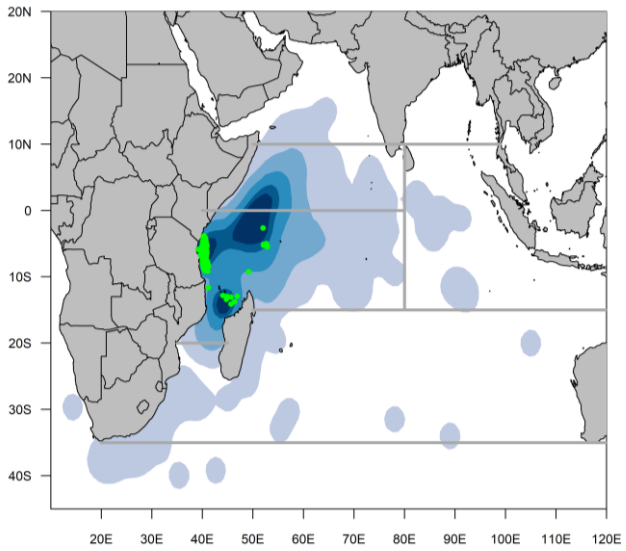

Figure 10: Location of releases (green) and density of recoveries for the bigeye tuna RTTO-IO tag Program

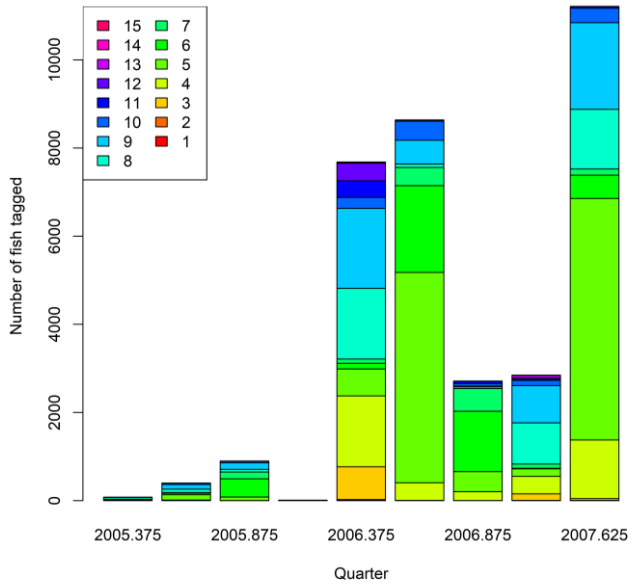

Figure 11 : Number of tag releases quarter and age class included in the assessment data set. Al tag releases occurred in region 1S. Ages were assigned based on the length.

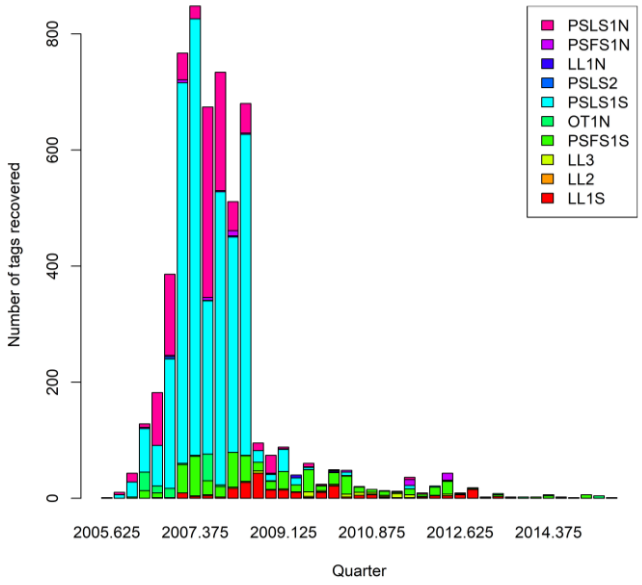

Figure 12: Bigeye tag recoveries by year/quarter and fishery included in the assessment model. Purse seine tag recoveries have not been corrected for reporting rate.

3. MODEL STRUCTURAL AND ASSUMPTIONS

3.1 Population dynamics

The model population structure is comprised of 41 quarterly age classes; the first age class represents fish aged 0–3 months (age 0) and the last age class accumulates all fish age 40+ quarters. The population is aggregated by sex and partitioned by region.

The model commences in 1975 and extends to the end of 2021 in quarterly intervals (188 time steps). The initial (1975) age structure of the population was assumed to be in an exploited, equilibrium state. The four main LL fisheries were operating prior to 1975 and initial fishing mortality parameters were estimated for each of these fisheries, based on early catches and size structure in the commercial catches in the early years. The resulting fishing mortality rates are applied to determine the initial numbers-at-age in each model region.

3.1.1 Recruitment

Recruitment of 0 age fish occurs in each quarterly time step of the model. Recruitment was estimated as deviates from the BH stock recruitment relationship (SRR). The recruitment deviates were estimated for the period that corresponds to the operation of the PSLS fishery which provides catch and length data for the smaller fish and, hence, may be informative regarding the variation in recruitment (for 1985–2020 (144 deviates).). Recruitment deviates were assumed to have a standard deviation (σ_R) of 0.6. The final model options included three (fixed) values of steepness of the BH SRR (h 0.7, 0.8 and 0.9). These values are considered to encompass the plausible range of steepness values for tuna species such as bigeye tuna and are routinely adopted in tuna assessments conducted by other tuna RFMOs (Harley 2011, ISSF 2011).

The recruitment for bigeye remains uncertain as the areas where larvae and early juveniles are concentrated have never been sampled nor studied by scientists (Fonteneau 2004). While the temperate regions are generally believed to be feeding grounds, recruitment is assumed to occur in all regions (hence differentiating between recruitment into the population, vs. spawning.) The overall proportional distribution of recruitment among the four regions was estimated. There is little information to indicate that there are significant differences in the pattern of recruitment between the regions; i.e. the CPUE

trends are broadly comparable between the equatorial regions and the length composition data from the longline fisheries do not appear to be informative regarding recruitment. Length composition data from the small fish fisheries are available from the western equatorial regions only. The relative distribution of recruitment between the four regions (1N, 1S, 2, 3) was initially assumed to be temporally invariant. However, regional recruitment distribution was allowed to vary for 2001–2019 in the basic model, to account for as the divergent regional CPUE trends in more recent years.

A full log-bias adjustment factor ($-\frac{1}{2}\sigma^2$) is applied to the recruitment deviates (as recruitment variability is assumed to be lognormally distributed, see Methot et al. 2013). Potential underestimation of recruitment variability due to uninformative data implies further bias correction may help ensure that the population scaling parameter R0 represent the long-term average recruitment. The optimal bias correction ($-\frac{1}{2}b\sigma^2, b \leq 1$) can be determined from the relationship between the assumed and estimated recruitment variability (Methot and Taylor 2011). With this approach, bias correction was applied to recruitment deviations in the period that is sufficiently informative about the full range of recruitment variability.

3.1.2 Growth and Maturation

Eveson *et al* (2012) derived estimates of Indian Ocean bigeye tuna growth from otolith age data and tag release/recovery. Growth estimates are available for both sexes combined (an updated analysis by Eveson *et al* (2015) estimated very similar growth parameters for males and females). The quarterly growth deviates from a von Bertalanffy growth function with considerably lower growth for quarterly age classes 4–8 (Figure 13–left). Maximum average length (L_∞) was estimated by Eveson *et al* (2012) at 150.9 cm (fork length). The growth model was unable to reliably estimate the standard deviation of length-at-age; however, the most appropriate level of variation in length for all age classes was considered to be represented by a coefficient of variation of 0.10 (P. Eveson, pers. comm.). The growth function was implemented in SS using age-specific deviates on the *k* growth parameter.

Farley et al. (2021) estimated age and growth using otoliths collected in the Indian Ocean as part of the 'GERUNDIO' project, based a new method developed to estimate the age and growth of bigeye tuna from counts of daily and annual growth zones in otoliths. The preliminary age validation work using otoliths and data from the IOTTP provides evidence that the otolith ageing method used in this study is accurate. The two-stage, VB-LogK growth curve is quite different from the integrated VB-logK curves of Eveson et al. (2012) (Figure 13–left). The new estimates represent a size-at-age that is significantly larger, with a much higher mean asymptotic length (L^∞=168 cm FL). Both growth estimates were examined in the current assessment.

The size of sexual maturity was equivalent to that applied by Shono et al (2009) and used in the subsequent assessments. Female fish were assumed to attain sexual maturity from 100 cm (F.L.) with full sexual maturity at about 125 cm (Figure 13–right). Zudaire et. al (2022) estimated reproductive parameters for bigeye tuna in the Indian Ocean as part of the 'GERUNDIO' project. The shape of the preliminary maturity ogive obtained is very different to the ogive currently used in the stock assessment, although the estimates of length at 50% maturity are similar (112.7 cm versus 110.9 cm FL). The proportion mature at length does not reach 100% as expected in the larger length classes and requires further investigation.

The length-weight relationship are based on estimates by Chassot et al. (2016) ($a=2.217 \times 10^{-5}$, b= 3.01211).

.

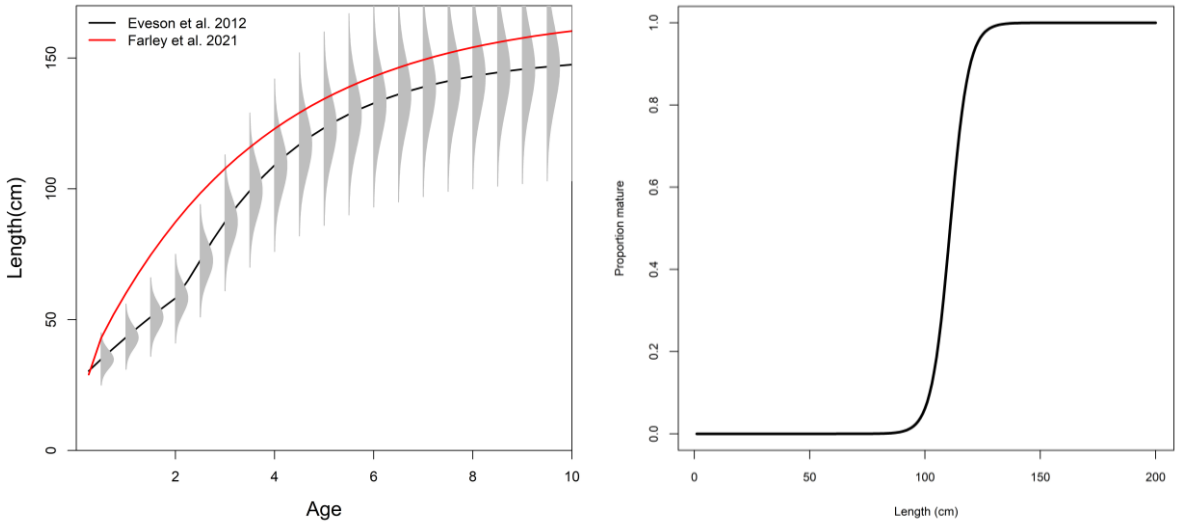

Figure 13: Fixed growth function for bigeye tuna by Eveson et al. 2012 and by Farley et al. 2021 (left), and length-based maturity Ogive following Shono et al (2009). For growth function of Eveson et al. 2012, the shaded distributions represent the assumed variability of mean size-at-age in the assessment .

3.1.3 Natural mortality

In the previous assessment, two alternative levels of age-specific natural mortality were considered in the assessment. The higher level of natural mortality is comparable to IATTC and WCPFC bigeye tuna stock assessments with relatively high natural mortality for the younger age classes and natural mortality of about 0.1 per quarter for the adult age classes (IOTC_2019_hi, see Figure 14). A lower level of natural mortality was proposed based on a Lorenz curve analysis with a lower natural mortality for the adult age classes (0.0625 per quarter) (IOTC_2019, Figure 14). This is comparable to the level of natural mortality assumed for Atlantic bigeye tuna in the recent ICCAT stock assessment by (ICCAT 2015). This relationship between M and age/size (high M for juveniles and low M for adults) are well established for tuna (Hampton 2000) and corresponds well with some of the biological factors contributing to the variability of natural mortality of tuna (Fonteneau & Pallares 2004).

From the RTTP, a considerable number of tagged fish were captured after 7–8 years at liberty, indicating a considerable proportion of the tagged fish had reached an age of 8–10 years; 8 tags were recovered after 10 years at liberty and a few tags were recovered during the most recent year (2015), corresponding to an age at recovery of 11–12 years. The higher level of natural mortality would result in a very small proportion of the tagged fish reaching 12 years of age, suggesting that the lower level of natural mortality may be more plausible. The lower level of M is also supported by the aging study of bigeye tuna in the eastern and western Australia water which suggested the longevity of bigeye is more than the 8–10 years which were the maximum age commonly thought (Farley et al. 2004).

Hoyle (2022) reviewed approaches for estimating natural mortality for bigeye tuna and proposed an approach to provide estimates of age dependent natural mortality. The approach involves determining a target level of M based on the maximum observed age, and the relative M at age based on the Lorenz curve analysis. The two components are then combined using the approach of Porch (2011) which rescale the Lorenzen curve so that the average mortality rate matches a target value over the relevant life history period. Using this approach, Hoyle (2022) provided four alternative values of target M based two alterative maximum observed ages for bigeye tuna (14.7 years in the Indian Ocean or 17 years in the Atlantic Ocean), and two empirical methods to predict M (Then et al. (2015) or Hamel and Cope in review) (Figure 14). These alterative M estimates are examined in the current assessment.

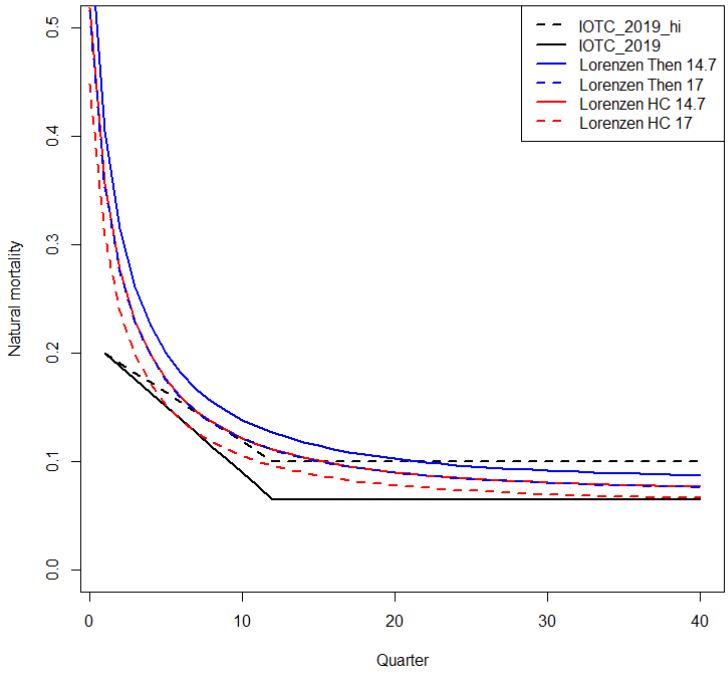

Figure 14: Age specific natural mortality (per quarter) patterns assumed for the IOTC_2019_hi and IOTC_2019 assessment model options, and four additional age dependent natural mortality proposed by Hoyle 2022.

3.1.4 Movement

In Stock Synthesis, movement is implemented as the proportional redistribution of fish amongst regions, including the proportion remaining in the home region. The redistribution of fish occurs instantaneously at the end of each model time step (quarter).

Movement of fish was estimated amongst the four model regions. Movement was parameterised to estimate differential movement from young (8 quarters) to old (≥15 quarters) fish to approximate potential changes in movement dynamics associated with maturation. For each movement transition, two separate movement parameters were estimated (for young and older fish). A linear interpolation between the age specific movement rates was applied to determine movement of the intermediate age classes. Fish younger than age 3 quarters were assumed to remain within the natal region. Movement rates were assumed to be temporally invariant.

3.2 Fishery dynamics

Age based selectivity were assumed for all fisheries. Selectivity is more likely to be a length-based process for most gears. However, as the model has adopted a quarterly resolution, the age selectivity is considered adequate in approximating the length-based process. Separate selectivity functions were estimated for each of the four main longline fisheries where a logistic function was used for LL1N and 1S fisheries, and a double normal function was used for the LL2 and 3 fisheries. A logistic selectivity was assumed for the FL2 longline fishery.

The selectivities of the PSLS fisheries were estimated using a double normal functional form. Separate selectivity functions were estimated for the PSLS1N and PSLS1S fisheries. For the PSLS1N and PSLS1S fisheries, there was a marked shift in the length composition of the fishery catch in the mid-2000s. the modelling option of accounting for the apparent change in the selectivity of the PSLS1 fishery was explored by incorporating a random walk on the estimation of the selectivity parameters

related to the age of the peak selectivity and the width of the ascending limb of the selectivity. The temporal shift in selectivity was not included in the final model options.

To account for the bimodal length composition of the catch from the PSFS fishery, the selectivity was modelled using a cubic spline with 6 nodes. The selectivity of the PSFS1N and PSFS1S fisheries was assumed to be equivalent.

Limited data were available to estimate the selectivity of either the PSLS2 or PSFS2 fisheries. The selectivity of these fisheries was constrained to be equivalent to the corresponding fishery selectivity in the western equatorial region 1S.

Limited size data are available from the "Other" fisheries. During the previous assessment, attempts to estimate independent selectivities for these fisheries were not successful, partly due to the variability in the length composition between samples. In aggregate, the length compositions are bimodal and similar to the length composition from the PSFS fishery. On that basis, the selectivities for the two "Other" fisheries (OT1N and OT2) were assumed to be equivalent to the PSFS fishery. Similarly, limited length data are available for the LINE2 fishery, and the selectivity was assumed to be equivalent to the main longline fishery. Further it has been suggested the length samples from the "baitboat" fishery (mostly from Maldives pole and line fishery) are of very poor quantities (Fabio Fiorellato, per. comm.), therefore the selectivity of this fishery was assumed to be equivalent to the PSLS 1S fishery.

Fishing mortality was modelled using the hybrid method that estimates the harvest rate using Pope's approximation and then converts it to an approximation of the corresponding *F* (Methot & Wetzel 2013).

3.3 Dynamics of tagged fish

3.3.1 Tag mixing

In general, the population dynamics of the tagged and untagged populations are governed by the same model structures and parameters. The tagged populations (tag groups) are monitored over time intervals following release. The predicted number of tags in each region and subsequent time intervals are derived based on the movement parameters, natural mortality and fishing mortality. For each time interval, the number of tags recovered by a specific fishery is predicted based the modelled number of tags in each age class in the region, the selectivity of the fishery and the fishing mortality of the specific fleet (fishery). The predicted number of tag recoveries is also moderated by the fishery specific reporting rate.

The assessment framework assumes that the probability of capturing a tagged fish is equivalent to the probability of catching an untagged fish. Violation of the assumption of homogeneous mixing of tagged fish at the relevant spatial scale (i.e. region) is likely to introduce a bias in the estimation of fish abundance. In Stock Synthesis, a mixing period is specified which partitions the tag data sets (by release group); tag recoveries (observed and predicted) from the mixing period are excluded from the tag likelihood and therefore do not influence the estimation procedure.

For bigeye tuna, almost all tags were released from a localised area of region 1S. The tagged bigeye were predominantly aged 4−8 quarters at release, while the selectivity of the PSLS1S is estimated to be 4−11 quarters. Consequently, there is likely to be a limited time period (4−8 quarters) during which most of the tagged fish would be available to the PSLS fishery. Thus, a mixing period of four quarters was chosen on the basis that sufficient numbers of tagged fish remained available to the PSLS fishery during the post mixing period, albeit for a relatively limited period.

An analysis of the spatial distribution of the tag recoveries from the purse-seine fishery (see Appendix A of Fu 2019) suggested that the four quarter mixing period may be sufficient to allow for a reasonable degree of mixing of tagged fish within the south-western equatorial region (Region 1S). The dispersal

of tags into the north-western equatorial region (Region 1N) will be mediated by the estimated movement rates (from Region 1S), however, the distribution of tagged fish in this region is unlikely to be homogeneous and it is likely that tag densities would be higher in the southern area of Region 1N (i.e. closer to the release location). Consequently, tag recoveries from the region may be influenced by the spatial distribution of the catch from the fishery.

Specifying a mixing period of 12 months (4 quarters) in the stock assessment model will effectively exclude 76% of all the FAD tag recoveries, while retaining 69% of the free-school recoveries (reducing the total tag recoveries by 66%). This effectively reduces the potential bias introduced by the FAD tag recoveries while maintaining most of the free-school tag recoveries. The remaining FAD tag recoveries are predominantly comprised of fish larger than 80 cm and, arguably, these larger fish are likely to be more evenly distributed that the smaller size category.

3.3.2 Tag Reporting

The observed number of tag recoveries for the purse seine fisheries were already adjusted to account for the differential tag reporting rates. On that basis, the reporting rates for the purse seine fisheries were fixed at 1.0. The model also incorporates the tag recoveries from the other fisheries, most notably the LL fisheries. There are no external estimates of tag reporting rates available for the longline fishery and, hence, the fishery specific reporting rates were estimated based on uninformative priors and were assumed to be temporally invariant. Tag recoveries from the longline fishery will be considerably less informative about stock abundance.

The tag mixing process is highly variable in time and space and is likely to vary by release group. Different release groups may experience different levels of tag loss and/or reporting due to tagger effects. Recent development in tag modelling has suggested the modelling of tags conditioned on the number returned, in order to minimise the bias due to the heterogeneity due to tag losses, reporting, or mixing amongst release groups. A new option has been added to the Stock Syntheses, that would ignore all release groups with a small number of returns. This option has been explored in the current assessment, with a threshold of a minimum number of 3 returns for each release groups in the post-mixing period.

3.4 Modelling methods, parameters, and likelihood

The total likelihood is composed of four main components: catch data, the abundance indices (CPUE), length frequency data and tag release/recovery data. There are also contributions to the total likelihood from the recruitment deviates and priors on the individual model parameters. The model was configured to fit the catch almost exactly so the catch component of the likelihood is very small. There are two components of the tag likelihood: the multinomial likelihood for the distribution of tag recoveries by fleets over time and the negative binomial distribution of expected total recaptures across all regions. Details of the formulation of the individual components of the likelihood are provided in Methot & Wetzel (2013).

The regional CPUE indices are assumed to represent the relative abundance (numbers of fish) of the proportion of the regional population that was vulnerable to the longline fishery. The weighting of the CPUE indices followed the approach of Francis (2011). A series of smoother lines were fitted to the CPUE index and the RMSE of the resulting fit to each set of CPUE indices was determined as a measure of the magnitude of the variation of each set of indices CPUE indices. The analysis performed to the annualised CPUE index (Kitakato et al. 2022) to remove the influence of seasonal variation in CPUE. On basis of the analysis, a CV of 0.2 was assigned to each set of CPUE indices in the base model, to ensure the stock biomass trajectories were broadly consistent with the CPUE indices while allowed for a moderate degree of variability in fitting to the indices.

The relative weighting of the tagging data was controlled by the magnitude of the over-dispersion parameters assigned to the individual tag release groups. Following Langley (2016), the over-dispersion

parameters for all tag release groups were estimated within the assessment model assuming a relatively uninformative beta prior (mean 10, sd 3). This prior reflected the variability in the tag-recapture data (variance of the standardised residuals) as determined from preliminary model runs (Langley 2016).

For all fisheries, except for the PSLS fisheries, the individual length frequency observations were assigned an effective sample size (ESS) of 1. For the PSLS fisheries an ESS of 10 was assigned to all length observations. The higher weighting of the purse seine PSLS length frequency data reflects the comprehensive nature of the port sampling programme monitoring the catch. There is a high degree of variation in the length composition data from the PSFS fisheries which appears related to the bimodal structure in the fishery length compositions; variation in the individual length samples may be attributable to sampling different proportions of the catch from each length mode. Based on the apparent level of sampling error an ESS of 1 was assigned to the length samples from the PSFS fisheries.

Two additional, alternative weighting schemes were considered for the length composition data: the Francis approach and the Dirichlet-Multinomial likelihood (Methot et al. 2013). The Francis approach is based on variability in the annual observed mean length, where the ESS are adjusted such that the fit of the expected mean length should be within the uncertainty intervals consistent with expected variability based on the adjusted sample sizes (Method "TA1.8") (Francis and Hilborn, 2011). The Dirichlet-Multinormal likehood use a new likelihood (as opposed to the standard multinomial) which includes an estimable parameter (theta) which scales the input sample size (Thorson et al. 2017). The DM has been shown to be capable of estimating ESS for compositional data and performs similarly to iterative re-weighting methods.

The Hessian matrix computed at the mode of the posterior distribution was used to obtain estimates of the covariance matrix, which was used in combination with the Delta method to compute approximate confidence intervals for parameters of interest.

4. ASSESSMENT MODEL RUNS

A basic model was configured that represents a continuity run from the 2019 assessment with updated data and a number of revisions of the model. A range of sensitivity or exploratory models were conducted explore alternative assumptions and parameter configurations. On basis of the analyses, final model options were tentatively proposed that include an ensemble of models running over permutations of plausible parameters and/or model settings, from which the stock status was estimated and uncertainty was quantified. The assessment was conducted using the 3.30 version of the Stock Synthesis software. The stock status was reported for the terminal year of the model (2021).

4.1 The basic model

In the 2019 assessment, final model options selected for quantify stock status by the WPTT21 included 12 models with alternative assumptions on levels of steepness, tag weighting, and LL selectivity assumption (IOTC 2019a). The model *cSci_sL_TagLambda01_h80* (steepness of 0.8, logistic longline selectivity, and tag likelihood lambda of 0.1) was considered as a reference model. The 2019 reference model was updated to ensure continuity, but some revisions were incorporated based on preliminary analyses. These revisions are to improve the assessment model, but they do not represent any major structural changes to the model. The revisions included:

- Optimising the parametrizations of regional recruitment and movement by removing redundant parameters
- Excluding the length data from the Taiwanese and Seychelles longline logbooks.
- Increasing the length bin size from 2 to 4 cm
- Estimating separate/independent longline selectivity in each region
- Changing the logistic selectivity function in region 2 and 3 to a double normal function
- Updating the Stock Synthesis platform from version 3.24 to 3.30

A sequential, stepwise approach was taken for the model updates (Table 4). The configuration of the resulting basic model is summarised in Table 5.

Table 4: Description of the sequence of model runs to update the 2019 base model.

Model	**Description**
cSci_sL_TagLambda01_h80	2019 reference model with steepness = 0.8, tag lambda =0.1
3.30	Updated Stock Synthesis from 3.24 to 3.30
1-update-catch	Updated and revised catch series, extended the model to 2021
2-update-LF	Updated and revised length composition data;
3-update-CPUE	Updated and revised longline CPUE indices;
Basic model	• Optimising movement and recruitment parameters. • increasing length bin size from 2 to 4 cm; • estimating separate/independent longline selectivity in each region; • Changing the logistic selectivity in region 2 & 3 the double-normal function
Bias_ramp	Implementation of recruitment bias correction (see Section 3.1.1)

Table 5: Main structural assumptions of the bigeye tuna *basic* model and details of estimated parameters. Changes to the 2019 reference model are highlighted in red.

Category	Assumptions	Parameters
Recruitment	Occurs at the start of each quarter as 0 age fish. Recruitment is a function of Beverton-Holt stock-recruitment relationship (SRR). Regional apportionment of recruitment to R1N, R1S, R2, and R3. Temporal recruitment deviates from SRR, 1975–2020. Temporal deviates in the proportion of recruitment allocated to R1N, R1S and R2 from 2001–2019.	R_0 Norm(10,10); h = 0.80 *PropR2* Norm(0,1.0) *SigmaR* = 0.6. 140 deviates.
Initial population	A function of the equilibrium recruitment in each region assuming population in an initial, exploited state in 1975. Initial fishing mortality estimated for LL1N,1S,2,3 fisheries.	Norm(0.10,99)
Age and growth	40 quarterly age-classes, with the last representing a plus group. Growth based on VonBert growth model with age-specific k to approximate the mean length at age determined by Eveson *et al* (2012). SD of length-at-age based on a constant coefficient of variation of average length-at-age. Mean weights (W_j) from the weight-length relationship $W = aL^b$.	*Linfinity* = 150.913 cm, k (base) = 0.332, k deviates for ages 1,8,9,10. CV =0.10 a = 2.217e-05, b = 3.01211
Natural mortality	Age-specific, fixed. Ramp function Age 0-12, initial 0.2 at age 0. Constant age 12-40 at 0.0625	
Maturity	Length specific logistic function from Shono *et al* (2009). Mature population includes both male and female fish (single sex model).	Mat50_Fem 110.888 cm Mat_slope_Fem -0.25
Movement	Age-dependent with two blocks; age classes 3-8 and 15-40. Ramp function Age 8-15. No movement prior to age class 3. Constant among quarters.	12 movement coefs. Norm(0,4).
Selectivity	Age specific, constant over time. Longline fisheries: Separate logistic selectivity parameters for LL1N and LL1S; Separate double normal selectivity parameters for LL2 and LL3 PSLS fisheries. Separate selectivity for PSLS1N, common selectivity PSLS1S and PSLS2 Common selectivity for all PSFS fisheries.	Logistic *p1* Norm(20,10), *p2* Norm(1,10) Double Normal Five node cubic spline

	LF2 fishery logistic selectivity. LINE2 share principal LL selectivity. BB1N fishery: double normal selectivity. OT 1N & 2 share PSFS selectivity. CPUE indices share principal LL selectivity.	
Catchability	Temporally invariant. Shared regional catchability coefficient. No seasonal variation in catchability for LL CPUE. LL2,3 CPUE indices have CV of 0.2; LL1N,1S CV 0.25.	Unconstrained parameter *LLq*
Fishing mortality	Hybrid approach (method 3, see Methot & Wetzel 2013).	
Tag mixing	Tags assumed to be randomly mixed at the model region level four quarters following the quarter of release. Accumulation after 28 quarters	
Tag reporting	All (adjusted) reporting rates constant over time. Common tag reporting rate fixed for all PS fisheries. Non PS tag reporting rates uninformative priors.	 PS RR 1.0 Other fisheries Norm(-0.7,5)
Tag variation	Over dispersion parameters estimated for each tag release groups.	Beta prior (mean 10, sd 3)
Length composition	Multinomial error structure. PSLS length samples assigned maximum ESS of 10. PSFS length samples assigned maximum ESS of 1.0. LL and Other fisheries length samples assigned ESS of maximum 1.0.	

4.2 Sensitivity models

This basic model served as a starting point for furher analysis. The exploratory phase investigated a range of model options related to the configuration of key data inputs, biological parameters, and model structures. The analysis complemented the suite of sensitivity models examined during the previous assessment, with the aim of identifying major sources of uncertainty that are likely to have an impact on the assessment results. Table 6 provides a description of the range of alternative model options considered.

Table 6: Description of the sensitivity runs for the 2021 assessment.

Model	**Description**
Spatial structure	
AreaAsFleet-LL1S	Single area, "fleet as area" model, using only the LL1S index
AreaAsFleet-LL2	Single area, "fleet as area" model, using only the LL2 index
AreaAsFleet-LL3	Single area, "fleet as area" model, using only the LL3 index
CPUE	
CPUELLq	Assuming a 1% annual catchability increase for all long line indices
CPUELSpe	Incorporated the purse seine CPUE on associated sets (assigned to region 1S)
Length data	
Ess5	Longline length frequency maximum sample size increased to 5;
Dirichlet	Dirichlet multinomial likelihood for the length freqnecy data
logistic	Separate Logistic selectivity for each of the regional longline fisheries
selrw	Random walk for purse seine associated school selectivity parameters 1984 – 2021
Tag data	
tag4	Retain only tag release groups if at least 4 tags were recaptured for that release group
Taglambda1	Tag likelihood lambda set to 1
Taglambda001	Tag likelihood lambda set to 1
Biological parameters	
growth	Using VB growth parameters estimated by Farley et al. 2021
Mhamel15	Lorenzo natural mortality with adult M estimated from the Hamel (2018) estimator assuming an maximum age of 14.7, see Hoyle 2021
Mhamel17	Same as Mhamel15 except assuming a maximum age of 17
Mthen15	Lorenzo natural mortality with adult M estimated from the Then (2015) estimator assuming an maximum age of 14.7, see Hoyle 2021
Mthen17	Same as *Mthen15* except assuming a maximum age of 17

4.3 Proposed model ensemble options

On basis of the sensitivity analysis, further model options were configured to capture the uncertainty related to selectivity configurations, steepness, and biological parameters which are considered to

contribute to the main source of uncertainty. Thus, the final models involved running a full combination of options on selectivity (2 options), and steepness (3 values), natural mortality (2 values), and growth (2 options) with a total of 24 models. All models have included the PSLS CPUE index (otherwise has similar configuration to the basic model)

The estimation uncertainty for each model was determined by calculating the Hessian matrix in order to obtain an estimate of the covariance matrix, which is used in combination with the delta method to compute approximate confidence intervals for quantities of interest (i.e., the biomass and recruitment trajectories). This was done for all models in the model ensemble and the estimation uncertainty was combined across models in a parametric bootstrap approach.

Table 7: Description of the final model options for the 2021 assessment. The final models consist of a full combination of options below, with a total of 24 models. The options adopted for the reference model is highlighted.

Model options	Description
Steepness	• h70 – Stock-recruitment steepness parameter 0.7
	• **h80 – Stock-recruitment steepness parameter 0.8**
	• h90 – Stock-recruitment steepness parameter 0.9
Growth	• ***Gbase*** **– growth estimates by Eveson et al. 2012.**
	• ***Gnew*** –VB growth parameters estimated by Farley et al. 2021
Natural Mortality	• ***Mbase*** **– base level natural morality as in the basic model**
	• ***Mhamel17*** – Lorenzo natural mortality with adult M estimated from the Hamel (2021) estimator assuming an maximum age of 17, see Hoyle 2021
selectivity	• **sD –** assuming dome-shaped selectivity for longline fisheries in R 2&3
	• **sL –** assuming asymptotic selectivity for longline fisheries in R 2&3

5. MODEL RESULTS

5.1 The basic model

5.1.1 2019 model continuity run

Upgrade to SS3.30 had no impact on model estimates. Updating the 2019 base model with the catch and length composition data yielded essentially identical estimates of historical stock biomass but biomass over 2019 – 2021 continued to drop under recent catches (Figure 15). However, the model indicated substantially lower spawning biomass and stock status than the prior assessment model due to the inclusion of the revised and updated longline CPUE(Figure 15, Table 8). This has been mostly caused by changes in CPUE indices for regions 2 and 3, which declined more rapidly than the previous indices from the late 1990s to the 2010s (see Figure 5). Consequently, compared to the prior assessment, the stock biomass decreased significantly during this time. The stock biomass is somewhat increased as a result of additional model configuration changes (the basic model, see Table 4), but the spawning biomass in 2018 (the terminal year in the most recent assessment) is still estimated to be below the

target level (B_{msy} and F_{msy}) (Figure 15, Table 8).

Little changed in the estimated stock abundance over the primary data period when the recruitment bias correction (b = 0.5) as established by Methot and Taylor (2011) was applied (however, the model needs to estimate the recruitment deviates from the initial year). The bias correction alters the relative contributions between R0 and recruitment deviates rather than the abundance estimates, which should be decided by the data. A smaller bias correction factor indicates a larger mean recruitment deviates and a lower estimate of R0 (and consequently, reference values that are dependent upon R0), as the bias correction is a downward adjustment on the mean recruitment deviates. For the basic model, the impact of the bias correction on reference quantities (e.g., B_{msy}) appears to be small (Table 8).

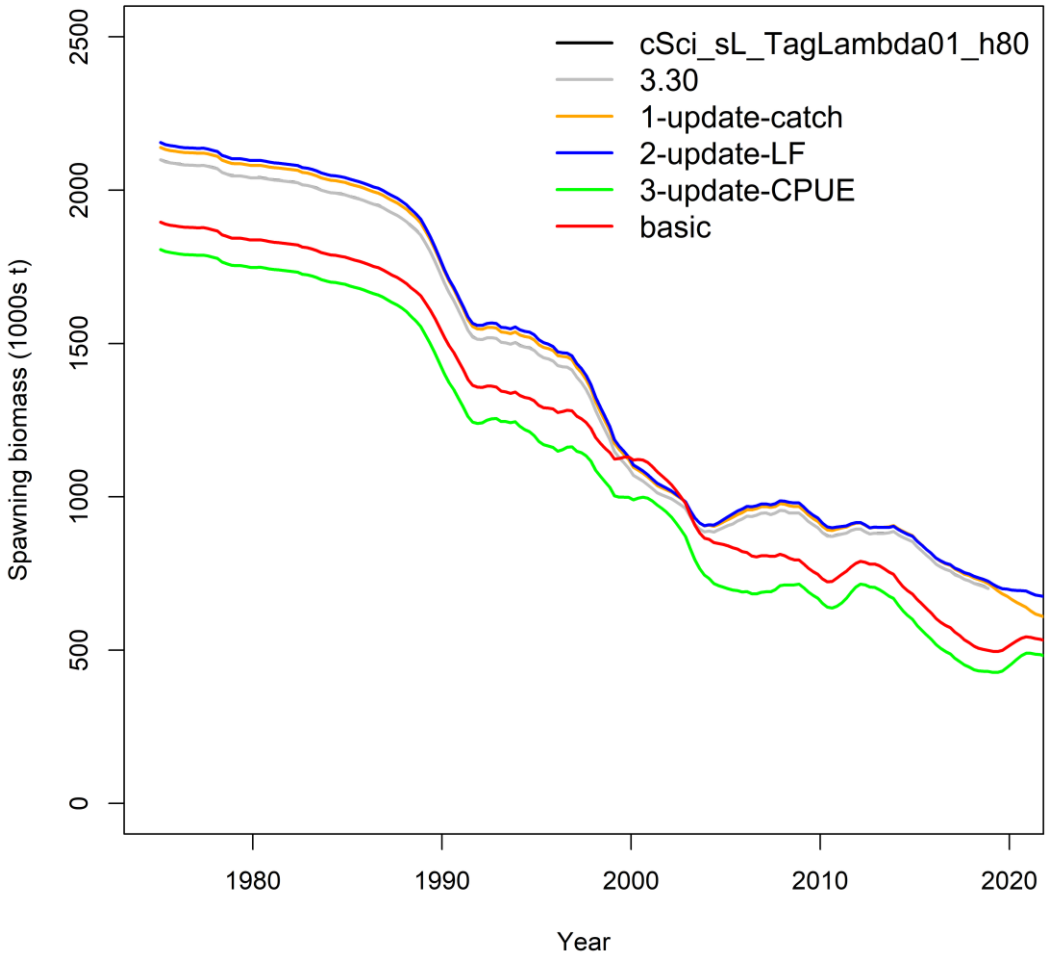

Figure 15: Spawning biomass trajectories for IO bigeye tuna from the step-wise model updates. (from the 2019 assessment reference model 'cSci_sL_TagLambda01_h80')

Table 8: Estimates of management quantities for the step-wise updates of the 2016 stock assessment reference model (*cSci_sL_TagLambda01_h80*).

Option	SB_0	SB_{MSY}	MSY	SB_{2018}	SB_{2021}	SB_{2018}/SB_{MSY}	SB_{2021}/SB_{MSY}	F_{2018}/F_{MSY}	F_{20121}/F_{MSY}
2019 model	2 216 640	514 365	86 554	710 000		1.38		0.98	
1-update-catch	2 256 850	555 256	91 795	727 000	617 000	1.31	1.11	0.93	1.14
2-update-LF	2 272 200	574 490	95 666	733 000	679 000	1.28	1.18	0.92	1.11
3-update-CPUE	1 925 150	531 526	89 671	433 000	486 000	0.81	0.91	1.23	1.70
basic	2 015 370	625 422	93 600	505 000	537 000	0.81	0.86	1.24	1.65
Bias_ramp	1 877 790	596 048	88 156	505 800	533 000	0.84	0.89	1.27	1.62

5.1.2 Model fits

The basic model fits the CPUE indices for the three main fisheries (LL1N, LL1S & LL2) and the seasonal CPUE indices from LL3 well (Figure 16). The trends in the LL1N&S and LL2 CPUE indices deviate during 2010–2017 and the model is able to accommodate the differences in these regional indices via varying levels of recruitment into these regions for more recent years. The residuals did not reveal any obvious patterns except this is a slight upward trend for region 1S (Figure 17) as the model has little flexibility to account for the differences in the CPUE trend for the early years. Overall, the variation in the residuals was broadly comparable to the S.E. initially assigned to the CPUE indices.

Overall, there was a good fit to the aggregated length frequency data for most of the main fisheries with comprehensive sampling (Figure 18). For the main purse seine fisheries (particularly the PSFS), the relative proportion of fish in the small (≤80cm) and large (>80cm) length mode is variable over time, probably due to size related schooling behaviour of adult bigeye tuna, resulting in less adequate fits to the length composition distributions. The recent trends in the predicted average fish size for the main longline and purse seine fisheries are broadly consistent with the sampling data. The average length of fish from LL2 is still over-estimated by the model throughout the 1980s and 1990s despite the use of a more flexible, double normal selectivity function. There is a marked decline in the average size of fish sampled from the purse seine FAD fisheries in both region 1S and region 1N (Figure 19), particularly during the mid-1990s. This trend is not evident in the predicted average fish size derived from the model for region 2. The average length of fish sampled from the PSFS is highly variable (Figure 19) probably reflecting the proportion of the catch sampled from the smaller and larger modes of the combined length composition. The model prediction of average length represents the length of fish in the intermediate length range (80–100 cm) There is an improvement in the fits to the length data from the fresh tuna longline fisheries in region 2. Given that the selectivity was assumed to be the same as the longline fishery, the model did not adequately fit the catch samples from the LINE fishery. Due to the small number of samples from this fishery, estimating a sperate selectivity did not work well.

The PSLS1S length frequency data showed some noticeable mode progression between 2008 and 2013, with new recruits appearing to occur in the fourth quarter, progressing through to the first and second quarter of the following year, and the model tracked these observed modes reasonably well (Figure 20). The PSLS LF data has some strong influence on the estimates of recruitment strength.

The fit to the observed number of tag recoveries was examined for those fisheries which accounted for most of the tag returns (e.g., PSLS1S). The fit to the number of tag recoveries was examined by recombining the tags into individual release periods (i.e., aggregating the releases by age class) and excluding those recoveries that occurred during the mixing period. The fit to the tag recoveries was examined by time period (quarters) and by age at recovery, and by time at liberty (quarters) for the individual release periods and the aggregated data set (all releases combined).

The number of tag recoveries varied considerably amongst the release periods (Figure 21 Figure 22). The tags released in 2005 and the first quarter of 2006 had very low recoveries, probably due to the small number of releases and high tag mortality in the initial phase of the program.

Most of the observed tag recoveries in the post mix period were from the PSLS1S fishery and a high proportion of the total recoveries occurred during the first four quarters following the mixing period Figure 21 Figure 22). Longer-term recoveries were less vulnerable to the PSLS1S fishery (due to the age specific selectivity) and, hence, numbers of recoveries declined considerably (Figure 21 Figure 22).

The fit to the tag recoveries from the PSLS1S fishery by age class (at recovery) suggested that the model under-estimated the overall number of tags recovered from the fishery in the older age classes (24–30 quarters) (Figure 23**Error! Reference source not found.**). This result indicates that the age-specific recoveries are inconsistent with the fishery selectivity functions. The tag recoveries from the PSLS fishery included a significant proportion of fish above 80 cm which generally were not vulnerable to

the commercial fishery. Limited numbers of tags were also recovered by the PSFS1S and LL1S fisheries after longer periods at liberty (compared to PSLS1S). The model tends to underestimate the number of tag recoveries throughout the age classes from the PSFS1S fishery. This may be indicating inadequate mixing of the tags with the fish population vulnerable to the PSFS fishery.

Overall, there was a reasonable fit to the tag recoveries from the PSLS 1S fishery during the main tag recovery period (to 2011) but the model over-estimates the number of longer term tag recoveries from the older age classes (at recovery), i.e. those fish at liberty for a longer period, this may reflected variable tag reporting over time or mis-specification of natural mortality. A small number of tags were recovered in region 1N and the model predicts a correspondingly low number of tag recoveries from the region. .

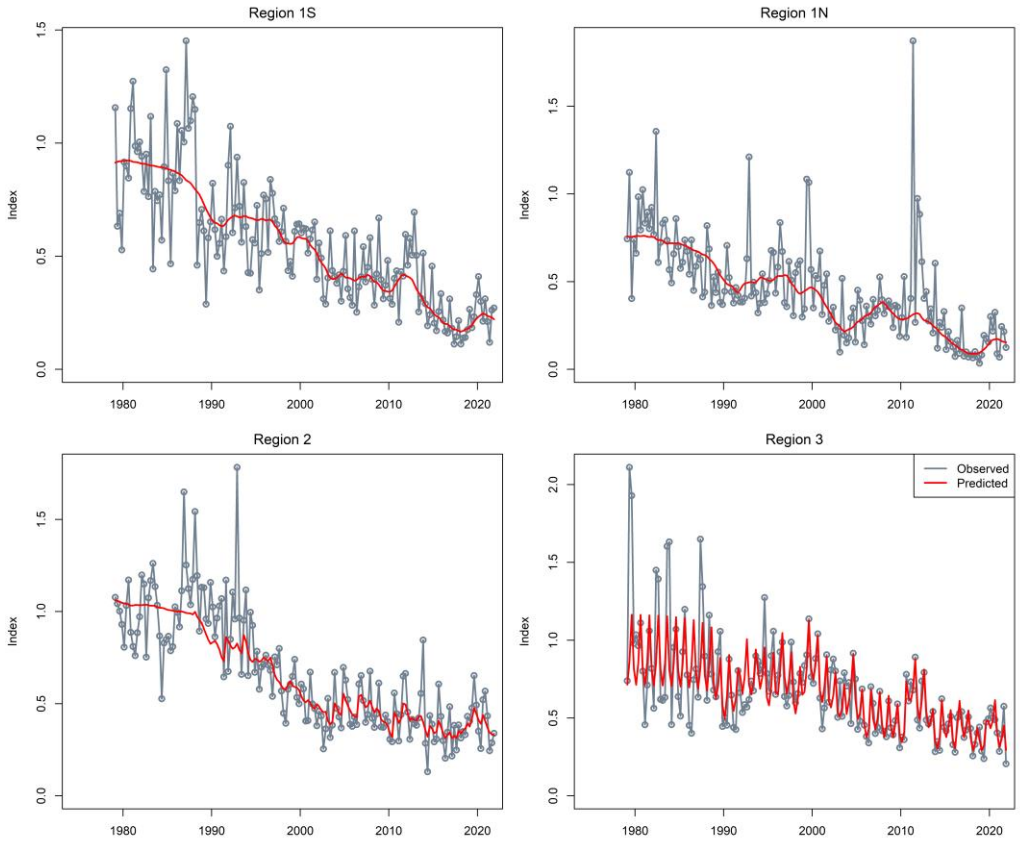

Figure 16: Fit to the regional longline CPUE indices, 1979–2021 from the basic model.

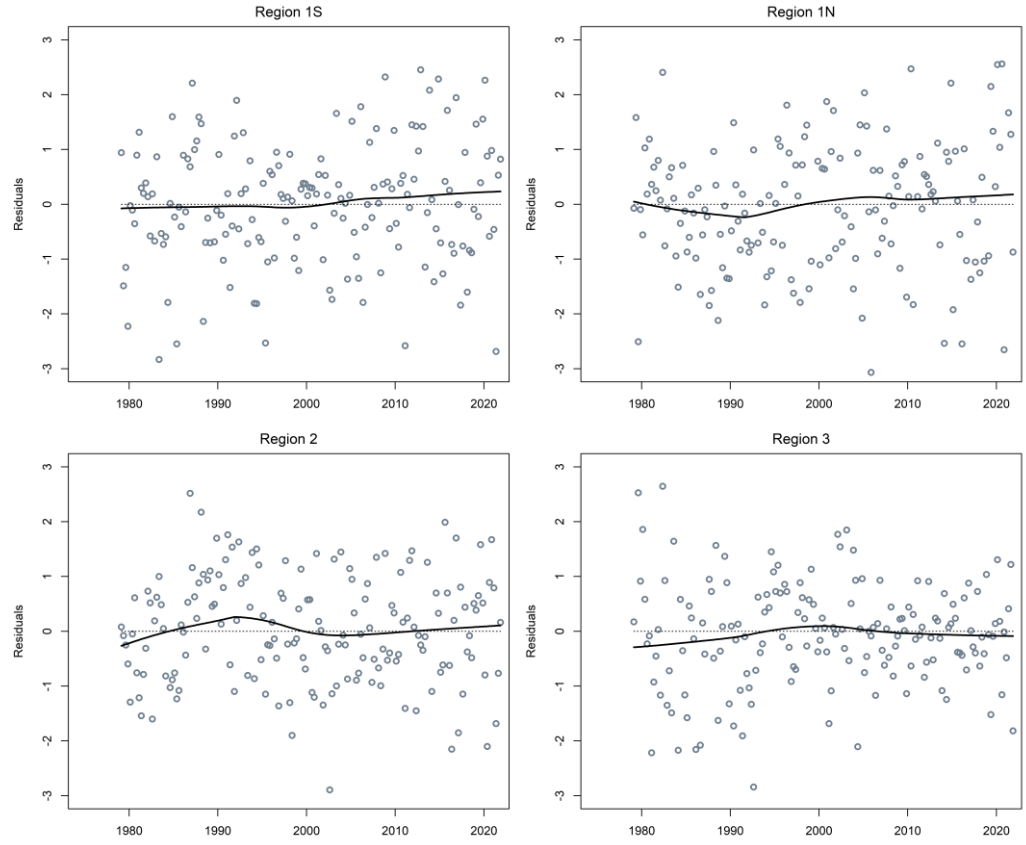

Figure 17: Standardised residuals from the fits to the CPUE indices from the basic model.

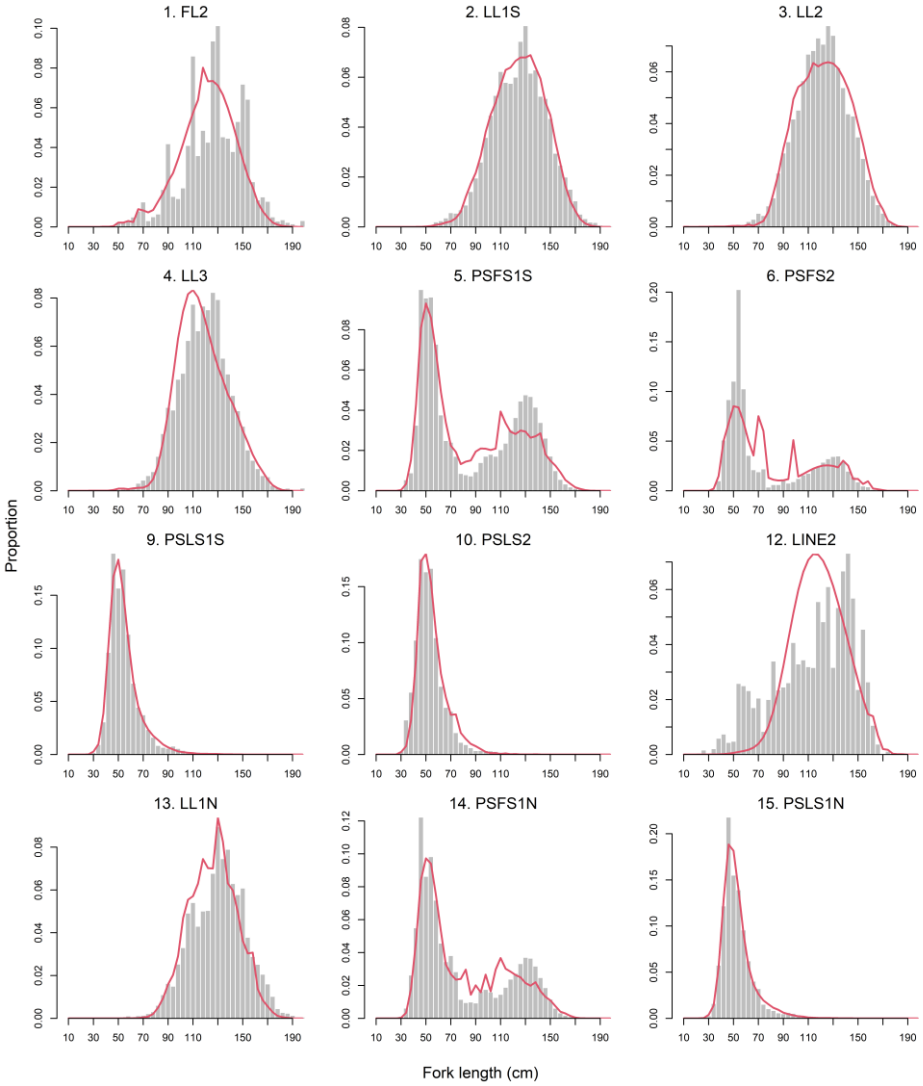

Figure 18: Observed (grey bars) and predicted (red line) length compositions (in 2 cm intervals) for each fishery of bigeye tuna aggregated over time for the basic model.

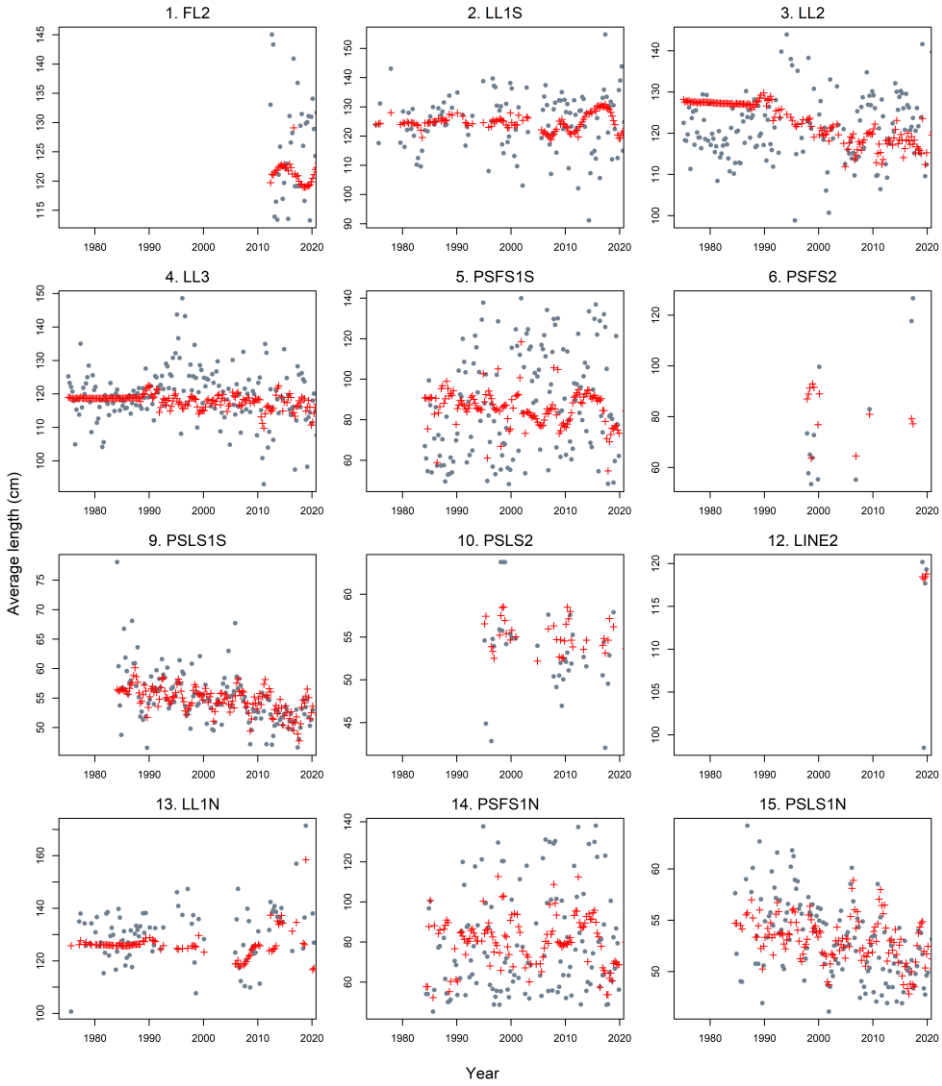

Figure 19: A comparison of the observed (grey points) and predicted (red points and line) average fish length (FL, cm) of bigeye tuna by fishery for the main fisheries with length data for the basic model.

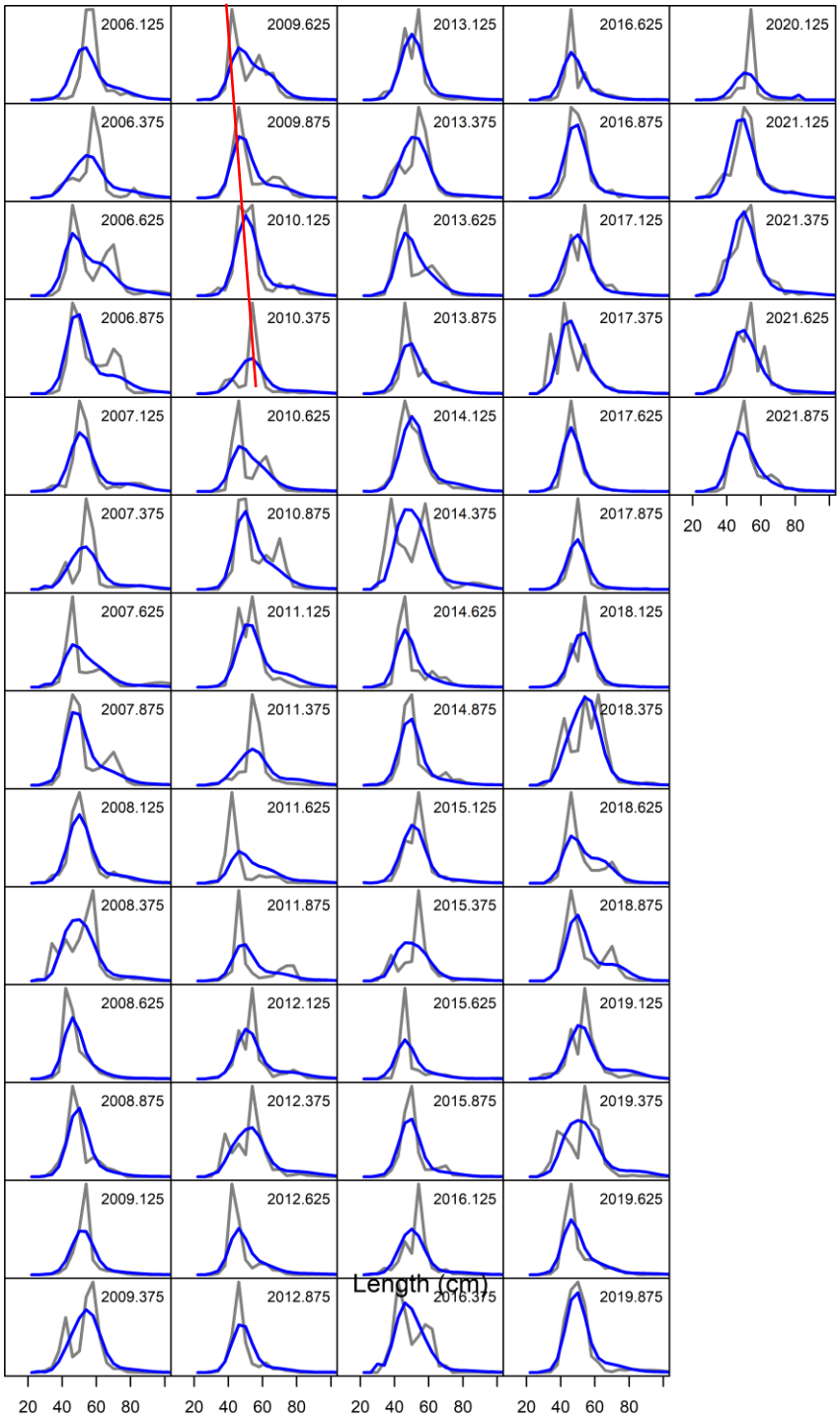

Figure 20: Observed (grey) and predicted (blue line) length compositions for the PSLS 1S fishery by year quarter 2006–2021 for reference model. The red line indicates a example of mode progression in the data.

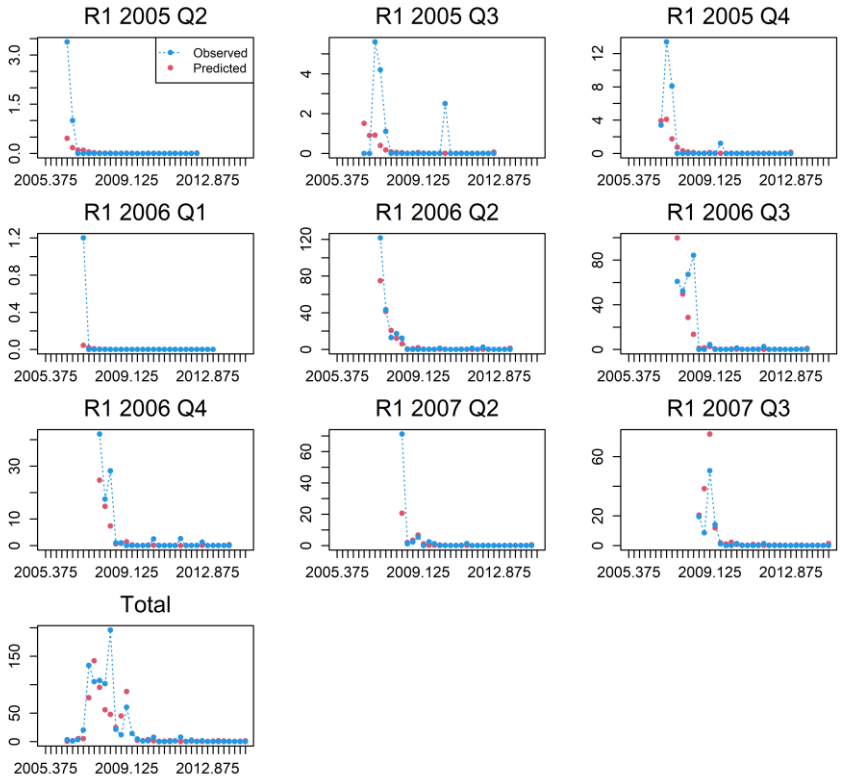

Figure 21: Observed and predicted number of tags recovered by quarter for the PSLS fishery in region 1S (PSLS 1S). Only tags at liberty after the four quarter mixing period are included. Tag recoveries are aggregated for each release group.

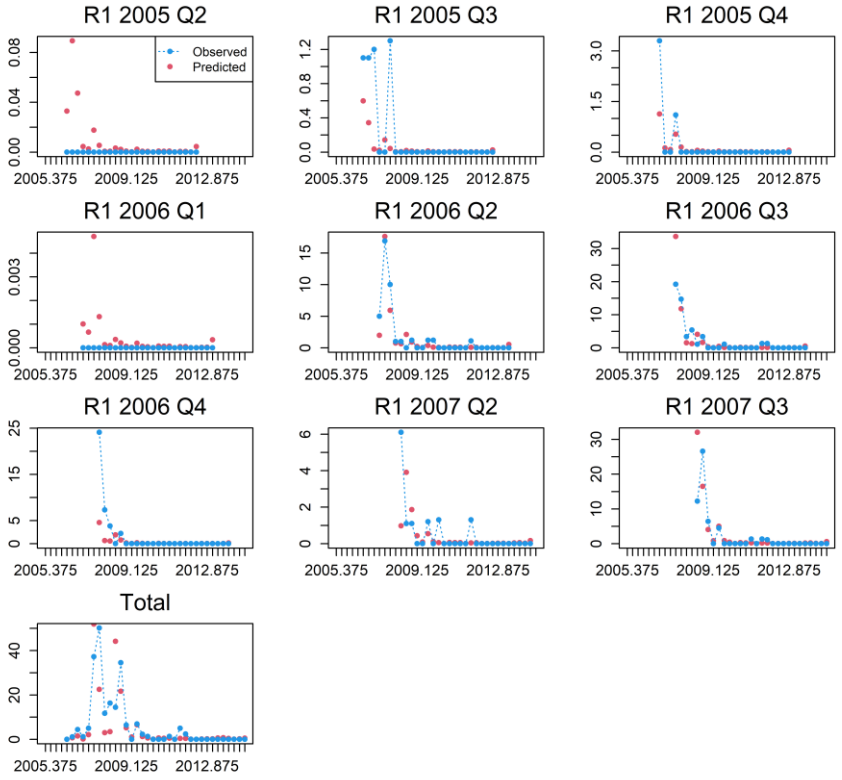

Figure 22: Observed and predicted number of tags recovered by quarter for the PSLS fishery in region 1N (PSLS 1N). Only tags at liberty after the four quarter mixing period are included. Tag recoveries are aggregated for each release group

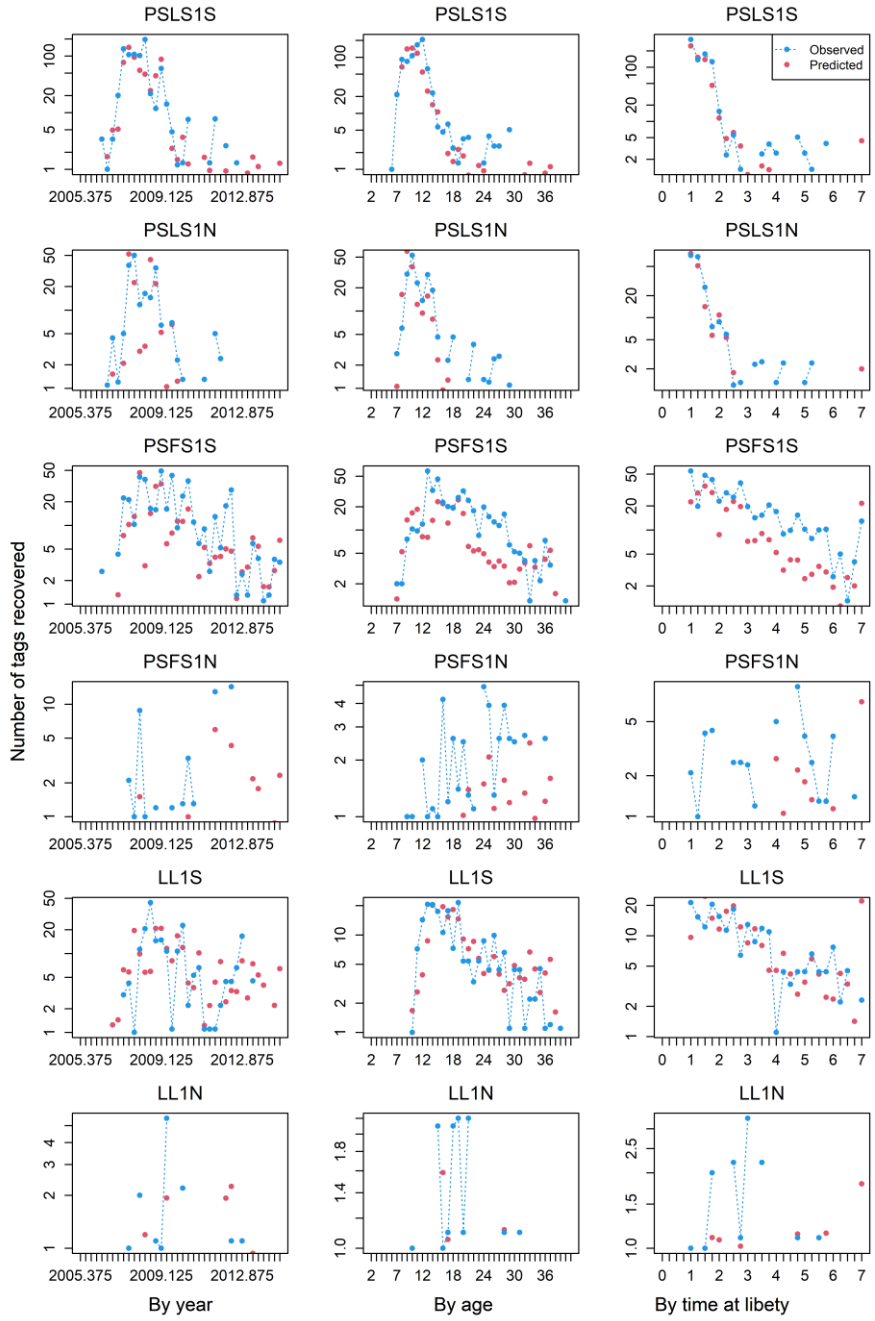

Figure 23: Observed and predicted number of tags recovered by year/quarter time-period (left), by age (mid), and by time at liberty (in quarters, right) for main Purse seine and longline fisheries in region 1N and 1S (PSLS 1S, 1N, PSFS 1S, 1N, and LL 1S, 1N) from the basic model. Only tags at liberty after the four-quarter mixing period are included. Tag recoveries are aggregated for each of the regional fisheries.

5.1.3 Model estimates

The estimated parameters in the basic model include: the overall population scale parameter *R0*, the time series of recruitment deviates, the distribution of recruitment among regions, age specific movement parameters, the fishery selectivity parameters, fishery tag reporting rates and the catchability parameters for the CPUE indices..

The age-specific selectivity functions are presented in Figure 24. Full selectivity is reached for the R1N and 1S longline fisheries at around age 18 (quarters). Selectivity for the longline fishery in R2 was predicted to be asymptotic with a steep transition. The selectivity for the longline fishery in R3 was estimated to be dome-shaped, with a diminishing right limb from roughly 18 to 22. Peak selectivity for the PSLS1N and PSLS1N fisheries occurs at ages 5–8 quarters. (Figure 24). For the PSFS fisheries, selectivity was estimated to be bimodal with a similar level of selectivity for the younger and older modes.

Recruitment deviates were estimated for the quarterly time steps from 1984–2020. Estimating the recruitment prior to 1984 was quite uncertain. There are longer-term trends visible in the recruitment deviates, with higher than average recruitment estimated for the late 1990s to early 2000s and reduced recruitment between the mid-2000s and 2015 (Figure 25). These trends correspond to period of higher and lower catches from the PSLS fishery. Recruitment for 2010–2016 was estimated to fluctuate around the long-term average with moderate variability.

Recruitment was assumed to occur in all regions and the distribution of recruitment was estimated to be apportioned 33% to Region 1N, 23% Region 1S, 18% to Region 2, and 25% to region 3. The basic model estimated a decreasing level of recruitment into region 1N for 2000–2015 (Figure 26).

Movement rates were estimated amongst the model regions. The model estimates low movement rates of mature fish amongst the regions, with some reciprocal movement between region 1S and region 3 (Figure 27). Very low mixing was estimated to occur between regions 1N and 1S.

Tag reporting rates were estimated for the non purse seine fisheries (Figure 28). For some of these fisheries, the estimated reporting rates are unlikely to be influential in the overall assessment as the reported tags were predominately recovered during the tag mix period. However, a considerable proportion of the tag recoveries from the LL1S and LL3 fisheries occurred during the post mixing phase and, hence, the tag reporting rates will have some influence in the model likelihood. For these fisheries, tag reporting rates were estimated at 0.21 and 0.52, respectively. while the reporting rate for the LL1N fishery was estimated to be considerably lower (0.05). The estimates for the LL2 and LL3 fisheries are associated with high uncertainty, and probably have reflected the large inter-annual variabilities in the tag recoveries (and reporting) from these fisheries.

For the basic model, Region 3 accounted for about 40% of the initial biomass (R2, 24%; R1S, 20%, R1N, 16%). Due to the adoption of a double normal selectivity function for the longline fisheries in areas 2 and 3, these estimates differ from the previous assessment. In region 3, the selectivity is estimated to be quite dome-shaped, indicating that there is a significant amount of mature biomass that is not vulnerable to longline fishing. On the other hand, regional scaling of the longline CPUE indices was primarily responsible for determining the relative distributions of vulnerable biomass among regions (see Section 2.5.1). Spawn biomass decreased across all regions until the 1990s and the beginning of the 2000s (Figure 29). In 2011–12, biomass somewhat increased before declining quickly to historical low levels in 2018. The spawning biomass increased in all regions over the last three years (Figure 29).

The estimates of fishing mortality for the fisheries in regions 2 and 3 were low (Figure 30). The mortality rates for the LL1N and LL1S fisheries were similar to those for the other two longline fisheries. Comparatively, fishing mortality rates for the PSLS fisheries were estimated to be rather high in regions 1N and 1S starting in the middle of the 1990s, with a substantial increase in Region 1S in 2018 and Region 1N in 2021. (Figure 30).

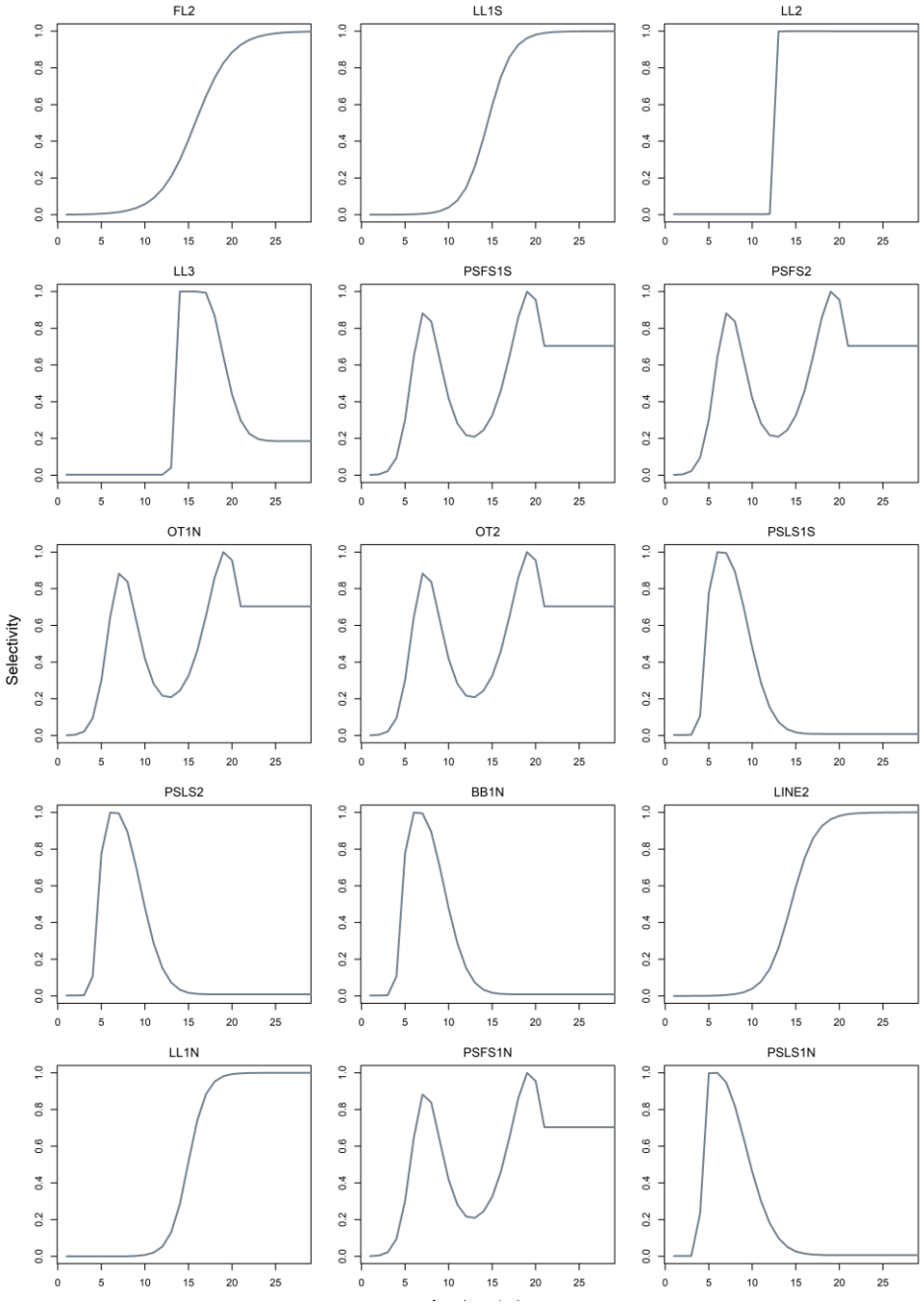

Figure 24: Age specific selectivity by fishery from the basic model.

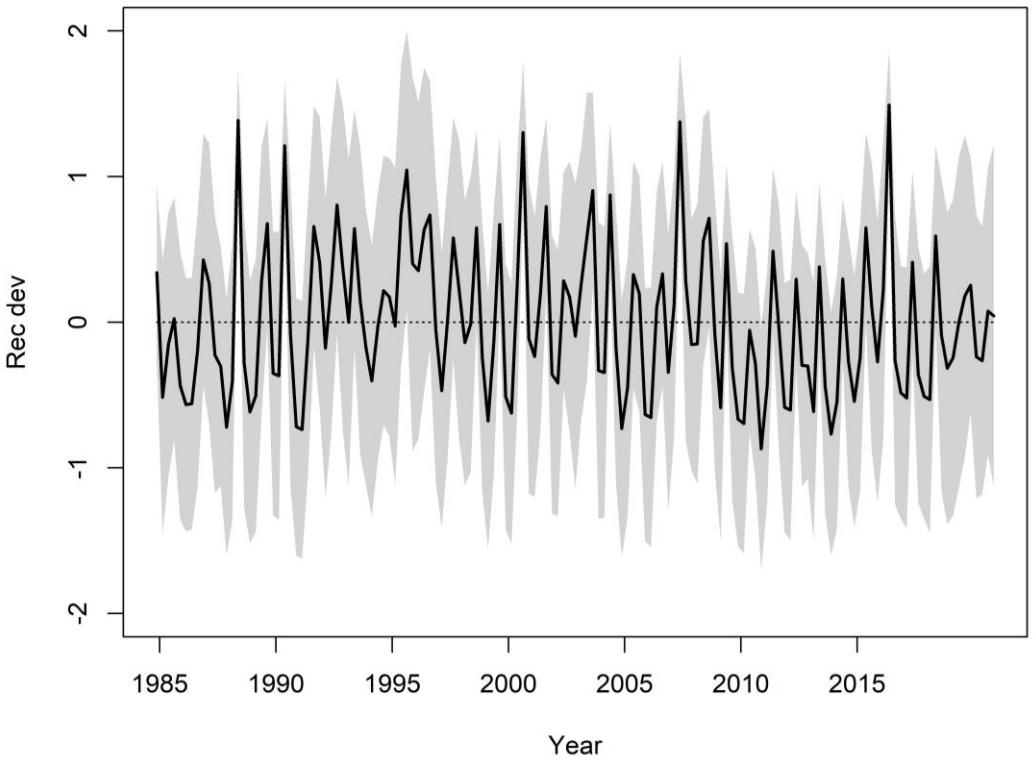

Figure 25: Recruitment deviates from the SRR with 95% confidence interval from the reference model

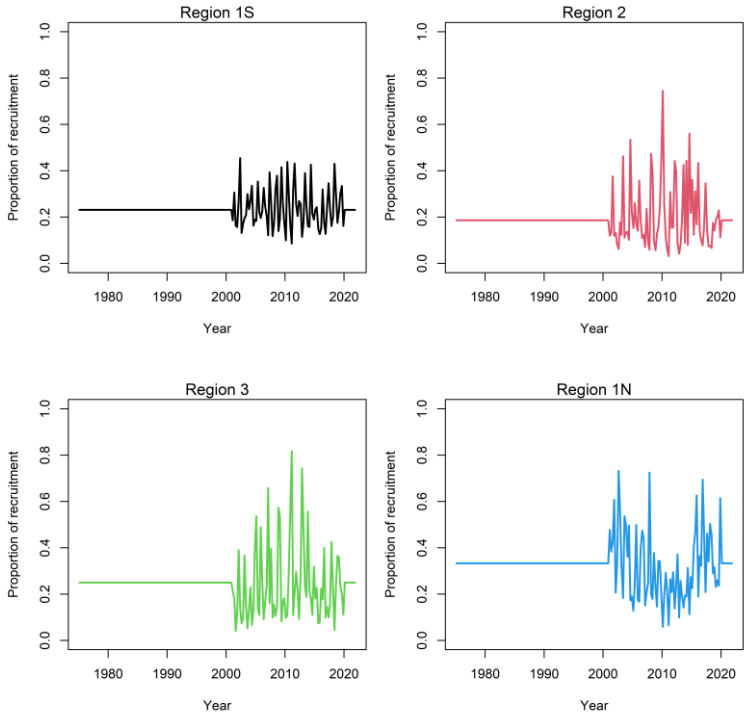

Figure 26: Proportion of the total quarterly recruitment assigned to each region for the basic model.

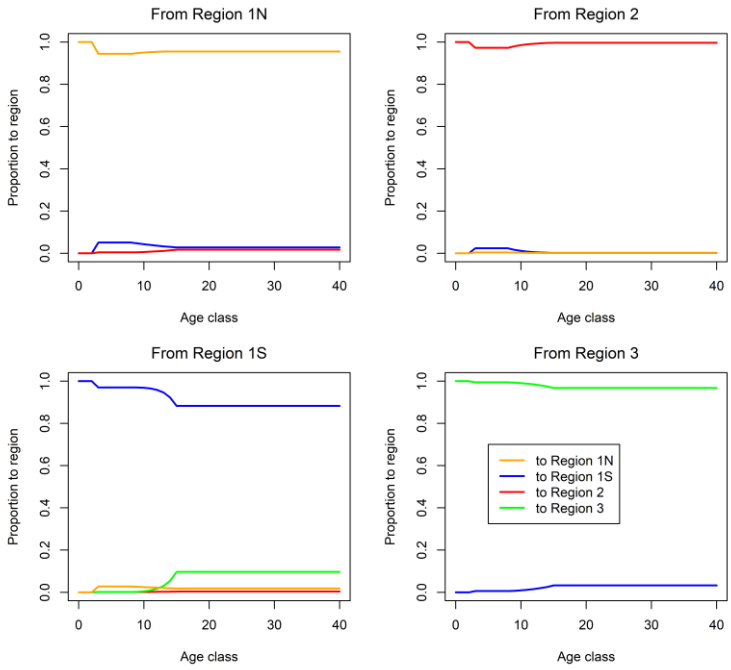

Figure 27: Estimated age specific movement parameters for the basic model.

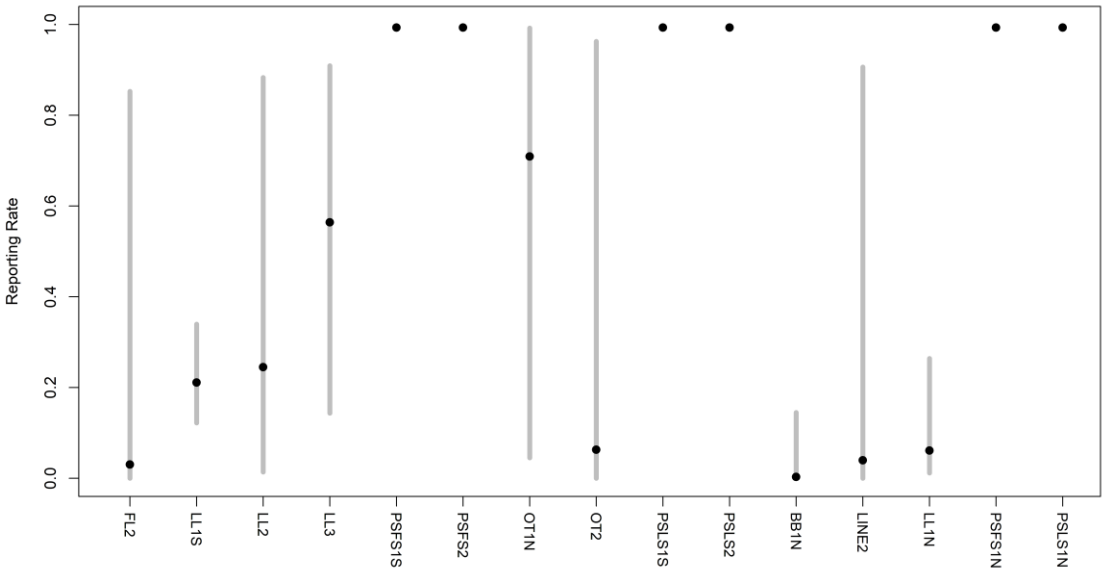

Figure 28: Tag reporting rates for each fishery from the reference model. Purse seine reporting rates were fixed at a value of 1.0. Reporting rates for the other fisheries were estimated. The grey lines represent the 95% confidence interval for the estimated values.

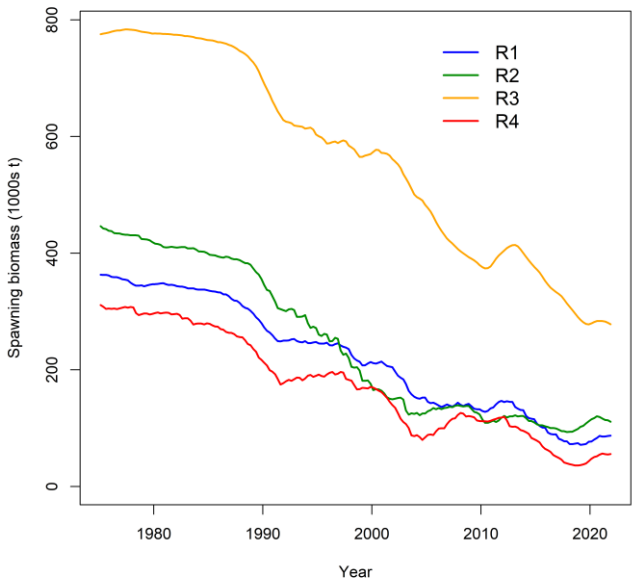

Figure 29: Estimated spawning biomass trajectories for the individual model regions from the basic model.

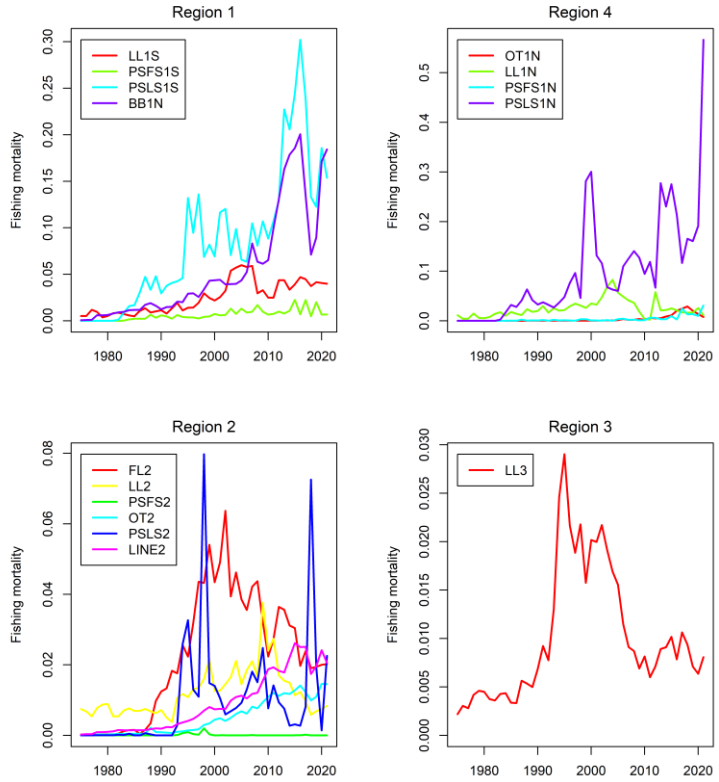

Figure 30:Trends in fishing mortality (quarterly) by fleet for the basic model.

5.1.4 Diagnostics

Several diagnostic tools were run for the reference model, including ASPM analysis, retrospective and hindcasting analysis.

ASPM analysis

The Age Structured Production Model (ASPM) analysis (Maunder & Piner 2015) was used to illustrate what is the main driver of the population trend, and whether the composition data has an undue influence on the estimates of abundance. The ASPM analysis involved running two variations of the reference model: *ASPMfixed* – where the length composition data were removed from the model (selectivity parameters fixed) and recruitment deviates were fixed to be zero; and *ASPMdev* – the same as *ASPMfixed* except that fixed recruitment deviates (estimates from the reference model) were added 7back.

The stock biomass from the two ASPM model runs are shown in Figure 31. The analysis indicated that the catches and abundance indices for the bigeye tuna stock generally agree, meaning that the catch by itself may adequately explain the overall degree of stock depletion seen in the historical CPUE indices. The stock is expected to fall more quickly between 1990 and 2010 and remain relatively steady over the following ten years, if there were no variations in recruitment. In order to account for the CPUE trend throughout 1990–2010 and 2011–2018, the model requires greater or lower than average recruitment for the two time periods, respectively. The analysis also revealed that the population scaling parameter estimate is only somewhat influenced by the length composition data.

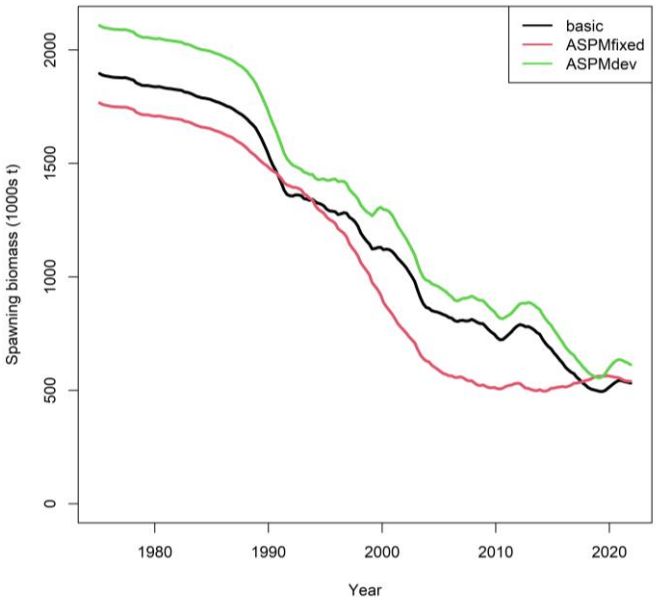

Figure 31: ASPM analysis for the reference model: ASPMfixed (no recruitment deviations), and ASPMdev (recruitment deviates from the reference model added back). Both runs excluded the length composition data and fixed the selectivity parameters.

Retrospective analysis

Retrospective analysis is diagnostic approach to evaluate the reliability of parameter and reference point estimates and to reveal systematic bias in the model estimation. It involves fitting a stock assessment model to the full dataset. The same model is then fitted to truncated datasets where the data for the most recent years are sequentially removed. The retrospective analysis was conducted to the reference model for the last 5 years of the assessment time horizon to evaluate whether there were any strong changes in model results. The selected period was intended to avoid removing any tag recovery data. The analysis involves sequentially removing 4 quarters of data at each trial.

The analysis conducted to the basic model indicated there is no apparent retrospective pattern for SSB estimates and the ratio SSB over SSB_0 (Figure 32). Overall the very low level of retrospective pattern provided some confidence on the robustness of the model with respect to the inclusion of recent observational data.

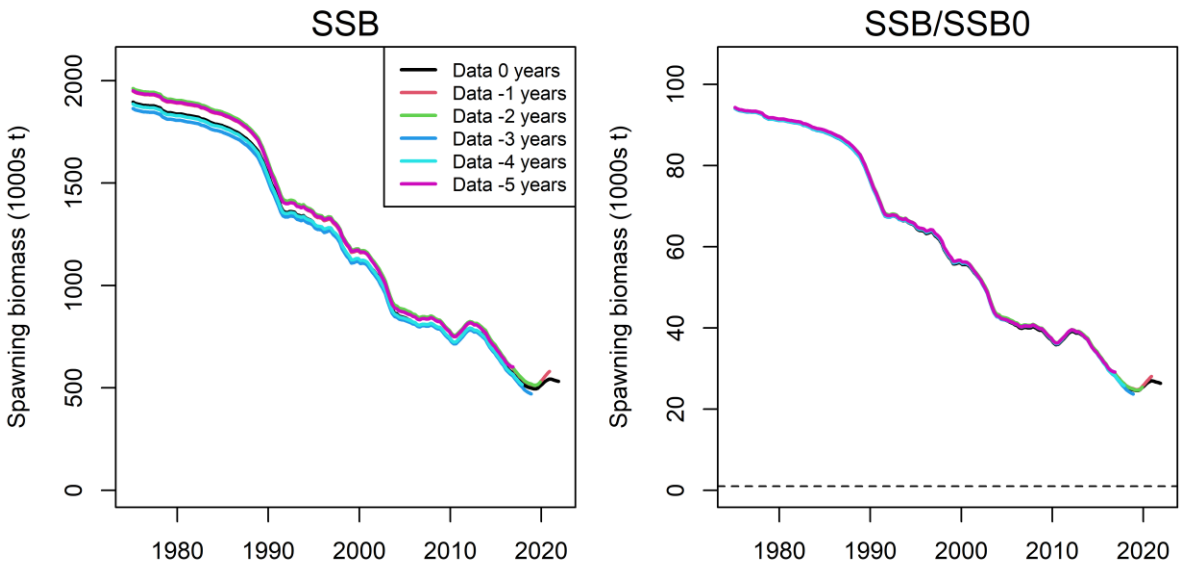

Figure 32: Retrospective analysis summary for the reference model.

Hindcasting analysis

Retrospective analysis evaluates the model's stability with respect to recent data. The Hindcasting analysis (Kell et al. 2016) further assesses the model's predictive power by making forward projections of the CPUE index using truncated models (i.e., models were fitted with data sequentially removed and were projected forward with catches added back in). The Hindcasting diagnostics were provided for the basic model using the tools provided by Carvalho et al., 2021. The results show that the predictive ability of the model is reasonably stable, as the vulnerable biomass predicted in the truncated model is quite close to the prediction in the full model (**Figure 33**). The mean absolute scaled error (MASE), calculated from the residuals as a measure of prediction errors, is less than 1 for most quarterly indices, (indicating the predictive ability is better than a random walk).

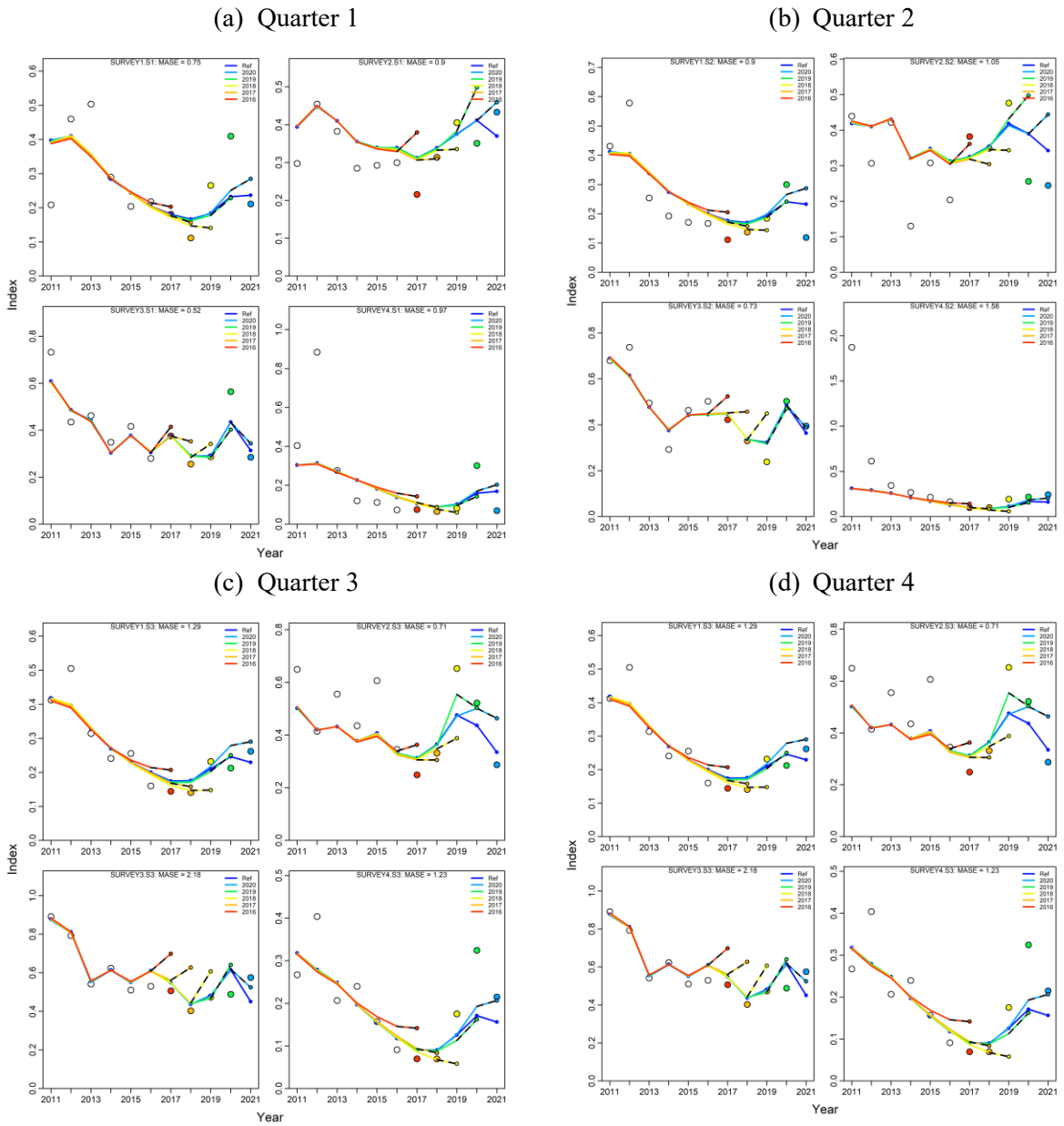

Figure 33: The Hindcasting analysis summary for the basic model: each panel shows the predicted quarterly longline CPUE index from models with data sequentially removed for 1, 2, 3, 4, 5 years.

5.2 Sensitivity models

The exploratory models investigated alternative options relating to parameter and structural assumptions and aimed to identify potential revisions to the assessment model. Key results of the exploratory runs are given in Appendix A and are also summarised below.

<u>CPUE indices</u>

The PSLS index was added in model *CPUEPSLSpe* (assumed to represent the relative abundance in region 1S). In addition to estimating the constant CV of 0.2 as the observation error, the model also estimated a further variance component for the index. The estimated value of the additional process error, which is around 0.05, shows that the PSLS and longline indices are rather consistent. The PSLS index was well fit by the model (Figure A2). The model estimated a stock abundance comparable to the basic model (Table A1, Figure A1)

The longline CPUE indices fall 33% more if an 1% annual catchability increase (effort creep) over the time series is assumed. This would result an estimate of a greater stock depletion (SSB_{2021}/SSB_0 was estimated to be 17% in model *CPUELLq* (27% for the basic model).

Length composition data

Individual length frequency data were given a maximum sample size (ESS) of 1 in the basic model (except for the PSLS fisheries an ESS of 10 was assigned). One iteration of Francis (2012) approach was applied, which indicated that the sample size for longline fisheries might be increased to about 5. (The Francis method set the sample size such that the standard error of normalised residuals of the mean length over the time series is close to 1). Model ess5, which increased the sample size for the longline fishery to a maximum of 5, appears to have little effect on estimates of stock abundance nevertheless (Figure A1)

Alternatively, a Dirichlet-multinomial (DM) likelihood for the length frequency data. The DM likelihood includes an estimable parameter (theta) which scales the input sample size. The Dirichlet estimates the effective sample size as Neff = $1/(1+\theta) + N*\theta /(1+ \theta)$, where θ is the estimable parameter and N is the input sample size. Estimated effective sample are very close to the input sample size for both the longline and purse seine fisheries. The model estimated a slightly lower level of stock biomass than the basic model (Figure A1).

There was a discernible decline in the fits to the length composition data in the two regions for the longline fisheries in region 2 and region 3 when using an asymptotic, logistic selectivity. When all the years are combined, the estimated length composition is biased in region 2. (Figure A3). In comparison to the model that used the double-normal selectivity function, the model's mean length prediction for the period 1975–2000 is worse. On the other hand, there is greater agreement between mature biomass and vulnerable biomass (to the longline fishery) when an asymptotic selection function is assumed (Figure A5).

The basic model predicts the observed decreasing trend in the mean fish length of the PSLS1S and 1N fisheries over time. The reason for the decline, nevertheless, is unclear; it could be due to combined effects of changes in abundance, fish behaviour, and/or fishing operations. Model *selrw* assumed that the diminishing fish length in PSLS fisheries is the result of shifting selectivity/vulnerability. The predicted shift in selection over time toward smaller fish eliminated potential abundance signals from the PSLS length composition data. The estimated recruitment pattern was impacted by this, and the model also estimated a higher stock abundance than the basic model (Figure A1).

Tag data

Model *tag4* reduces the number of release groups from 68 to 41 by limiting the tag release groups to those that had at least 4 positive returns. The release groups with fewer returns are thought to have more reflected the variability in the tagging process (e.g., high tagger induced morality, etc). The model estimated a small decrease in the average value of the overdispersion parameters (from 8.9 to 8.6). Other model estimations aren't much affected by this model, though (Figure A1).

The previous assessments suggested there is conflict between the tag release/recovery data and the CPUE data, and the relative weighting of each data type influences the population scale parameter (R0). In the basic model, the tag likelihood lambda was set at 0.1 (10% of natural weight). The value is arbitrary but serves to moderate the influence of tagging data on the estimates of abundance, as the assumption of homogeneous mixing of tags is very unlikely to have been met due to the limited tag dispersion. Further decreasing the tag lambda value to 0.01 (*taglambda001*) did not have appreciable impact on the model estimates (Figure A1), nor the quality of fits (Figure A6). On the other hand, Increasing the tag lambda to full weight (1) yielded substantially lower level of stock biomass (Figure A1), lower estimate of *MSY*, and change in stock status relative to SB_{MSY} and F_{MSY} compared to the basic model (Table A1). Not surprisingly, the model with a higher (lambda 1.0) weighting to the

tagging data exhibit a better fit to these data (Figure A6), particularly for the PSLS1S fishery, with a shift in PSLS1S selectivity towards larger fish (70–100cm).

Biological parameters

The mean size of the new growth (Farley et al., 2021) is larger across all age groups. According to the mean size at age, the new growth significantly altered the age distribution of the tagging data towards younger fish. Overall, there was not much of a difference in the fits to the CPUE, size, and tagging data. The new growth predicted lower population numbers but greater annual biomass estimations (Figure A1). Through the fits to the length composition data from the purse seine fishery, it had various effects on the estimations of the recruitment and selectivity pattern. In comparison to the basic model, the estimated selectivity in LL 3 has a substantially steeper falling right-hand limb (Figure A4), which widens the gap between the vulnerable biomass and mature biomass (Figure A5).

The four different natural mortality all provided good fits to the data, with the likelihood marginally increasing for the model with the lowest natural mortality (Mhamel17) and decreasing for the model with the highest natural mortality (MThen15). All models tended to have lower estimates of spawning biomass than the basic model (Figure A1, Table A1). The estimated selectivity for the LL 3 fishery is less domed with a higher level of natural morality (Figure A4), which reduces the gap between the vulnerable biomass and mature biomass (Figure A5)

Spatial structure

The 4-region spatial partitioning in the assessment model was to accommodate the distribution of fleets, differences in regional abundance trends, and the incomplete mixing of tags in the main area of recovery. The model requires a relatively large number of movements to be estimated. There is probably limited information to estimate movement rates within the model: all tags releases are limited to one region (R1S), the size structures in the commercial catches are similar among regions.

Models with a simplified (1-region) regional structure were briefly investigated. The tagging data was not included in the 1-region models. Utilizing the longline CPUE indices from 1S, 2, and 3 respectively, three models were fitted (the longline CPUE in 1N is very similar to 1S). The model indicated a lower biomass and higher depletion with the LL1S CPUE compared to the 4-region model, and a higher biomass and lower depletion with the LL2 or 3 CPUE. Overall, the estimates from the basic model are included in the range of biomass for the three 1-region models, showing a degree of stability in model estimates with regard to the various specific structures..

The single-region and 4-region models' estimates of selectivity differed, especially for the longline fishery. This is because that each fleet's selectivity is calculated in relation to the population structure of the area in which it operates. Asymptotic selectivity may not be appropriate when using the fleet-as-area approach to describe spatial fishing, as demonstrated by Waterhouse et al. in 2014.

5.3 Proposed final model options

On basis of the sensitivity models, final options were configured to capture the uncertainty related to assumptions on biological parameters including growth and natural mortality, stock-recruitment steepness, and selectivity configurations, which are shown to have contributed to the main sources of uncertainty around the key model estimates.

MThen15 had the highest natural mortality among the four alternative *M* explored in the sensitivity models, and it received less support from the likelihood values. The *M* values in *MHambel15* and *MThen17* are very comparable. It seems more reasonable to use *Mhambel17* because the M is based on the highest age that has been observed. Additionally, M values in *Mhambel17's* are closer to the basic model, ensuring some degree of continuity.

Given that the average fish size is generally smaller than those captured in region 1, the assumption of a dome-shaped selectivity function for the longline fisheries in region 2 and region 3 seems appropriate (see Figure 9). This, however, is a source of uncertainty since it suggests that a significant portion of mature biomass is not vulnerable to fishing. Therefore, the option of an asymptotic, logistic selectivity for the longline fisheries in region 2 and 3 was also included in the final models, although this option provided less accurate fits to the length data in those regions.

The basic model assumed a steepness of 0.8. The final model options also included two alternative values of steepness of the BH SRR (*h* 0.7 and 0.9). These values are considered to encompass the plausible range of steepness values for tuna species such as bigeye tuna and are routinely adopted in tuna assessments conducted by other tuna RFMOs.

The model is sensitivity the tag lambda value (weight). The tag lambda was set at 0.1 in the basic model, which represents an intermediate level of weighting of the tagging data. The previous assessment has included a tag lambda of 1.0 representing the native weighting of the tag recovery data (giving the tagging data a relatively high weighting). given the limited dispersion of tags, it appears more appropriate to downweight the tag data. Without significantly affecting the fits to the tag observations, the tag lambda of 0.1 could reduce any potential bias resulting from the violation of the tag mixing assumption. A tag lambda of 0.1 was therefore applied to all models.

Thus, the final models involved running a combination of options on, LL 2 and 3 selectivity configurations (2 scenario), steepness (3 values), growth (2 values), natural morality (2 levels) (Table 7). The final model grid is different from the assumptions of the 2019 assessment: it omits the alternative, native tag release mortality value, but adds alternative options for growth and natural mortality parameters. All final models included the purse seine CPUE index (thus, the models in the grid represents a one-off change to model *CPUEPSLSpe*). The model_h80_Gbase_Mbase_sD can be considered as a reference model in the final model ensemble (the difference between this model and the basic model is that it has included PSLS CPUE index). These models encompass a wide range of stock trajectories, with low steepness values generally yielding lower estimates of biomass (Figure 34).

Further diagnostics to detect model mis-specification using the “ss3diags” package (Carvalho et al., 2021) and to examine anomalous trends in process error time series (Merino et al. 2022) for the final models are provided in Appendix B.

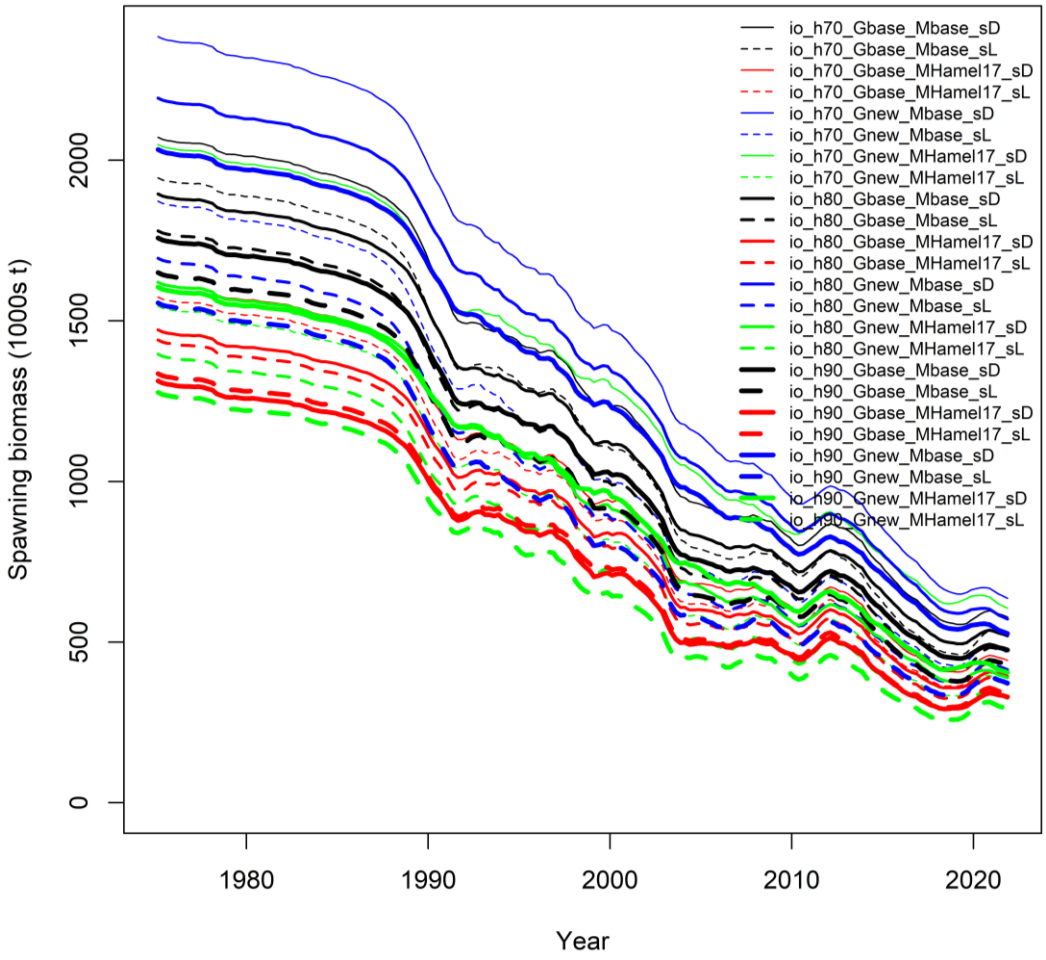

Figure 34: Spawning biomass trajectories from the final model options (details in Table 7)

6. STOCK STATUS

6.1 Current status and yields

MSY based estimates of stock status were determined for the final model options, including alternative assumptions on selectivity, alternative values of SRR steepness, growth, and natural mortality. Stock status was determined for individual models (Table 9), as well as the for all (24) models combined incorporating uncertainty from individual models based on estimated variance-covariance matrix of parameters (Table 10).

MSY based reference points were derived for the model options based on the average F-at-age matrix for 2019–2020. The period was considered representative of the recent average pattern of exploitation from the fishery. However, it is important to note that recent fishery catches from the fishery have been quite variable (PSLS catches in region 1N doubled in 2021); variation in the proportion of catches between the main fishing gears (LL and PSLS) are likely to influence the F-at-age matrix and, hence, *MSY* based indicators.

For the selected model options, point estimates of *MSY* ranged from 83,688 mt to 117,530 mt (Table 9) compared to most recent annual catches of about 116, 538mt (Table 9). Model options with higher steepness generally yielded comparatively higher estimates of *MSY*. On average fishing mortality rates have remained well below the F_{MSY} through to 1990s and 2000s, increased significantly after mid-2010s (Figure 35**Error! Reference source not found.**). Biomass was estimated to have declined considerably

from the late 1990s before stabilizing through the 2000s and declined rapidly following a small increase after 2011 – 12 (Figure 35**Error! Reference source not found.**). Current fishing mortality (F_{2021}) was estimated 8 – 72% higher than F_{MSY}, and current biomass (SSB_{2021}) ranged from 26% lower to 20% higher than SSB_{MSY} (Table 9, Figure 35). In general, current stock status relative to the *MSY* based benchmarks are not fundamentally different for the range of model options, although the proximity to the *MSY* benchmarks is sensitive to the different of model assumptions. Current (2021) fishing mortality was estimated to be above the F_{MSY} level ($F_{2021}/F_{MSY} > 1.0$) for all models; current spawning biomass was estimated to be below the SB_{MSY} level ($SB_{2021}/SB_{MSY} < 1.0$) except for four models (they are associated with high steepness of 0.9 and the low natural mortality option).

Estimates were combined across from the 24 models to generate the final KOBE stock status plot (Figure 36). For individual models, the uncertainty is characterised using the multivariate lognormal Monte-Carlo approach (Walter et al. 2019, Walter & Winker 2019, Winker et al. 2019), based on the maximum likelihood estimates and variance-covariance of the untransformed quantities F/F_{MSY} and SSB/SSB_{MSY}. Thus, estimates of stock status included both within and across model uncertainty. Combined across the model ensemble, SSB_{2021} was estimated to be of 0.90 SSB_{MSY} (0.75–1.05), and F_{2021} was estimated 1.43 F_{MSY} (1.10–1.77) (Table 10). Thus, the stock is considered to be overfished, and is subject to overfishing in 2021.

.

Table 9: Estimates of management quantities for the stock assessment model options. Current yield (mt) represents yield in 2021 corresponding to fishing mortality at the FMSY level.

Option	SB_0	SB_{MSY}	SB_{MSY}/SB_0	SB_{2021}	SB_{2021}/SB_0	SB_{2021}/SB_{MSY}	F_{2021}/F_{MSY}	MSY
h70_Gbase_Mbase_sL	2 061 400	592 810	0.29	527 652	0.26	0.89	1.70	83 688
h70_Gbase_Mbase_sD	2 190 390	699 352	0.32	586 098	0.27	0.84	1.72	86 445
h70_Gbase_MHamel17_sL	1 679 440	482 639	0.29	417 456	0.25	0.86	1.65	88 243
h70_Gbase_MHamel17_sD	1 727 800	523 207	0.30	450 023	0.26	0.86	1.62	88 997
h70_Gnew_Mbase_sL	1 996 680	628 643	0.31	476 617	0.24	0.76	1.70	84 583
h70_Gnew_Mbase_sD	2 522 400	844 401	0.33	647 237	0.26	0.77	1.54	102 544
h70_Gnew_MHamel17_sL	1 657 730	513 086	0.31	378 357	0.23	0.74	1.68	89 622
h70_Gnew_MHamel17_sD	2 166 390	755 294	0.35	616 810	0.28	0.82	1.26	108 601
h80_Gbase_Mbase_sL	1 896 030	478 147	0.25	475 934	0.25	1.00	1.47	88 841
h80_Gbase_Mbase_sD	2 013 860	573 637	0.28	526 925	0.26	0.92	1.48	90 876
h80_Gbase_MHamel17_sL	1 546 420	387 928	0.25	377 251	0.24	0.97	1.40	93 984
ih80_Gbase_MHamel17_sD	1 578 550	420 580	0.27	399 568	0.25	0.95	1.40	93 683
h80_Gnew_Mbase_sL	1 819 780	519 528	0.29	422 377	0.23	0.81	1.52	88 523
h80_Gnew_Mbase_sD	2 330 710	701 998	0.30	582 100	0.25	0.83	1.35	108 144
h80_Gnew_MHamel17_sL	1 508 440	420 047	0.28	334 262	0.22	0.80	1.49	93 848
h80_Gnew_MHamel17_sD	1 738 300	534 925	0.31	396 373	0.23	0.74	1.45	104 440
h90_Gbase_Mbase_sL	1 766 350	367 171	0.21	435 668	0.25	1.19	1.23	94 259
h90_Gbase_Mbase_sD	1 876 880	465 577	0.25	481 659	0.26	1.03	1.27	95 338
h90_Gbase_MHamel17_sL	1 441 150	300 099	0.21	345 809	0.24	1.15	1.17	99 803
h90_Gbase_MHamel17_sD	1 419 250	315 151	0.22	334 569	0.24	1.06	1.25	96 525
h90_Gnew_Mbase_sL	1 680 650	425 657	0.25	380 025	0.23	0.89	1.34	92 214
h90_Gnew_Mbase_sD	2 169 840	594 207	0.27	535 738	0.25	0.90	1.18	112 406
h90_Gnew_MHamel17_sL	1 389 440	337 824	0.24	299 325	0.22	0.89	1.31	97 761
h90_Gnew_MHamel17_sD	1 721 810	437 387	0.25	413 086	0.24	0.94	1.08	116 538

Table 10: Estimated Status of bigeye tuna in the Indian Ocean from the model ensemble.

Catch in 2021:	95 021
Average catch 2016–2021:	87 728
MSY (1000 t) (plausible range):	96 (83 –108)
F_{MSY}	0.26 (0.18–0.34)
SB_0(1000 t) (80% CI):	1831 (1445–2218)
SB_{2021} (1000 t) (80% CI):	450 (322–577)
SB_{MSY}	513 (332–694)
SB_{2021}/SB_0 (80% CI):	0.25 (0.23–0.27)
SB_{2021} / SSB_{MSY}	0.90 (0.75–1.05)
F_{2021} / F_{MSY}	1.43 (1.10–1.77)

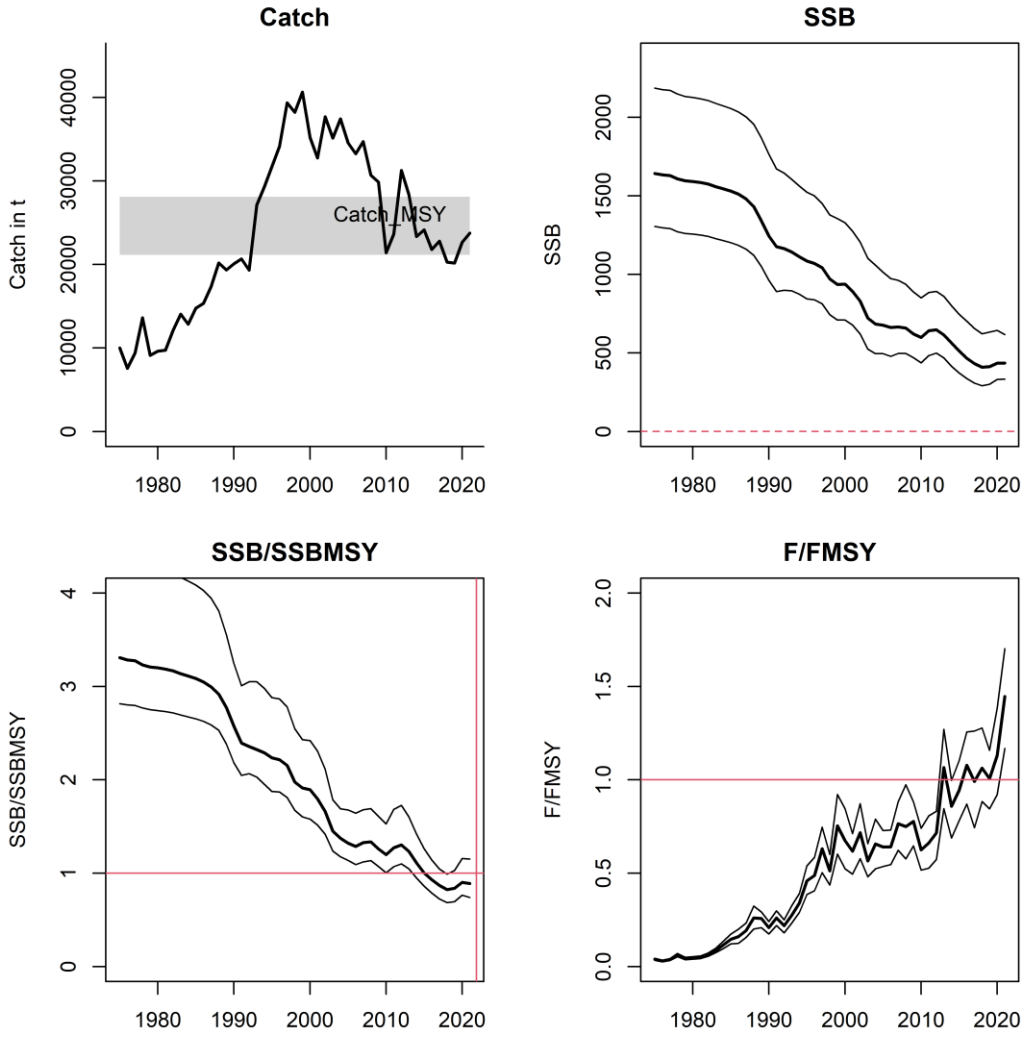

Figure 35: Estimated stock trajectories for the Indian Ocean yellowfin tuna from the final model grid. Thick black lines shaded areas represent 5th and 95th percentiles across all models. In the catch plot, dotted lines represent estimate of MSY (quarterly), the shaded area represents 5th and 95th percentiles.

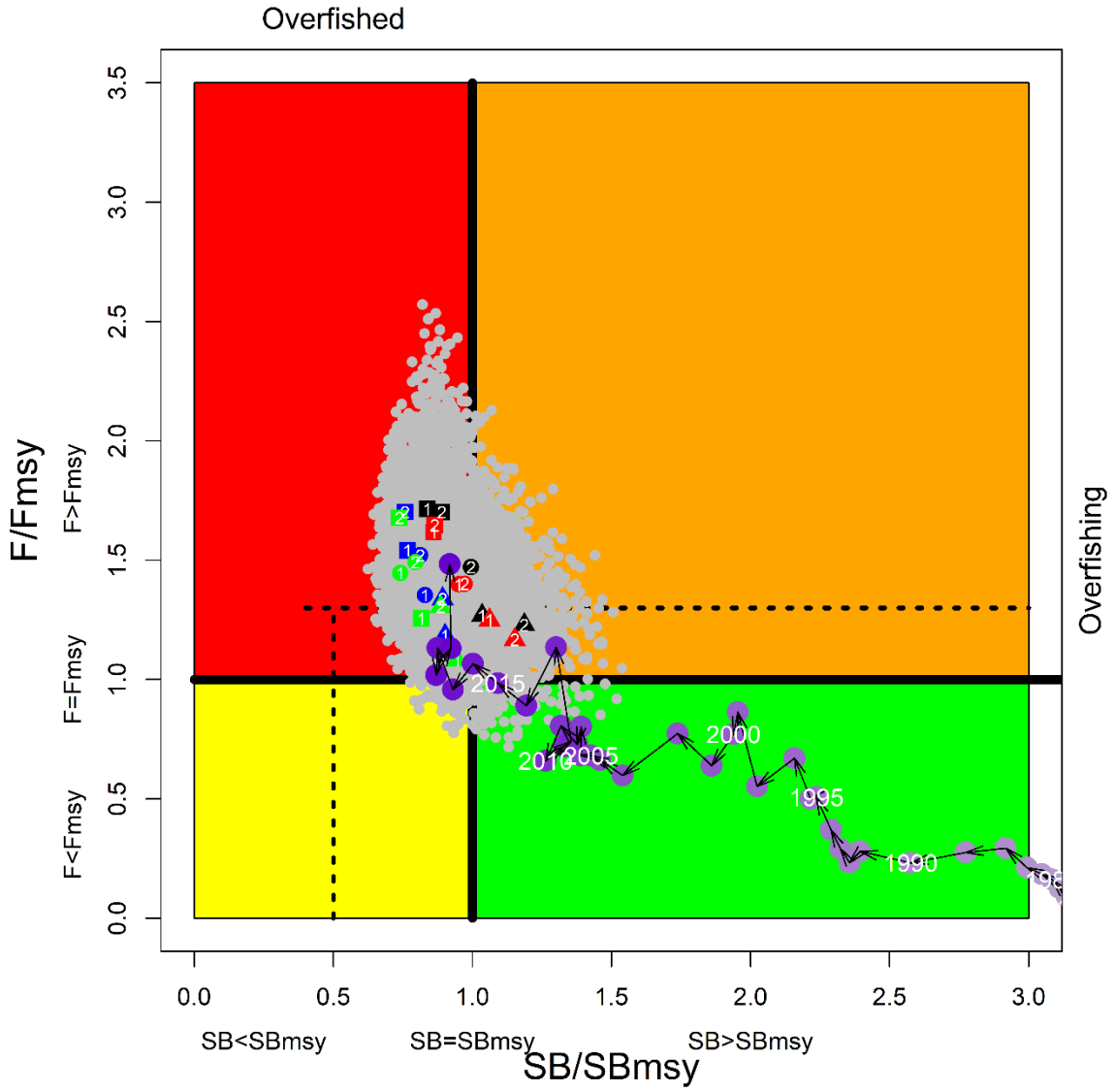

Figure 36: current stock status, relative to SB_{MSY} (x-axis) and F_{MSY} (y-axis) reference points for the final model options. Coloured symbols represent MPD estimates from individual models: square, circle, and Triangles represents steepness options h70, h80, and h90 respectively; black, red, blue, and green represents growth and natural mortality option combination Gbase_Mbase, Gbase_MHamel17, Gnew_Mbase, and Gnew_MHamel17 respectively; 1,2, represents selectivity options sD and sL respectively. The purple dot and arrowed line represent estimates of model "io_h80_Gbase_Mbase_sD". Grey dots represent uncertainty from individual models. The dashed lines represent limit reference points for IO yellowfin tuna (SB_{lim} = 0.5 SB_{MSY} and F_{lim} = 1.4 F_{MSY}).

7. DISCUSSION

This report presents a preliminary stock assessment for Indian Ocean bigeye tuna using a spatially explicit, age structured model. It represents an update and revision of the 2019 assessment model with newly available information. There are no fundamental changes in the structure of the current assessment models compared to the previous assessment (Fu 2019), with most revisions concerning observational data, e.g., the inclusion of revised regional LL CPUE indices, and the incorporation newly avaiable biological information including growth and natural mortality. A range of exploratory models are also presented to explore the impact of key data sets and model assumptions.

As earlier assessments, the models presented here, while providing a reasonable fit to some key data sets (e.g., the CPUE indices), also show some signs of poor fit (e.g. LF data). There are conflicts amongst observational datasets, noticeably between the CPUE and tag data, and the model estimates are sensitive to the relative weighting of these data. Estimates of movement rates were probably more influenced by model configurations than tag data. The nature and extent of the dispersal of tagged fish remains a key uncertainty in the assessment. However, the retrospective analysis provided some confidence on the robustness of the model with respect to recent data, yet the uncertainly on levels of recent recruitment may undermine the predictive capabilities of the model.

The overall stock status estimates obtained from a range of model options is somewhat more pessimistic compared to from the previous assessment: current spawning biomass remained to be below SSB_{MSY} (SSB_{2021}/SSB_{MSY} = 0.90), and fishing mortality is estimated to be above F_{MSY} (F_{2021}/F_{MSY} = 1.43) (Current SSB was estimated to be above SSB_{MSY} in the previous assessment). This has been mostly caused by changes in CPUE indices for regions 2 and 3, which declined more rapidly than the previous indices from the late 1990s to the 2010s. Consequently, compared to the prior assessment, the stock biomass decreased significantly during this time. As such, the model estimated a spawning biomass that dropped be below the target since 2018. The number of fish caught by the purse seine FAD fishery increased significantly in 2021 (by over 100% in region 1N), which caused a considerable increase in fishing mortality since the most fish caught by this fishery were juveniles. The average catch over the last few years, however, are lower than the estimated MSY from the final model ensemble, and the trend of diminishing spawning biomass was reversed from 2018 to 2021.

The scale of the abundance indices can be found in both CPUE and length composition. The two data sources frequently include contradictory information. The best practice is to place greater focus on the CPUE data because it is more direct, whereas length composition often suffers from sampling problems, and it is impossible to totally eliminate the influence of biased length samples. In this assessment, only length composition from major fisheries (i.e., longlines, purse seine, and longlines for fresh tuna) is incorporated into the model. Following Hoyle et al. (2021), the longline fishery excludes Taiwanese and Seychelles length data due to sampling bias, and size data from the bait boat, line, and other fisheries are not used because the samples are of poor quality and representativeness, even though these fisheries' selectivity is linked to fisheries with a similar pattern of selection. By doing so, the impact of these length samples on estimates of the abundance is lessened.

Growth is one major source of uncertainly. The otolith aging approach utilized in the growth study of Farley et al. (2021) is supported by preliminary age validation work. The new growth curve is quite different from the integrated VB-logK curves of Eveson et al. (2012). According to Farley et al. (2021), The very slow growth for fish < 50 cm and the lower mean asymptotic length in Eveson et al. 2012) may be due to the low number of fish >150 cm FL in the tag-recapture data available at the time. Further Eveson and Farley (2021) suggested the differential growth exhibited in different tagging cohorts may not have been handled well by the integrated model of Eveson et al. (2012) and that the new otolith method is likely more reliable. However, the modal progress shown in the length data from the purse seine associated sets between 2006 and 2009 seems to be more compatible with the growth function of is Eveson et al. (2012), and does fit well with the growth function of Farley et al (Figure A7, Appendix A). The Eveson et al. (2012) growth estimate is based on tag data recovered from the purse seinc fishery

during that time, and the samples from Farley et al. 2021 are obtained from a wider area, so this may not be too surprising. Despite this, given the new study's small sample size, there is still a great deal of uncertainty surrounding the revised growth estimates. The large discrepancy between the two growth estimates is anticipated to significantly increase the level of uncertainty in the assessment.

The assessment model adopted a 4-region spatial structure. Movement rates between regions were estimated to be very low. There is very little information on the movement dynamics of bigeye tuna and a low level of mixing among subpopulation may be possible. Alternative models assuming hypothetical high mixing rates did not yield very different estimates of stock abundance but was not consistent with the extent of spatial heterogeneity as observed in the regional CPUE indices. Models with less disaggregated regional partitioning (e.g. three regions) reduce the complexity of movement dynamics but is likely to introduce bias if the incomplete tag dispersal within the main tag recovery region is not adequately accounted for. The assessment indicated that the data did not adequately inform movement rates. A substantial number of tags were recaptured in region 1N (released 1S), although 73% of them were caught before the expected mixing period (4 quarters). The model estimated a higher rate of movement from 1S to 1N when shorter mixing periods were assumed (e.g., 0). If the tagging data is truly informative of regional movement, omitting tag recovery during the pre-mixing period would result in bias in the estimation of movement rate. One method is to compute "unmixed" fishing mortality values for each recapture occurrence in the expected non-mixing timeframe so all recoveries can be incorporated without violating the mixing assumption. Stock Synthesis does not presently implement this option.

Almost all bigeye tuna caught from the purse seine FAD fishery are less than 80 cm (fish caught by longliners are generally greater than 100 cm). The of the impact of these catches of small tuna on other tuna fisheries is frequently raised in fishery management meetings (Hampton 2002). The fishing impact analysis (Minto 2016) performed to the bigeye assessment model showed that the relative impact attributed to different fishing sectors is sensitive to the natural mortality assumption, e.g. the PSLS will have a much larger impact than the longline fishery if the juveniles experience a much lower natural mortality (Fu 2019). The uncertainty in the scale natural morality across various life stages will have important management implications for the bigeye tuna stock. Figure A6 showed that the fishing impact of Purse seine fishery is much larger under the MThen15 compared to the basic model.

The population scaling parameter R0 was intended to accurately reflect the long-term average recruitment through the recruitment bias adjustment. The application to the basic model demonstrates that additional bias correction should change the relative contributions of recruitment deviates and R0 rather than the abundance estimations. However, applying bias correction to a larger model grid is more challenging, necessitating the development of correction factors for individual models and careful tuning to ensure that the overall biomass estimations are unaffected. Initial investigation indicated that this isn't always the case. Using the same bias correction for all models is another option. Future assessments should look into applying recruitment bias adjustment to the entire model grid.

8. ACKNOWLEDGMENTS

I am grateful to the many people that contributed to the collection of this data historically, analysts involved in the CPUE standardization, and developers for providing the SS3 software, and in particular to Adam Langley who conducted the previous assessments.

9. REFERENCES

Akia, S., Guery, L., Grande, M., Kaplan, D., Baéz, J.C., Ramos, M. L., Uranga, J., Abascal, F., Santiago, J, Merino, G., Gaertner, D. 2022. European purse seiners CPUE standardization of Big Eye tuna caught under dFADs. IOTC-2022-WPTT24-12.

Appleyard SA, RD Ward, PM Grewe. 2002. Genetic stock structure of bigeye tuna in the Indian Ocean using mitochondrial DNA and microsatellites. J. Fish Biol. 60: 767- 770.

Carvalho, F., Winker, H., Courtney, D., Kapur, M., Kell, L., Cardinale, M., Schirripa, M., Kitakado, T., Yemane, D., Piner, K.R., Maunder, M.N., Taylor, I., Wetzel, C.R., Doering, K., Johnson, K.F., Methot, R.D., 2021. A cookbook for using model diagnostics in integrated stock assessments. Fish. Res. 240, 105959. https://doi.org/https://doi.org/10.1016/j.fishres.2021.105959

Chassot E, Assan C, Esparon J,, Tirant A, Delgado d, Molina A, Dewals P, Augustin E, Bodin N. 2016. Length-weight relationships for tropical tunas caught with purse seine in the Indian Ocean: Update and lessons learned. IOTC-2016-WPDCS12-INF05.

Díaz-Arce, N., Grewe, P., Krug, I Artetxe, I., Ruiz, J., et al. (2020). Evidence of connectivity of bigeye tuna (Thunnus obesus) throughout the Indian Ocean inferred from genome-wide genetic markers. IOTC-2020-WPTT22(AS)-16.

Eveson, P., Million, J., Sardenne, F., Le Croizier, G. 2012. Updated growth estimates for skipjack, yellowfin and bigeye tuna in the Indian Ocean using the most recent tag-recapture and otolith data. IOTC-2012-WPTT14-23.

Eveson, P., Million, J., Sardenne, F., Le Croizier, G. 2015. Estimating growth of tropical tunas in the Indian Ocean using tag-recapture data and otolith-based age estimates. Fisheries Research 163, 58–68,

Eveson, P., Farley, J., 2021. Investigating growth information for yellowfin and bigeye tuna from the IOTTP tag-recapture data.

Farley, J.H., Clear, N.P., Leroy, Bruno., Davis, T.L.O., McPherson, G. 2004. Age and growth of bigeye tuna (Thunnus obesus) in the eastern and western AFZ.

Farley, J., Krusic-Golub, K., Eveson, P., Clear, N., Luque, P.L., Artetxe-Arrate, I., Fraile, I., Zudaire, I., Vidot, A., Govinden, R., Ebrahim, A., Romanov, E., Chassot, E., Bodin, N., Murua, H., Marsac, F., Merino, G. 2021. Estimating the age and growth of bigeye tuna (Thunnus obesus) in the Indian Ocean from counts of daily and annual increments in otoliths. IOTC-2021-WPTT23-BET growth.

Fonteneau, A., Pallares, P. 2004. Tuna natural mortality as a function of their age: the bigeye tuna case. IOTC-2004-WPTT-INF02.

Fonteneau, A., Ariz, R., Delgado, A., Pallares, P., Pianet, R. 2004. A comparison of bigeye stocks and fisheries in the Atlantic, Indian and pacific oceans. IOTC-2004-WPTT-INF03.

Francis, R.C. and Hilborn, R. 2011. Data weighting in statistical fisheries stock assessment models. Canadian Journal of Fisheries and Aquatic Sciences 68(6): 1124–1138. doi:10.1139/f2011-025.

Fu, D. 2017. Indian ocean skipjack tuna stock assessment 1950-2016 (stock synthesis). IOTC–2017–WPTT19–47_rev1.

Fu, D. 2019. Preliminary Indian Ocean Bigeye Tuna Stock Assessment 1950-2021 (Stock Synthesis). IOTC–2019–WPTT21–61.

Fu, D., Langley, A. Merino, G., Ijurco, A.U. 2018. Preliminary Indian ocean yellowfin tuna stock assessment 1950-2017 (Stock Synthesis). IOTC–2018–WPTT20–33.

Gaertner, D., Hallier, J.P. 2015. Tag shedding by tropical tunas in the Indian Ocean and other factors

affecting the shedding rate. Fisheries Research. 2015/163.

Hampton. J. 2000. Natural mortality rates in tropical tunas: size really does matter. Can. J. Fish. Aquat. Sci. 57: 1002–1010 (2000).

Harley, S.J. 2011. Preliminary examination of steepness in tunas based on stock assessment results. WCPFC SC7 SA IP-8, Pohnpei, Federated States of Micronesia, 9–17 August 2011.

Hillary, R.M., Eveson, J.P., 2015. Length-based Brownie mark-recapture models: derivation and application to Indian Ocean skipjack tuna. Fish. Res. 163, 141–151.

Hillary, R.M., Million, J., Anganuzzi, A., Areso, J.J. 2008a. Tag shedding and reporting rate estimates for Indian Ocean tuna using double-tagging and tag-seeding experiments. IOTC-2008-WPTDA-04.

Hillary, R.M., Million, J., Anganuzzi, A., Areso, J.J. 2008b. Reporting rate analyses for recaptures from Seychelles port for yellowfin, bigeye and skipjack tuna. IOTC-2008-WPTT-18.

Hoyle, S.D., Leroy, B.M., Nicol, S.J., Hampton, J. 2015. Covariates of release mortality and tag loss in large-scale tuna tagging experiments. Fisheries Research 163, 106-118.

Hoyle, S.D., Kitakado, T., Matsumoto, T., Kim, D.N., Lee, S.I., Ku, J.E., Lee, M.K., Yeh,Y., Chang, S.T., Govinden, R., Lucas, J., Assan, C., Fu, D. 2017a. IOTC–CPUEWS–04 2017: Report of the Fourth IOTC CPUE Workshop on Longline Fisheries, July 3th–7th, 2017. IOTC–2017–CPUEWS04–R. 21 p.

Hoyle, S., Satoh, K., Matsumoto, T. 2017b. Exploring possible causes of historical discontinuities in Japanese longline CPUE. IOTC–2017–WPTT19–33 Rev1.

Hoyle, S.D., Okamoto, H. (2015). Descriptive analyses of the Japanese Indian Ocean longline fishery, focusing on tropical areas. IOTC-2015-WPTT17-INF08.

Hoyle, S.D., Langley, A. 2018. Indian Ocean tropical tuna regional scaling factors that allow for seasonality and cell areas. IOTC-2018-WPM09-13.

Hoyle, S., Chang, ST., Fu, D., Geehan, J., Itoh, T., Lee, S.I., Matsumoto, T., Yeh, Y.M., Wu, R.F. 2021. IOTC-2021-WPTT(DP)23-08: Review of size data from Indian Ocean longline fleets, and its utility for stock assessment.

Hoyle 2022. Natural mortality ogives for the Indian Ocean bigeye tuna stock assessment. IOTC–2022-WPTT24(DP)-17.

IOTC 2016. Report of the 18th Session of the IOTC Working Party on Tropical Tunas. Seychelles, 5–10 November 2016. IOTC–2016–WPTT18–R. 126 pp.

IOTC 2018a. Report of the 20th Session of the IOTC Working Party on Tropical Tunas. Seychelles, 29 October – 3 November 2018. IOTC–2018–WPTT20–R. 127 pp.

IOTC 2018b. Review of the statistical data and fishery trends for tropical tunas. IOTC-2018-WPTT20-07 Rev_1. IOTC-2004-WPTT-INF04.

IOTC 2019a. Report of the 21st Session of the IOTC Working Party on Tropical Tunas. Seychelles, 21 - 26 October 2019. IOTC–2019–WPTT21–R: 146 pp.

IOTC 2019b Report of the 15th Session of the IOTC Working Party on Data Collection and Statistics. IOTC, Karachi, Pakistan, 27-30 November 2019.

IOTC 2021. Report of the 23nd Session of the IOTC Working Party on Tropical Tunas. Online, 22 - 24 June 2020. IOTC–2021–WPTT23(DP)–R[E]: 35 pp.

IOTC 2022. Report of the 24th Session of the IOTC Working Party on Tropical Tunas, Data Preparatory Meeting. Online, 30-May – 03 June 2022. IOTC–2022–WPTT24(DP)–R. 37 pp.

ISSF (2011). Report of the 2011 ISSF stock assessment workshop. Technical Report ISSF TechnicalReport 2011-02, Rome, Italy, March 14-17, 2011.

Kell, L.T., Kimoto, A., Kitakado, T., 2016. Evaluation of the prediction skill of stock assessment using hindcasting. Fisheries research, 183, pp.119-127.

Kitakado, T., Wang, S.P., Matsumoto, T., Lee, S.I., Satoh, K., Yokoi, H., Okamoto, K., Lee, M.K., Lim, J.H., Kwon, Y., Tsai, W.P., Su, N.J., Chang, S.J., Chang, F.C. 2022. Joint CPUE indices for the bigeye tuna in the Indian Ocean based on Japanese, Korean and Taiwanese longline fisheries data up to 2020. IOTC–2022-WPTT24(DP)-15

Kolody, D., Herrera, M., Million, J., (2010). Exploration of Indian Ocean Bigeye Tuna Stock Assessment Sensitivities 1952-2008 using Stock Synthesis (updated to include 2009). IOTC-2012-WPTT10-4.

Kolody, D. 2011. Can length-based selectivity explain the two stage growth curve observed in Indian Ocean YFT and BET. IOTC–2011–WPTT13–33.

Langley, A.; Herrera, M.; Sharma, R. 2013a. Stock assessment of bigeye tuna in the Indian Ocean for 2012. IOTC-2013-WPTT15-30.

Langley, A.; Herrera, M.; Sharma, R. 2013b. Stock assessment of bigeye tuna in the Indian Ocean for 2012. IOTC-2013-WPTT15-30-Rev_1.

Langley, A. 2016. Stock assessment of bigeye tuna in the Indian Ocean for 2016 — model development and evaluation.

Matsumoto, T. 2016. Consideration on the difference of average weight by estimation method for tunas caught by Japanese longline in the Indian Ocean. IOTC-2016-WPDCS12-16.

Method, R.D., Taylor, I.G. 2011. Adjusting for bias due to variability of estimated recruitments in fishery assessment models. Can. J. Fish. Aquat. Sci. 68: 1744–1760.

Methot, R.D. 2013. User manual for Stock Synthesis, model version 3.24f.

Methot, R.D., Wetzel, C.R. 2013. Stock synthesis: A biological and statistical framework for fish stock assessment and fishery management. Fisheries Research 142 (2013) 86–99.

Maunder. A concise guide to developing fishery stock assessment models.

Merino, G., Urtizberea, A., Fu, D., Winker, H., Cardinale, M., Lauretta, M. V., Murua, H., Kitakado, T., Arrizabalaga, H., Scott, R., Pilling, G., Minte-Vera, C., Xu, H., Laborda, A., Erauskin-Extraminiana, M., Santiago, J., 2022. Investigating trends in process error as a diagnostic for integrated fisheries stock assessments. Fish. Res. 256, 106478.

Maunder, M.N., Piner, K.R., 2015. Contemporary fisheries stock assessment: many issues still remain. ICES J. Mar. Sci. 72, 7–18.

Nishida, T., Rademeyer, R. (2011). Stock and risk assessments on bigeye tuna (*Thunnus obesus*) in the Indian Ocean based on AD Model Builder implemented Age-Structured Production Model (ASPM). IOTC-2011-WPTT-42.

Okamoto, H. 2005. Recent trend of Japanese longline fishery in the Indian Ocean with special reference to the targeting. Is the target shifting from bigeye to yellowfin? IOTC-2005-WPTT-11.

Shono, H., K. Satoh, H. Okamoto, and T. Nishida. (2009). Updated stock assessment for bigeye tuna in the Indian Ocean up to 2008 using Stock Synthesis III (SS3). IOTC-2009-WPTT-20.

Then, A.Y.; Hoenig, J.M.; Hall, N.G.; Hewitt, D.A. Evaluating the predictive performance of empirical estimators of natural mortality rate using information on over 200 fish species. ICES Journal of Marine Science. 72:82-92; 2015

Thorson, J.T., Johnson, K.F.,Methot, R.D., and Taylor, I.G. 2017. Model-based estimates of effective sample size in stock assessment models using the Dirichlet-multinomial distribution. Fisheries Research 192: 84–93. doi:10.1016/j.fishres.2016.06.005.

Vincent, M. T., Pilling, G.M., Hampton, J. 2018. Incorporation of updated growth information within the 2017 WCPO bigeye stock assessment grid, and examination of the sensitivity of estimates to alternative model spatial structures. WCPFC-SC14-2018/ SA-WP-03.

Waterhouse, L, Sampson DB, Maunder M, Semmens BX. 2014. Using areas-as-fleets selectivity to model spatial fishing: Asymptotic curves are unlikely under equilibrium conditions. Fisheries Research. 158:15-25.

Walter, J., Hiroki, Y., Satoh, K., Matsumoto, T., Winker, H., Ijurco, A.U., Schirripa, M., 2019. Atlantic bigeye tuna stock synthesis projections and kobe 2 matrices. Col. Vol. Sci. Pap. ICCAT 75, 2283–2300.

Walter, J., Winker, H., 2019. Projections to create Kobe 2 Strategy Matrices using the multivariate log-normal approximation for Atlantic yellowfin tuna. ICCAT-SCRS/2019/145 1–12.

Winker, H., Walter, J., Cardinale, M., Fu, D. 2019. A multivariate lognormal Monte-Carlo approach for estimating structural uncertainty about the stock status and future projections for Indian Ocean Yellowfin tuna. IOTC–2019–WPTT21–xx.

Waterhouse, L, David B. Sampson, D., Maunder, M., Semmens, B. 2014. Using areas-as-fleets selectivity to model spatial fishing: Asymptotic curves are unlikely under equilibrium conditions. Fisheries Research 158 (2014) 15–25.

Williams, A., Jumppanen, P., Preece, A., Hillary, R. 2022. Running the IOTC Bigeye Tuna Management Procedure for 2022. IOTC-2022-WPM13-10.

Williams, A., Preece, A., Hillary, R. 2022 Specifications of the IOTC Bigeye Tuna Management Procedure. IOTC-2022-WPM13-11.

Iker Zudaire, Iraide Artetxe-Arrate, Jessica Farley, Hilario Murua, Deniz Kukul, Annie Vidot, Shoaib Abdul Razzaque, Mohamed Ahusan, Evgeny Romanov, Paige Eveson, Naomi Clear, Patricia L. Luque, Igaratza Fraile, Nathalie Bodin, Emmanuel Chassot, Rodney Govinden, Ameer Ebrahim, Umair Shahid, Theotime Fily, Francis Marsac, Gorka Merino. Preliminary estimates of sex ratio, spawning season, batch fecundity and length at maturity for Indian Ocean bigeye tuna. IOTC-2022-WPTT24(DP)-18.

APPENDIX A: RESULTS FROM THE EXPLORATORY MODELLING

Table A1. Maximum Posterior Density (MPD) estimates of the main stock status indicators from the sensitivity model options.

	SB_0	SB_{MSY}	SB_{MSY}/SB_0	SB_{2021}	SB_{2021}/SB_0	SB_{2021}/SB_{MSY}	F_{2021}/F_{MSY}	MSY
basic	2 015370	625 422	0.31	536 864	0.27	0.86	1.65	93 600
basic1950	2 013140	624 917	0.31	534 842	0.27	0.86	1.66	93 586
CPUELSpe	1 923940	550 245	0.29	473 099	0.25	0.86	1.64	88 209
CPUELLq	1 855390	565 862	0.30	318 263	0.17	0.56	2.26	95 098
dirichlet	2 022570	630 740	0.31	536 411	0.27	0.85	1.69	93 887
ess5	1 990370	589 180	0.30	515 697	0.26	0.88	1.62	94 066
selrw	2 117460	666 302	0.31	581 692	0.27	0.87	1.66	91 907
logistic	1 887400	540 494	0.29	473 630	0.25	0.88	1.70	91 916
growth	2 434350	803 813	0.33	659 335	0.27	0.82	1.27	111 491
MHamel15	1 266460	354 605	0.28	308 300	0.24	0.87	1.45	101 218
MHamel17	1 511480	429 984	0.28	358 859	0.24	0.83	1.69	94 580
MThen15	1 060180	286 830	0.27	249 889	0.24	0.87	1.30	106 734
MThen17	1 277050	357 887	0.28	311 313	0.24	0.87	1.46	101 014
taglambda1	1 756840	589 454	0.34	425 673	0.24	0.72	2.08	84 184
taglambda001	2 080980	627 032	0.30	559 322	0.27	0.89	1.54	95 394
tag4	2 019730	625 555	0.31	538 786	0.27	0.86	1.64	93 896
areaAsFleet_1	1 846500	553 474	0.30	319 888	0.17	0.58	2.24	95 482
areaAsFleet_2	2 115830	629 453	0.30	592 445	0.28	0.94	1.29	94 462
areaAsFleet_3	2 358240	692 113	0.29	836 406	0.35	1.21	1.03	97 343

Table A2: Details of objective function components for the exploratory model options.

	TOTAL	CPUE	Length_comp	Tag_comp	Tag_negbin	Recruitment	Parm_priors	Parm_devs	Catch	Soft bounds
basic	911.9	-524.5	1034.4	226.8	167.6	-22.1	12.7	12.7	0.0	0.0
basic1950	911.9	-524.6	1034.6	226.7	167.6	-22.1	12.6	12.6	0.0	0.0
CPUELSpe	891.3	-545.9	1033.2	225.9	166.5	-18.9	12.8	12.8	0.0	0.0
CPUELLq	909.7	-529.1	1042.5	226.6	166.0	-25.4	12.2	12.2	0.1	0.0
dirichlet	4328.8	-530.9	4455.9	227.1	168.0	-21.6	12.9	12.9	0.0	0.0
ess5	1094.4	-510.2	1206.4	226.7	166.2	-22.9	11.9	11.9	0.1	0.0
selrw	818.4	-526.9	939.3	224.4	168.3	-27.3	18.5	18.5	0.0	0.0
logistic	942.6	-479.0	1027.0	224.0	165.9	-21.6	12.6	12.6	0.2	0.0
growth	973.8	-546.6	1158.1	217.0	155.5	-44.6	19.1	19.1	0.6	0.0
MHamel15	912.0	-533.9	1043.6	227.3	170.0	-26.1	13.5	13.5	0.0	0.0
MHamel17	912.6	-522.5	1032.9	226.1	167.4	-21.4	13.0	13.0	0.0	0.0
MThen15	926.2	-538.6	1061.1	227.9	173.0	-29.3	14.0	14.0	0.0	0.0
MThen17	911.6	-533.8	1043.1	227.3	169.9	-25.9	13.4	13.4	0.0	0.0
taglambda1	4282.7	-495.2	1061.7	2143.6	1490.9	-10.7	73.6	73.6	0.5	0.0
taglambda001	550.9	-526.4	1032.2	24.4	17.4	-24.4	10.6	10.6	0.0	0.0
tag4	887.1	-524.2	1034.2	220.4	148.4	-22.2	13.5	13.5	0.0	0.0

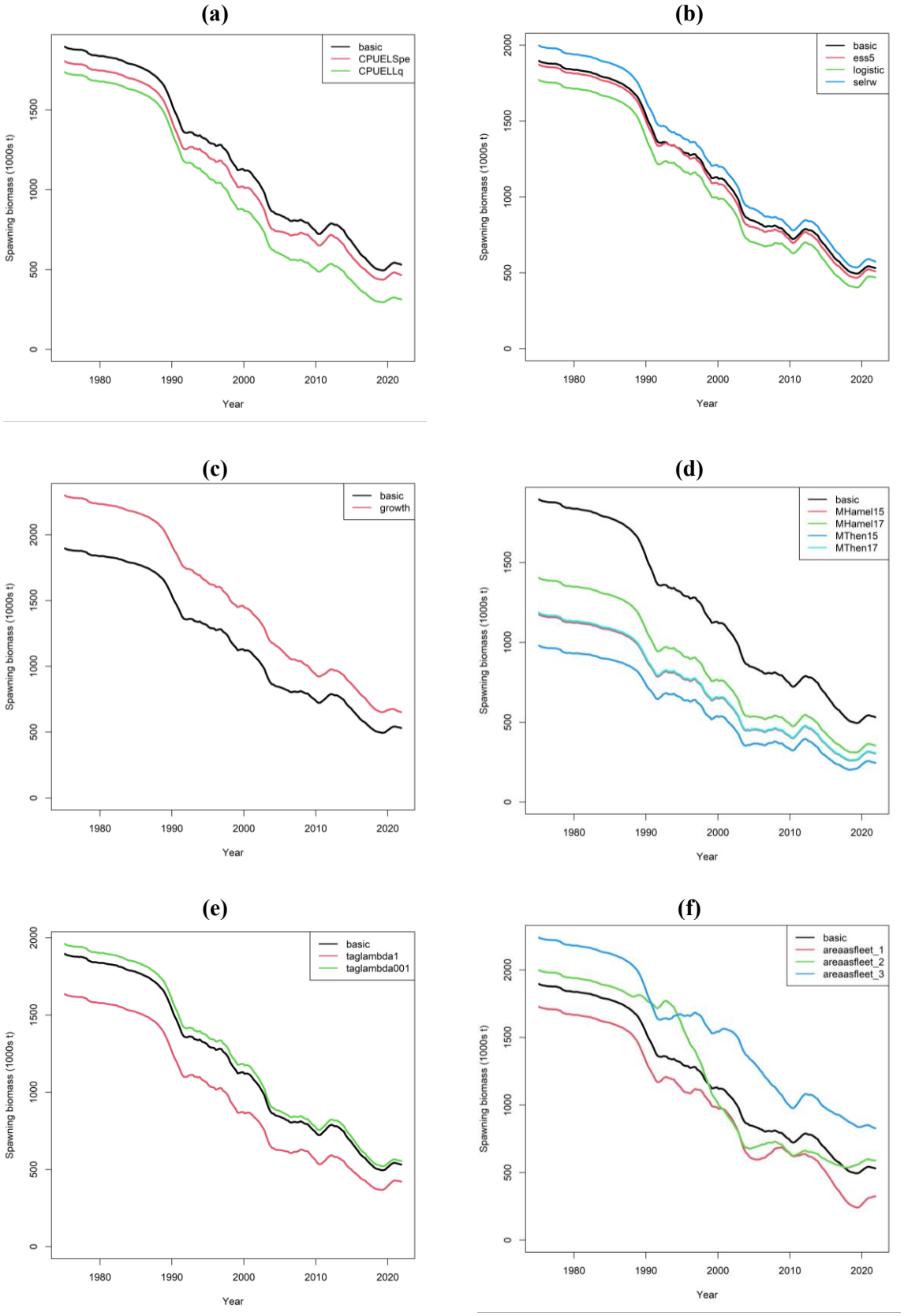

Figure A1: A comparison of estimated SSB for between selected sensitivity models and the basic model.

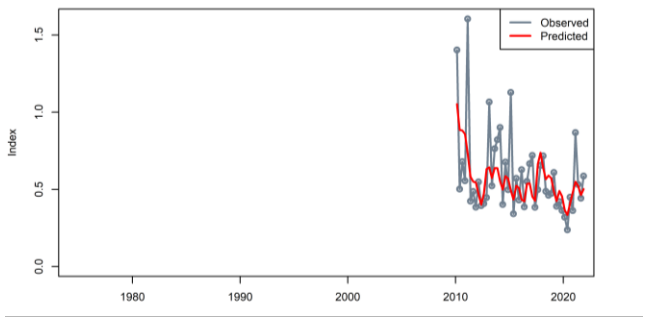

Figure A2: Fit to the PSLS CPUE index, 2010–2021 from model "*CPUELSpe*".

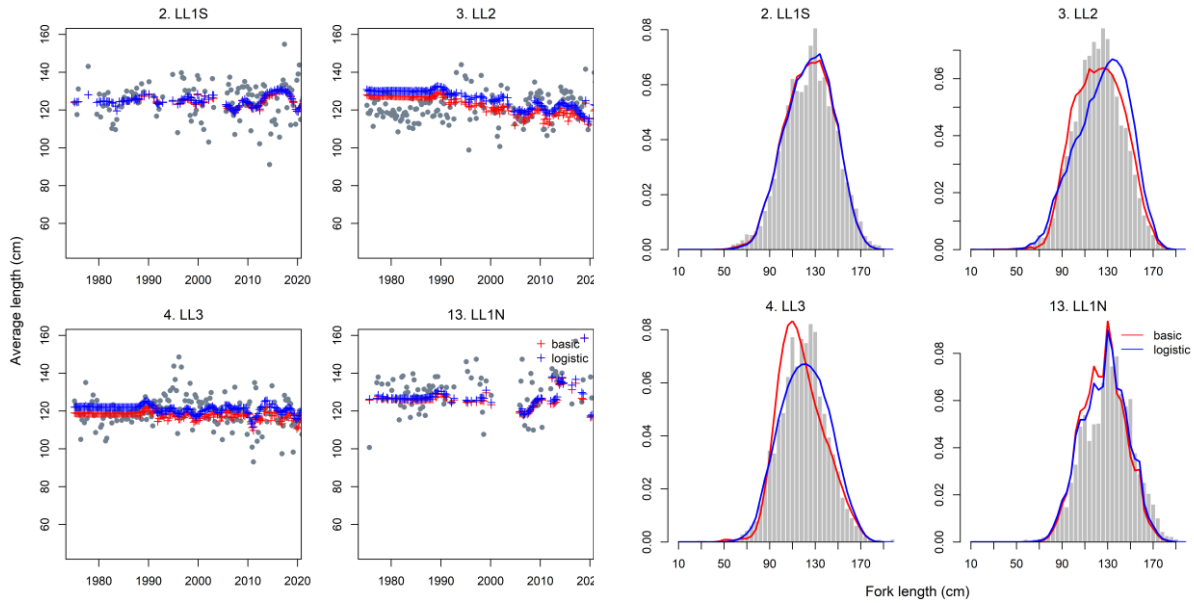

Figure A3: A comparison of fits to the mean annual length frequencies and the aggregated length frequency for the four regional longline fisheries between models "*basic*" and "*logistic*".

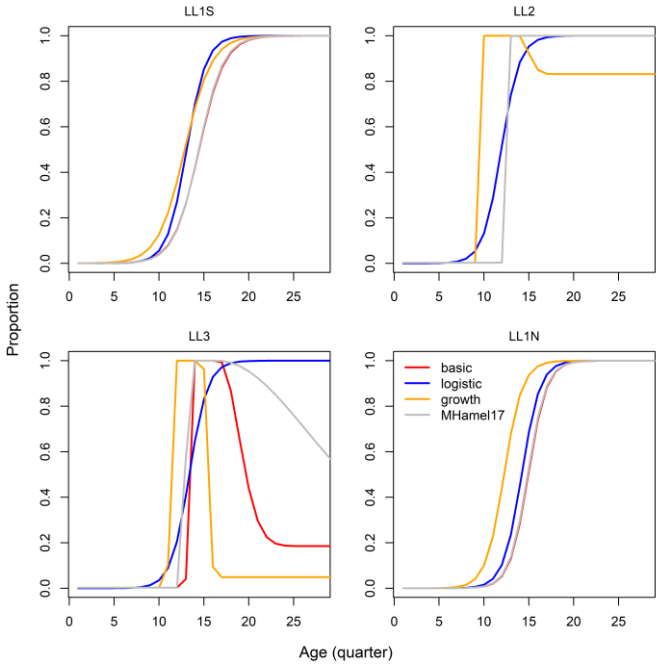

Figure A4: A comparison of estimated selectivity for the four regional longline fisheries amongst models "basic", "logistic", "growth", and "HMamel17".

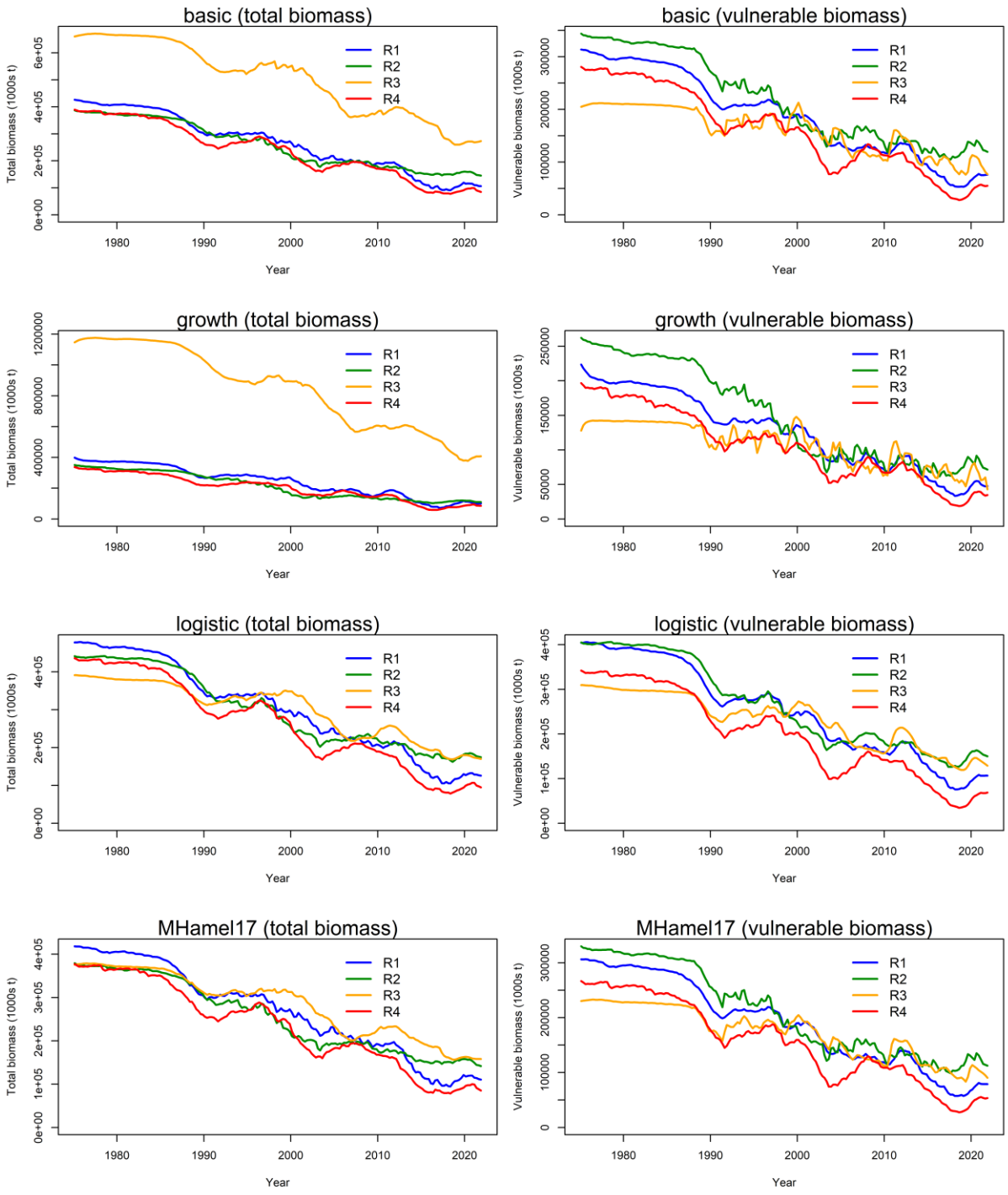

Figure A5: A comparison of estimated total biomass and vulnerable biomass (with respect to the regional longline fisheries) among models "basic", "growth", "logistic", and "MHamel17".

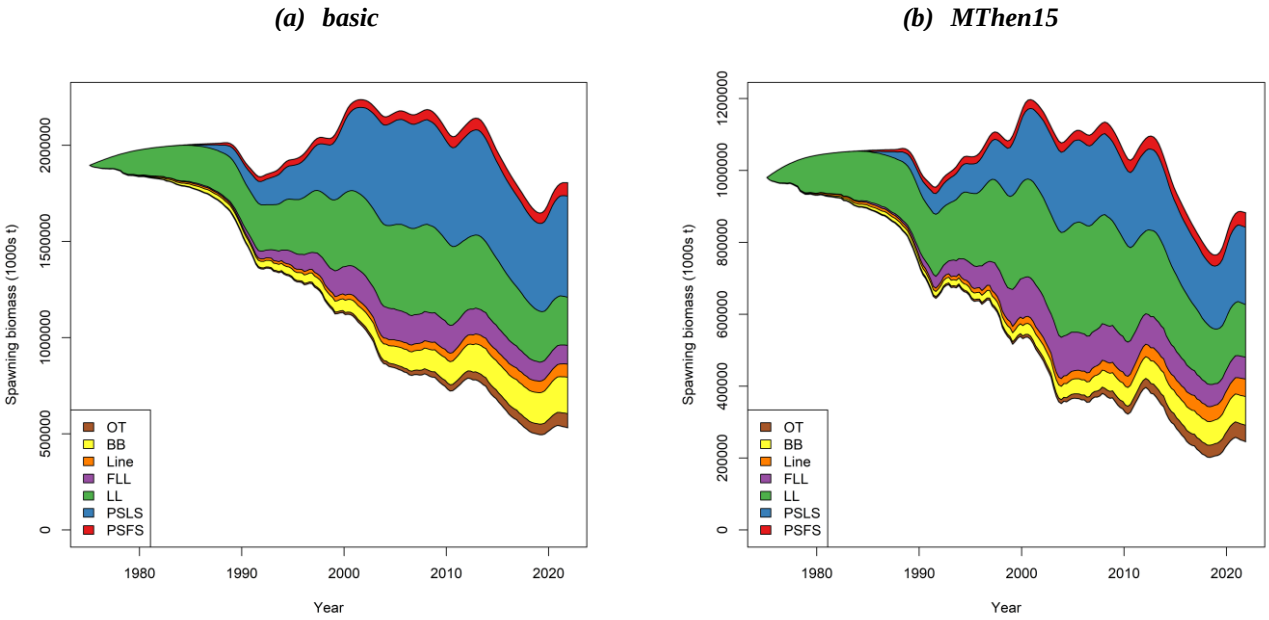

Figure A6: A comparison of estimated fishing impact (reduction in spawning biomass due to fishing over attributed to various fishery groups) for exploratory models with high (eMhigh, left) and low natural mortality options (eMconst, right).

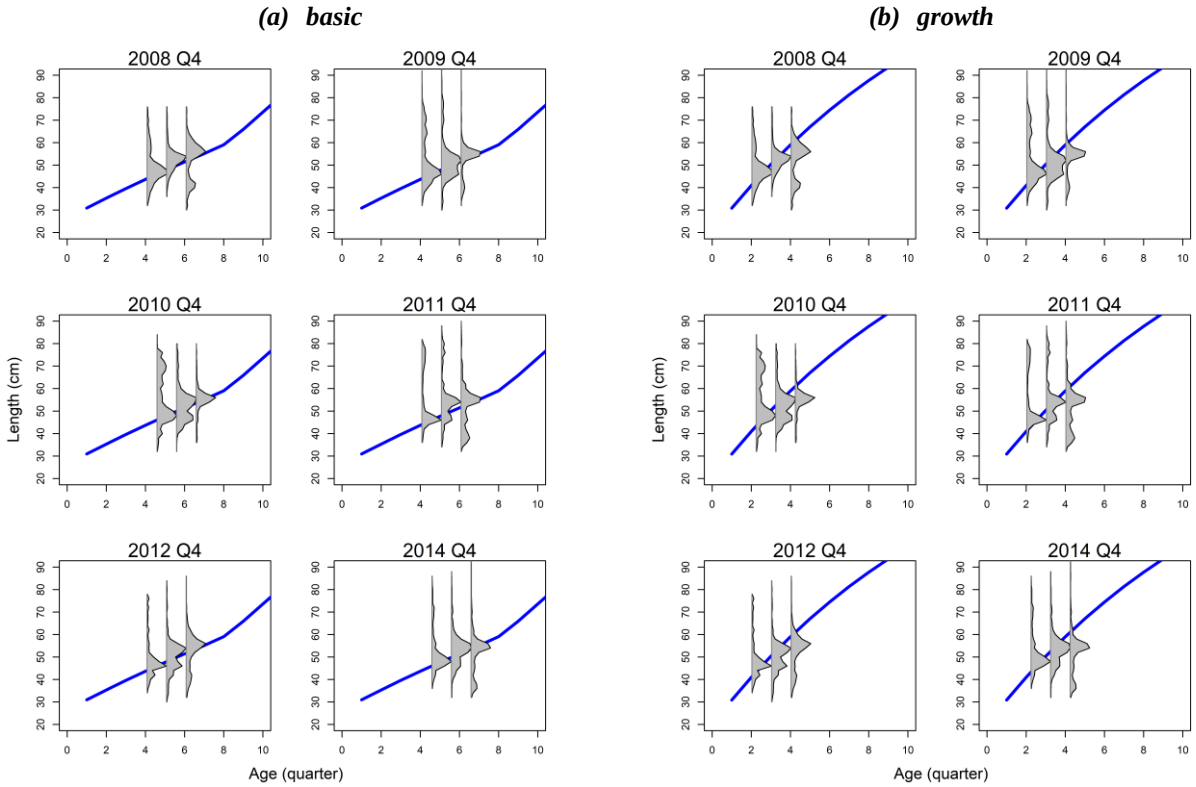

Figure A7: A comparison of the growth curve with the modal progression exhibited in the PSLS length frequency distribution, for the basic model (Eveson et al. 2012 growth) and in the "growth" (Farley et al. 2021 growth). In each panel, three consecutive quarterly length frequency (starting in the 4th quarter of 2008, 2009, 2010, 2011, 2012 and 2014, respectively), and were overlaid with the age-length relationship in the respective model. The age of the mode in the first length frequency in each panel was assigned to the closest age according to the growth curve used.

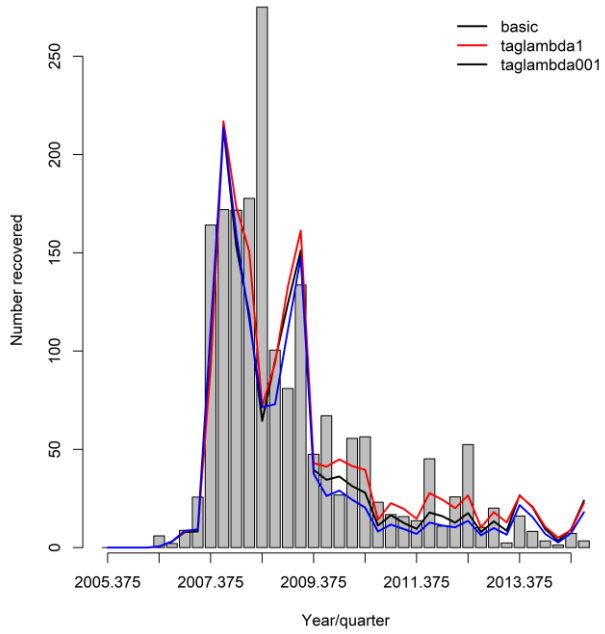

Figure A8: A comparison of fits to the tag recoveries aggregated for all fisheries amongst models "basic", "taglambda001", and "tagLambda1"

APPENDIX B: DIGNOSTICS FOR THE FINAL MODELS

Table B1: Summary statistics from retrospective and hindcasting diagnostics for the final models

Models	rec.p	sigR	rho.AR1	runs.p	Mohns.B	Mohns.F	MASE	PRMSE	MASE.I1	MASE.I2	MASE.I3	MASE.I4	MASE.I5
Criteria	>0.05				[-0.15,0.2]	[-0.15,0.2]							
io_h70_Gbase_Mbase_sL	0.45	0.50	0.50	0.06	-0.06	0.11	1.00	0.45	1.29	0.99	0.62	0.88	1.03
io_h70_Gbase_Mbase_sD	0.77	0.50	0.41	0.04	0.02	0.01	1.00	0.45	1.17	1.06	0.64	0.91	1.04
io_h70_Gbase_MHamel17_sL	0.34	0.50	0.52	0.04	-0.08	0.11	1.00	0.45	1.22	1.06	0.62	0.89	1.04
io_h70_Gbase_MHamel17_sD	0.59	0.48	0.39	0.07	0.01	0.01	1.01	0.45	1.20	1.07	0.63	0.90	1.05
io_h70_Gnew_Mbase_sL	0.16	0.41	0.34	0.08	-0.02	0.13	0.97	0.44	0.92	0.96	0.68	1.03	1.03
io_h70_Gnew_Mbase_sD	0.82	0.47	0.17	0.06	0.01	0.23	0.92	0.41	0.89	0.96	0.58	0.93	1.00
io_h70_Gnew_MHamel17_sL	0.15	0.36	0.39	0.07	-0.19	0.26	0.97	0.44	0.92	0.95	0.67	1.03	1.04
io_h70_Gnew_MHamel17_sD	0.61	0.46	0.17	0.10	0.00	0.25	0.92	0.41	0.93	0.97	0.57	0.93	0.99
io_h80_Gbase_Mbase_sL	0.32	0.50	0.50	0.06	0.00	0.06	1.00	0.46	1.21	1.00	0.65	0.87	1.06
io_h80_Gbase_Mbase_sD	0.50	0.50	0.41	0.05	0.03	0.00	1.00	0.45	1.14	1.06	0.65	0.90	1.04
io_h80_Gbase_MHamel17_sL	0.21	0.50	0.52	0.11	-0.06	0.09	1.00	0.45	1.12	1.07	0.61	0.90	1.05
io_h80_Gbase_MHamel17_sD	0.36	0.48	0.40	0.07	0.02	-0.01	1.00	0.45	1.11	1.07	0.65	0.88	1.06
io_h80_Gnew_Mbase_sL	0.06	0.40	0.31	0.12	-0.02	0.13	0.97	0.44	0.94	0.93	0.71	0.99	1.03
io_h80_Gnew_Mbase_sD	0.63	0.47	0.18	0.05	0.02	0.23	0.92	0.41	0.88	0.96	0.57	0.93	1.00
io_h80_Gnew_MHamel17_sL	0.10	0.40	0.28	0.11	0.09	0.04	0.96	0.44	0.89	0.95	0.66	1.01	1.03
io_h80_Gnew_MHamel17_sD	0.44	0.45	0.18	0.13	0.00	0.25	0.92	0.41	0.94	0.97	0.57	0.93	0.99
io_h90_Gbase_Mbase_sL	0.18	0.50	0.51	0.06	-0.03	0.12	1.00	0.45	1.21	1.02	0.66	0.87	1.04
io_h90_Gbase_Mbase_sD	0.29	0.50	0.42	0.05	0.04	-0.01	1.00	0.44	1.15	1.06	0.66	0.88	1.04
io_h90_Gbase_MHamel17_sL	0.13	0.50	0.52	0.10	0.04	0.00	1.00	0.45	1.13	1.06	0.65	0.88	1.05
io_h90_Gbase_MHamel17_sD	0.21	0.48	0.40	0.10	0.03	-0.04	1.01	0.45	1.15	1.07	0.67	0.87	1.06
io_h90_Gnew_Mbase_sL	0.04	0.40	0.32	0.13	0.12	0.06	1.00	0.45	0.93	0.92	0.86	0.98	1.06
io_h90_Gnew_Mbase_sD	0.45	0.47	0.19	0.05	0.02	0.23	0.92	0.42	0.88	0.96	0.56	0.93	1.00
io_h90_Gnew_MHamel17_sL	0.05	0.38	0.36	0.02	-0.05	0.13	1.00	0.45	0.84	0.96	0.74	1.13	1.05
io_h90_Gnew_MHamel17_sD	0.23	0.45	0.19	0.15	0.01	0.24	0.92	0.42	0.92	0.97	0.56	0.93	0.99

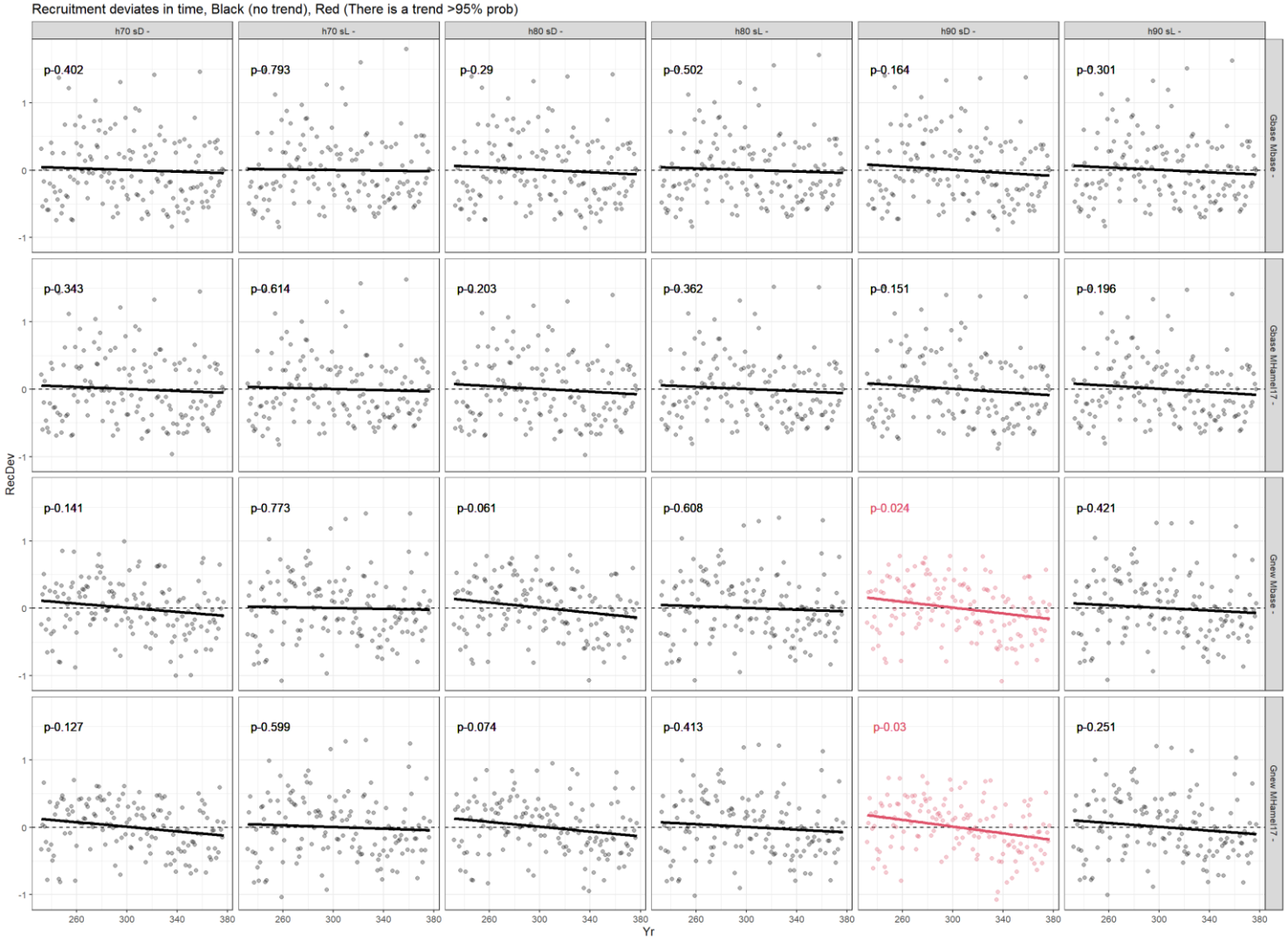

Figure B1: Recruitment deviates for the 24 models of the bigeye tuna stock assessment of 2021. Scenarios with a p-value of the no-trend test lower than 0.05 are identified in black. Lines represent a linear regression to the recruitment deviates